EFFECTS AND MECHANISM OF ENVIRONMENTAL AND GENETIC FACTORS ON FEMALE PUBERTY AND REPRODUCTION

by

RONG LI

(Under the Direction of Xiaoqin Ye)

Abstract

Both environmental and genetic factors can affect female puberty and reproduction. In Chapter 1, these factors with focuses on one environmental factor, genistein, and one genetic factor, olfactomedin 1 (OLFM1) are reviewed. In Chapter 2, the effects of postweaning dietary genistein exposure on female puberty and early pregnancy in C57BL/6J mice are studied. Dose-response study reveals that genistein diets (5-500 ppm) have dose-dependent effects on advancing age at vaginal opening, increasing duration of estrus stage, and accelerating mammary gland development; 5 ppm genistein diet promotes ovulation. Despite the effects on female puberty, postweaning dietary genistein exposure does not have significant effects on early pregnancy. In Chapter 3, the influence of body fat on the effects of genistein on female pubertal development is studied. *Berardinelli-Seip Congenital Lipodystrophy 2* (*Bscl2*)$^{-/-}$ female mice with lipodystropy are used as a low body fat animal model. Postweaning 500 ppm genistein dietary exposure advances vaginal opening and increases mammary gland area in *Bscl2*$^{-/-}$ females. In Chapter 4, the function and mechanism of OLFM1 on female puberty and fertility using *Olfm1*$^{-/-}$ mouse model are investigated. *Olfm1*$^{-/-}$ females have delayed pubertal

development and impaired fertility. Rescued ovulation and fertility by superovulation, normal basal Follicle-stimulating hormone (FSH) and Luteinizing hormone (LH) levels, and normal Gonadotropin-releasing hormone (GnRH) induced LH surge indicate a functional Hypothalamus-pituitary-gonad (HPG) axis. High expression level of OLFM1 in the olfactory systems, unresponsiveness to male bedding stimulation on estrous cycle and pubertal development in *Olfm1*$^{-/-}$ females coupled with a 41% reduction of cFOS positive cells in mitral layer of accessory olfactory bulb indicate that the function of OLFM1 in olfaction contributes to the defective pubertal development and fertility in *Olfm1*$^{-/-}$ female mice. In Chapter 5, the dissertation and future directions of study are summarized.

INDEX WORDS: puberty, reproduction, genistein, vaginal opening, estrous cycle, ovulation, mammary gland, hypothalamus-pituitary-gonad axis, lipodystrophy, olfactomedin1, olfaction.

EFFECTS AND MECHANISM OF ENVIRONMENTAL AND GENETIC FACTORS ON FEMALE PUBERTY AND REPRODUCTION

by

RONG LI

B.E. Shanghai Jiaotong University, Shanghai, China, 2007

M.S. Nanjing University, Nanjing, Jiangsu, China, 2010

A Dissertation Submitted to the Graduate Faculty of The University of Georgia in Partial Fulfillment of the Requirements for the Degree

DOCTOR OF PHILOSOPHY

ATHENS, GEORGIA

2016

EFFECTS AND MECHANISM OF ENVIRONMENTAL AND GENETIC FACTORS ON FEMALE PUBERTY AND REPRODUCTION

by

RONG LI

Major Professor: Xiaoqin Ye

Committee: Julie A. Coffield
Nickolay M. Filipov
Mary Alice Smith
Jia-sheng Wang

Electronic Version Approved:

Suzanne Barbour
Dean of the Graduate School
The University of Georgia
August 2016

ACKNOWLEGEMENTS

Six years of PhD study is the one of the most valuable treasure in my life. I have received warm encouragement, insightful advises, and sincere help from a lot of people. They make my study more smoothly, and my life more enjoyable.

First of all, I want to express my deep gratitude to my advisor, Dr. Xiaoqin Ye. She has guided me through my PhD study. Every project I did, every paper I published, and every award I won could never be accomplished without her support. I am always admiring her quick thinking, sharp eyes, funny words, and smiling all the time. What I learned from her, not only have my PhD project finished successfully, but also my confidence established and my potentials developed. Thank you very much for all you've done! It has been wonderful to work in your lab.

Here I want to say thanks to all my lab mates. Honglu Diao, Shuo Xiao, and Fei Zhao, Elizabeth A. Dudley who already left have helped me a lot. Especially, Fei zhao, he was my "teacher" at the beginning of PhD study. He taught me the techniques as well as driving. Jun Zhou has been in our lab for only one year, but he is very nice and willing to help all the time. And my current lab mates Ahmed E. El Zowalaty, Zidao Wang, and Lianmei Hu have accompanied me for one to four years, all the kindness and help I received from them I will always remember. Thank you all for all your support! You make me truly feel our lab as a family!

I also want to say thanks to all my committee members, Dr. Julie A Coffield, Dr. Nickolay M. Filipov, Dr. Mary Alice Smith, Dr. Jia-sheng Wang. They have always been very supportive. I really appreciate that they have done a lot in order to attend my

committee meeting and give many insightful suggestions during the meeting and in private discussion. Every progress of my study you are all involved. Thank you very much for keeping an eye on my PhD study. Your support is essential for me!

I also want to thank Joanne Mauro, Misty Patterson, Kali King and Jackie Yearwood who helped me to deal with all kinds of issues and filled many types of documents to finish my PhD study. And my sincere thanks to the professors in our department, especially Dr. Wan-I Olive LI, who helped with my class, Dr. Jesse Schank, who provided great suggestions and cFOS antibody for my OLFM1 project, and Dr. Edwards, who taught me the basic knowledge of neuron system and sent many recommendation letters for me. And there are many other people in UGA who have helped me and I would like to say thank you here. And many thanks to my friends. You are very important for me all the time.

In the end, I would like to thank my parents, my mother Cuixia Wang and my father Guanghong Li. They make me believe that I can do anything, and they are always standing behind me. Through the PhD study, your caring is my greatest motivation. And my love to you both is more than I can say!

TABLE OF CONTENTS

Page

LIST OF TABLES

Page

LIST OF FIGURES

LIST OF ABREVIATION

Olfm1: Olfactomedin 1; **HPG**: Hypothalamus-pituitary-gonad; **GnRH**: Gornadotropin-releasing hormone; **FSH**: Follicle-stimulating hormone; **LH**: Luteinizing hormone; **P4**: Progesterone; **E2**: estrogen; **E**: Embryonic; **PND**: Postnatal day; **GABA**: Gamma-aminobutyric acid; EB: Estradiol-benzonate; **ERα**: Estrogen receptor α; P-ERα: Phospho-ERα; **ESR1**: Estrogen receptor 1; **ERβ**: Estrogen receptor β; **ESR2**: Estrogen receptor 2; **PR**: Progesterone receptor; **VMH**: Ventromedial nucleus of the hypothalamus; **ARH**: Arcuate nucleus of hypothalamus; **ZP**: Zona pellucida; **TE**: Trophectoderm; **ICM**: Inner cell mass; **PE**: Primitive endoderm; **EPI**: Epiblast; **VE**: Visceral endoderm; **PaE**: Parietal endoderm; **AVPV**: anteroventral periventricular nucleus; **MEPO**: Median preoptic nucleus; **PVpo/a**: Anterior hypothalamic divisions of the periventricular nucleus; **iHH**: idiopathic hypogonadotropic hypogonadism; **Kiss**: Kisspeptin; $\mathbf{t_{1/2}}$: half-life; **SD**: Sprague Dawley; **WAP**: White adipose tissue; **SCN**: Suprachiasmatic nucleus; **MOS**: Main olfactory system; **AOS**: Accessory olfactory system; **MOE**: Main olfactory epithelium; **MOB**: Main olfactory bulb; **VNO**: Vomeronasal organ; **AOB**: Accessory olfactory bulb; **OSN**: Olfactory sensory neuron; **VSN**: Vomeronasal sensory neuron; **POA**: Preoptic area; **CL**: Corpus luteum; **CK**: Cytokeratin; **Areg**: Amphiregulin; **Wnt4**: Wingless type MMTV integration site family, member 4; **VO**: Vaginal opening; **wks**: Weeks; **Gapdh**: Glyceraldehyde-3-phosphate dehydrogenase; **Hprt1**: Hypoxanthine Phosphoribosyltransferase 1; **TEB**: Terminal end bud; **GEN**: Genistein; **GR**: Glucocorticoid receptor; **LE**: Luminal epithelium; **GE**: Glandular

epithelium; **eCG**: Equine chorionic gonadotropin; **hCG**: human chorionic gonadotropin; **COCs**: Cumulus oocyte complexes; **ABSN**: Axons bundles of sensory neurons.

CHAPTER 1

INTRODUCTION AND LITERATURE REVIEW

This dissertation focuses on the effects of genistein exposure and mechanism of OLFM1 on female puberty and reproduction. Postweaning genistein exposure is used to study environmental effects, and OLFM1 deletion in mouse is used to study genetic mechanism. Chapter 1 reviews the background information related to the studies in this dissertation.

1.1 Female Puberty and Reproduction

1.1.1 Overview

Female reproductive system contains ovary, fallopian tubes (human)/oviduct (rodents), uterus, vagina, and mammary gland, etc. The structure of female reproductive system is formed before puberty, but the full reproductive power is only achieved after pubertal development [1]. Detailed description of puberty and the index of reproduction, such as reproductive cycle, female sexual receptivity and early pregnancy, is included in this chapter. Puberty and reproduction are under the control of multiple hormones, such as estrogen, progesterone, prolactin, etc. These hormones are coordinated by peripheral organs, i.e., ovary and adipose tissues, and central nervous system, i.e., hypothalamus. In mammals, the coordination is mainly exerted by hypothalamus-pituitary-gonad (HPG) axis [2, 3].

HPG axis is consisted of hypothalamus, pituitary and gonads (ovary in female, testis in male) (see Fig. 1.1). At the central level, gonadotropin-releasing hormone (GnRH)

is synthesized and released by a population of hypothalamic neuroendocrine neurons, GnRH neurons. GnRH travels down to the pituitary, which is located at the bottom of the brain to regulate the synthesis and release of two gonadotropins, follicle-stimulating hormone (FSH) and luteinizing hormone (LH). FSH and LH travel through the circulation system to regulate the follicle development and hormone production in the ovary. At the peripheral level, ovarian hormones, i.e. progesterone (P4) and estrogen (E2), etc., not only directly regulate the reproductive system, but also provide negative and/or positive feedback toward the central pituitary and hypothalamus (Fig. 1.1) [2]. Thus, the HPG axis tightly regulates the reproductive system as a single entity.

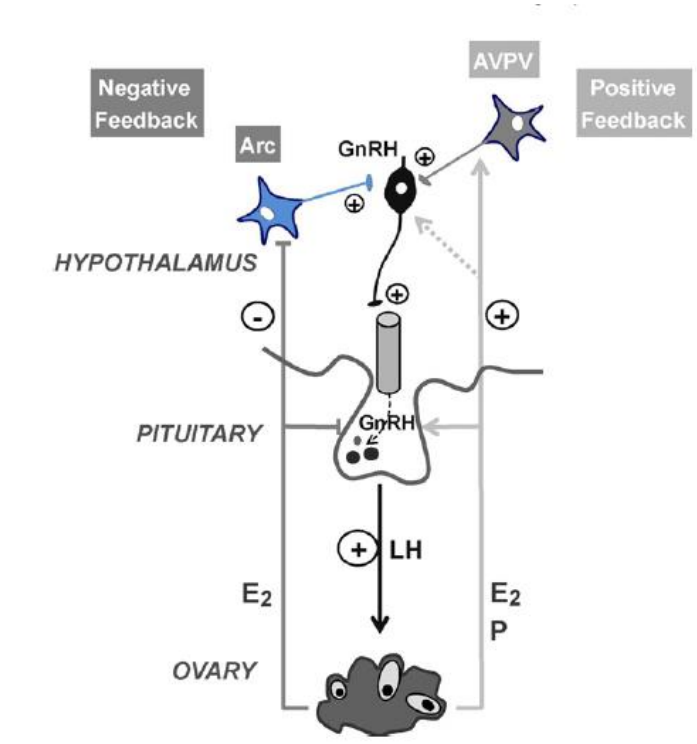

Figure 1.1. Female HPG axis with positive and negative feedback. E2, Estrogen; P, progesterone; GnRH, gonadotropin-releasing hormone; Arc: arcuate; AVPV: anteroventral periventricular. Cited from Fig. 3 in reference [4].

1.1.2 Female Puberty

Puberty is a transient period from the childhood to adulthood accompanied with dramatically physical and psychological changes to reach sexual maturation. For humans, the physical changes include sexual maturation, body composition changes, and rapid skeleton growth [5]. The psychological changes include the establishment of emotional independence, ethnical systems, the development of self-identity, self-motivation, and empathy, etc. [6].

In humans, female pubertal development can be assessed using several external makers, such as adrenarch, thelarche, and menarche. Adrenarche, the first appearance of pubic hair, is induced by the adrenal produced androgen, independent of the ovary [7], thus could not provide any developing information of HPG axis. Thelarche, the enlargement of mammary bud into Tanner B stage, mainly results from the onset of estrogenic actions [8]. Menarche, the occurrence of the first menstruation, happens at the late stage of puberty, followed by regular ovulation within a few years [9].

In rodents, female pubertal development can be determined by vaginal opening, first vaginal estrus, first vaginal plug, and first ovulation. Vaginal opening, an opening of vaginal cavity to the skin, is an external indicator which is induced by elevated estrogen levels and initiated by the apoptosis of vaginal epithelium [10]. Vaginal opening has been used as a standard endpoint for assessing pubertal development by U.S. Environmental Protection Agency (EPA)

(http://www.epa.gov/endo/pubs/pubertal_protocol_2007_v7.2c.pdf) and it has been used in many rodent studies to indicate pubertal onset [11-15]. Furthermore, a consistent sequential pattern following vaginal opening was found with other biomarkers for puberty, such as first estrus, first ovulation, etc. [15, 16]. Therefore, vaginal opening can be used as an easily obtainable noninvasive biomarker for pubertal onset in rodents [15].

Mammary gland development is used to monitor pubertal development in both humans and mice. Similar as human, mammary gland development in rodents is significantly accelerated during puberty and mainly caused by estrogen [17, 18]. Ovulation is initiated at the late stage of puberty by the maturation of HPG axis [16]. In rodents, the presence of corpus luteum in the ovary is one strong evidence that ovulation has occurred [19]. Therefore, the appearance of corpus luteum in the ovary could also be used as one indicator for pubertal development in mice. Mice have to be sacrificed to obtain these two pubertal markers.

Regardless of the various changes in the peripheral organs and largely unknown mechanisms of initiation of pubertal development, HPG axis plays an essential role in female pubertal development, indicated by the increased pulsatile release of GnRH from the hypothalamus [20]. In mice, GnRH neurons are generated in olfactory placode from embryonic day 9.5 (E9.5) to E12.5 [21], migrate across the nasal septum toward olfactory bulb around E12-16, and finally disperse in the forebrain [22]. GnRH neurons reach the destined loci in the hypothalamus before term in both primates and rodents [23, 24]. In contrast with a 15-fold increase of GnRH mRNA levels from E16 to postnatal day (PND) 60 in female mice [25], comparable mRNA levels of GnRH was found between juvenile

and adult monkeys [26]. This is consistent with the fact that the released GnRH, rather than the GnRH transcription levels in the brain, is important to initiate the puberty.

Low levels of GnRH release conjures a quiescent state of GnRH neurons before puberty in both primates and rodents [20]. The quiescent state might be caused by two specie-specific mechanisms in primates and rodents [27]. In primates, central inhibition plays an important role. It has been found GABAergic neurons inhibited GnRH neurons before puberty, and reduction of Gamma-aminobutyric acid (GABA) inhibition resulted in precocious puberty in monkeys [28, 29]. In rodents, rather than the existence of inhibition system, the absence of an excitatory system, such as glutamatergic inputs maintains the pre-pubertal period [30].

Mechanisms of pubertal initiation by removing the inhibition system in primates or establishing the excitatory system in rodents are not completely understood. Substantial progress has been made recently. On the molecular levels, the coordinated activity of gene sets organized into a functional network is required for the initiation of puberty, and epigenetic changes at these genes have been considered as one essential mechanism [31]. The interplay of various environmental cues and genetic differences is widely accepted as playing a critical role in pubertal development in individuals [32, 33].

1.1.3 Reproductive cycles

In sexually mature females, regular reproductive cycle is essential for fertility. In humans, the reproductive cycle is called menstrual cycle consisting of menstruation, proliferative and secretory phase lasting for about 28 days [34]. In rodents, the reproductive cycle is called estrous cycle consisting of proestrus, estrus, metestrus, and diestrus stage lasting for about 4 days [35]. Reproductive cycle is synchronized with

ovarian cycles. Within each reproductive cycle, the pituitary gonadotropins and ovarian hormones are tightly connected with the ovarian follicle development [36].

The cyclic patterns of gonadotropins and ovarian hormones in the circulating system have been well described in the estrous cycle of rodents. In each estrous cycle, estrogen starts to rise on late metestrus, and reaches a peak at noon of proestrus and falls before the peak of other hormones; the first rise of progesterone occurs from 0900h metestrus to 0900h diestrus, and the second rise of progesterone occurs with the rise of LH from noon of proestrus to midnight of proestrus, while the rise of FSH lasts from noon of proestrus to noon of estrus [37, 38].

Gonadotropins are the major regulators of the follicle development in the ovary. Follicle develops through primordial, primary, secondary, antral to pre-ovulatory stages [39]. About 300,000-400,000 (humans) primordial follicles are present in the ovary before puberty [40]. Most of them stay at primordial stage while only a small fraction of them is recruited into the growing pools continuously. It is generally accepted that it is hormone independent from primordial to pre-antral development. Afterwards, sustained high level of FSH plays a very important role as it selects only a cohort of antral follicles to continue growth [36]. At the pre-ovulatory stage, a rapid LH surge is essential for stimulating ovulation. After ovulation, the remaining follicles undergo luterinization and form corpora lutea. If embryo implantation does not happen after ovulation, the corpora lutea will degenerate after a few days. If embryo implantation happens, the corpora lutea would survive until lactation, and the wave of follicle development will be suppressed during pregnancy [41].

The production of ovarian hormones is in accordance with the wave of follicle development. Follicles at antral and later stages are the primary source of estrogen, and corpora lutea are the major source of progesterone [42]. Therefore, estrogen levels are increased with the development of antral follicles, and progesterone levels are increased with the formation of corpora lutea.

1.1.4 Female receptivity

Female receptivity refers to the ability to copulate with a male regardless of her motivational state [43]. For female mice, the sexual receptivity is physically manifested as lordosis, a stereotypic arching of back. This is a reflex behavior induced by male stimulation: pheromone (odor) and mounting (physical behavior), and the frequency of lordosis is widely used as an indicator of female sexual receptivity [44].

Unlike male, female mice are sexually receptive at late proestrus/early estrus stage. In this period the female mice could successfully copulate with a stud male [45]. Therefore, the presence of the estrus stage and the presence of a vaginal plug after mating can be used as indicators of female receptivity. The estrus stage is determined by the presence of dominant cornified epithelial cells in the vagina smear [46], and a vagina plug can be detected using a pair of blunt forceps the morning after mating.

To establish the female receptivity, adequate hormone stimulation on the central nervous systems is essential [47]. Naturally, sexual behaviors of female mice are generated by estrogen priming followed by progesterone stimulation. Estrogen priming, which refers to the rising levels of estrogen at proestrus stage, initiates the sexual behaviors. Progesterone surge coincident with the pre-ovulatory LH surge promotes the maximum sexual receptivity. Accordingly, exogenous hormonal priming, such as a high

dose of estradiol or long-lasting estradiol-benzonate (EB) or repeated doses of estradiol or estradiol plus progesterone, has been used to induce sexual receptivity in the spayed mice [48].

Estrogen acts through estrogen receptor α (ERα, also called ESR1)-mediated signaling pathway in the ventromedial nucleus of the hypothalamus (VMH) to stimulate female receptivity [49, 50]. Progesterone induced sexual behavior in estrogen primed females is mainly through progesterone receptor (PR)-mediated signaling pathway [51, 52], althrough ligand independent PR pathways and PR independent pathways have also been reported [51, 53].

The participation of GnRH in regulating female receptivity has also been reported. GnRH is essential to mediate leptin or progesterone induced lordosis and it may even directly act at the spinal cord [54-56]. Since estrogen initiates lordosis at the arcuate nucleus of hypothalamus (ARH) and it involves pro-opiomelanocortin neurons that project to the medial preoptic area and μ-opioid receptor neurons that project to VMH, it is highly possible that the GnRH neurons in the hypothalamus directly act on the neuron circuits of female receptivity (reviewed in [57]).

1.1.5 Early pregnancy events

Mating and ovulation are tightly correlated to each other and are required to for fertilization in vivo. After ovulation, oocytes with zona pellucida (ZP) and cumulus cells will be picked up by the oviduct in rodents (fallopian tubes in humans) [58]. In non-mated females, the dispersion of cumulus cells might finish 15h to 20h after ovulation, and in mated females, sperm protease could induce the dispersion of cumulus cells during fertilization [59, 60]. Oocytes and sperm meet and interact at the *ampulla* of oviduct. In

mice, ovulation might happen after midnight, around 2:00 to 3:30 am, and fertilization would happen within 2h after mating [61]. Once a sperm successfully fertilizes an oocyte, an intracellular calcium wave will be generated to induce multiple activation processes in the fertilized egg [62].

After fertilization, the embryo moves forward in the oviduct by the beat of the cilia, smooth muscle contraction, and tubal flow [63]. The communications between the mother and the embryo are evident as the transport rate of oviduct is reduced and the uterine artery morphology is changed when an embryo is moving through the oviduct [63].

The pre-implantation embryo development is comparable between humans and mice, involving mitotic cell division, compaction, and cavitation [64, 65]. At 8-cell stage, two distinct cell lineages, trophectoderm (TE) and inner cell mass (ICM), start to differentiate [66]. Subsequently, TE cells divide symmetrically to form the outer layer of the embryo, whereas ICM cells aggregate and attach to the basal surface of TE.

Mature TE cells become flattened and joined by tight junctions, and begin to pump fluid into first intracellular, later extracellular space, forming the blastocoelic cavity at 32-cell stage. Na^+, K^+, Ca^{2+}, Mg^{2+}, and Cl^- are concentrated in the blastocoelic cavity by ion pumpers in the TE cells to create the osmosis gradients for the entry of water. Simultaneously, the ICM cells facing the cavity differentiate into primitive endoderm (PE), and the remaining cells differentiate into epiblast (EPI). Eventually, PE develops into visceral endoderm (VE) and parietal endoderm (PaE); EPI develops into the embryo proper and extraembryonic mesoderm. The differentiation of ICM into PE and EPI is completed around embryo implantation [66, 67].

Embryo implantation is a process by which an embryo comes into intimate physical and physiological contact with the uterine endometrium, invades into the stroma and establishes the placenta [68]. If the day of vaginal plug detection is defined as gestation day (D) 0.5, an embryo will be in the uterus on D3.5, embryo implantation will be initiated ~D4.0 (midnight) [69]. Successful embryo implantation requires both a receptive uterus and a competent embryo. Uterine receptivity is established by appropriate ovarian hormone regulation and paracrine communication between uterine luminal epithelium and stroma [69, 70]. A competent embryo is at blastocyst stage when the blastocoel cavity is formed and the three cell lineages TE, PE EPI are differentiated. Embryo implantation could be divided into three stages: apposition, adhesion and invasion [71], and regulated by diverse molecular signaling, such as steroid hormone, lipid, adrenergic signaling, etc. [72, 73]. Therefore, embryo implantation can be used as one indicator of early pregnancy.

1.1.6 Hypothalamus and extra-hypothalamus regulation

Hypothalamus is the central regulator of HPG axis, correspondingly, central regulator of puberty and reproduction. Many environmental factors and internal signals are integrated at this level. The interactions between hypothalamus and other brain regions, such as accessory olfactory bulb, amygdala, hippocampus, and brain stem, etc., are essential to generate a favorable state for pubertal development and reproduction.

GnRH neurons are accounted for the direct regulation of HPG axis in the hypothalamus. The population of GnRH neurons extends caudally from the diagonal band of Broca, the optic chiasm, and into the medial basal hypothalamus [74]. In most mammals, the majority of GnRH neurons is found in the preoptic area and anterior hypothalamus; in higher primates, the caudal cells are predominant [74]. Most axons of

GnRH neurons are extended to a highly circumscribed region in the median eminence of hypothalamus to release GnRH into the pituitary portal system [74]. The total number of GnRH neurons in a mouse is ~800 [75].

The major GnRH neurons are spontaneously active and have variant firing patterns from bursting to continuous to silent, but the functional correlation of this heterogeneity is still unknown [76-78]. Due to the technical limitation, the secretion of GnRH from the hypothalamus is hard to be detected in the rodents. Studies in the ewe showed that strictly pulsatile GnRH release was interrupted by an explosion of massive GnRH release in an episodic pattern [79, 80], indicating that GnRH secretion include both pulse and surge phases in females.

As we mentioned above, ovarian hormones produce feedback on the GnRH neurons. Estrogen has been regarded as the key driver for the episodic release pattern of GnRH [80]. The presence of estrogen receptors (ERs), especially ERα, and progesterone receptor (PR) on GnRH neurons have been argued for decades [81-84].

However, it is widely accepted that GnRH neurons could be innervated by the set of neurons in anteroventral periventricular nucleus (AVPV), median preoptic nucleus (MEPO), and preoptic and anterior hypothalamic divisions of the periventricular nucleus (PVpo/a), through stimulatory signals, e.g., norepiepherine, kisspeptin, and glutamate, etc., as well as some inhibitory signals, e.g., β-endorphin, gonadotropin inhibiting hormone, and interleukin-1, etc. [85-87]. Besides mediating the effects of ovarian hormones, this set of neurons might also mediate the effects of many other environmental factors and internal signals to act as an extra-hypothalamus regulation. Three major neurotransmitters in the hypothalamus are briefly introduced below.

Gamma-aminobutyric acid (GABA) and glutamate are the first and second most dominant neurotransmitters in the hypothalamus, respectively [88, 89]. They interact in various frames to generate action potentials in GnRH neurons [90]. Both excitation and inhibition effects could be exerted upon GABA binding with the two GABA receptors, $GABA_A$ and $GABA_B$ receptors that are found in the GnRH neurons [91-93]. The fast synaptic currents, axo-dentrite and axo-somatic contacts, are frequent between GABAergic and GnRH neurons [92, 94-97]. On the contrary, glutamate is the primary fast excitatory neurotransmitter in the hypothalamus, and suppression of glutamate transmission might induce estrogen negative feedback [89, 98, 99]. Diverse ionotropic and metabotropic glutamate receptors are expressed in GnRH neurons, mainly at the dendritic spines of the GnRH neurons [100].

Kisspeptin has been studied intensively since the mutations of its receptor were first correlated with idiopathic hypogonadotropic hypogonadism (iHH) in humans in 2003. It is the most potent and efficacious neurotransmitter to excite GnRH neurons [101, 102]. Kisspeptin is a family of peptides encoded by the metastasis suppression gene *Kiss-1* via post-translational regulation and is the natural ligand for G protein-coupled receptor GPR54 [103]. Kisspeptin neurons are located at two discrete regions of hypothalamus, AVPV and arcuate nucleus (ARC), in humans, rhesus monkeys, and rodents, etc. [104-107]. The axons of AVPV kisspeptin neurons are in close association with the cell bodies of GnRH neurons, and are proposed to modulate the preovulatory GnRH surge; while the axons of ARC kisspeptin neurons make close apposition to GnRH axons in the median eminence to modulate the pulsatile GnRH release [108-111]. More than 90% GnRH

neurons express the kisspeptin receptor GPR54, nearly 100% adult GnRH neurons are responsive to kisspeptin [109, 112, 113].

1.2 Factors Influencing Female Puberty and Reproduction

1.2.1 Overview

The interplays among environmental factors, such as endocrine disruptors, and internal factors, such as body fat, can potentially influence female puberty and reproduction [3, 114, 115]. Here one environmental factor, genistein, and one internal factor, body fat, are discussed below.

1.2.2 Phytoestrogen genistein

Endocrine disruptors are chemicals that interfere with the endocrine system. They can potentially cause over or under production of endogenous hormones, or change the metabolism of the endogenous hormones, or mimic a natural hormone to over-respond or respond at inappropriate times to the stimulus, or interfere with hormone receptors, to disrupt the endocrine system.

Gensitein is a heterocyclic diphenol with three hydroxyl groups and its chemical name is 4',5,7-trihydroxy-isofavonethe or 5,7-dihydroxy-3-(4-hydroxyphenyl)-4H-1-benzopyran-4-one. Two benzene rings are linked through a heterocyclic pyran ring to form the isoflavone nucleus of genistein, a similar structure like 17β-estradiol (E2) [116]. The aromatic hydroxyl of genistein could form hydrogen bonds with the amino acids in ligand binding domain (LDB) of ERs to enhance its binding affinity [117, 118]. The relative binding affinity of genistein is lower than E2, but genistein induced gene transcription level is slightly higher than E2 [117, 118]. Genistein has ~30 folds higher affinity with ERβ compared to ERα [117], but genistein-induced ERα and ERβ transcriptional activities are

comparable, which is consistent with the fact that genistein could not induce the optimal agonistic conformation of ERβ [119, 120]. Genistein is considered as a full agonist for ERα and a partial agonist for ERβ [119, 120].

Genistein is a phytoestrogen abundant in soy [121]. High levels of genistein are found in traditional soy food, such as soy milk, tofu, miso, etc., as well as a variety of processed food, such as meatless burger, energy bar and soy yogurt, etc. [122]. The estimated daily intake of genistein in US adults is ~0.6 mg/day based on National Health and Nutrition Examination Survey 1999-2002 data [123], and ~6-19 mg/day in Asian people [124-126]. Since US FDA approved the health claims of soy diet on reducing coronary disease in 1999 [127], soy consumption in US has been steadily increasing [128].

As a natural estrogenic chemical, genistein is readily metabolized in the body. The estimated half-life ($t_{1/2}$) of total genistein for oral intake in human is 6-9hs, and 3-46hs in rodents (reviewed in [129]). Genistein is mainly presented as β-glucosides in the food. However, food processing methods like fermentation could increase aglycone levels in the soy products, like soy milk, temphe, miso, etc. (reviewed in [130]). Aglycoside genistein is rapidly absorbed through stomach and intestine [131, 132], while glycones need to be hydrolyzed by gut bacteria and intestinal β-glucosidase before absorption [133, 134]. Aglycoside genistein is a small lipophlic molecule, passively diffuses through the membrane. High permeability rate of genistein was observed in the human intestinal Caco-2 cells [135].

Upon absorption, most genistein is metabolized by enterocytes through phase I and phase II pathways [133, 136]. The rest aglycones would be oxidized and conjugated in the liver [137, 138]. Genistein glucuronide and sulfates are the major conjugates found

in the plasma and urine (reviewed in [129]). Genistein and its conjugates are distributed in multiple organs of the body, with the highest levels found in the gut and liver, and lower levels in the brain, mammary gland, reproductive organs vagina, uterus, ovary, prostate, and fat tissues [139-143]. After conjugation, genistein is hydrophilic and can be easily secreted through intestinal, biliary, and renal pathways. Among them, urine is the main pathway for glucuronide or sulfate conjugates [140, 144].

Genistein could affect human health as a weak estrogen [117, 145]. The beneficial effects of genistein include relieving menopausal symptom, protecting cardiovascular system, preventing breast cancer, etc. [146-149], while the adverse effects on reproduction and development have also been identified by many studies and recognized in the NTP-CERHR Expert Panel Report [150].

In male rodents, genistein alone or soy mixture (genistein, daidzein, and glycin) exposure could change the hormone levels, i.e., testosterone, estradiol, LH, etc. [151-156], modulate gene expression and cause histopathology in the reproductive organs locally [152, 154, 157-164], reduce the sperm number in rats [165, 166], and impair the mating behaviors [154].

Estrogen is an essential hormone for female. Genistein toxicity has also been observed in females. Acute exposure of genistein after ovariectomy had similar effects as E2 by reducing fat deposit in the body, increasing uterine and vaginal weights and changing their morphology, etc. [160, 167-176]. Defective fertility was observed upon long-term genistein exposure [177, 178]. One National Toxicology Program (NTP) multi-generation study using Sprague Dawley (SD) rats fed with 500ppm genistein diet showed

abnormal estrous cycle, advanced vagina opening, and mammary gland hyperplasia, but negligible effects on fertility [11].

A systematic study of neonatal genistein exposure on CD-1 mice showed multiple adverse consequences at different life stages including incompetent pre-implantation development of embryos [179, 180], embryo implantation failure [13], increased incidence of multiple oocyte follicles during prepuberty [181], extended diestrus and estrus stages after puberty [13], cystic ovary at 18 months old [182], and reduced branching and alveoli in mammary gland [183].

Genistein exposure can potentially affect hormonal levels. It was reported that genistien decreased estrogen level in prepubertal long evans rats and increased estrogen level in ovariectomized SD rats [184, 185]. A meta-analysis of multiple human trials indicates that genistein significantly increased FSH and LH levels in pre-menopause women [186]. Direct disruption of HPG axis have also been reported: genistein excited the central regulators GnRH neurons in the juvenile mice [187]; it stimulated gonadotropin-producing cells in the pituitary [188]; and it inhibited steroidogenesis in the follicles from immature rats and human granulosa-luteal cells [189, 190]. In addition, developmental exposure of genistein could modify neurons in multiple regions of the brain, especially the kisspeptin neurons [191-195], while adult genistein exposure could affect the hormone receptor expression in the brain [196] thus the functions of hypothalamus.

The connections between genistein and pubertal onset were found in both humans and rodents. A longitudinal study in UK including 1920 girls showed a positive correlation between soy formula intake during infancy and earlier menarche age [197]. Since menarche is an indicator of human puberty [198] and genistein is the major phytoestrogen

in the infant plasma after soy formulate consumption [199], it is most likely that genistein contributes to the puberty advancement upon infant soy formulate consumption. A case-control study of 150 6-12 years old precocious girls and 90 age-matched control girls in Korea revealed a significantly higher plasma level of genistein in the precocious group [200], implying that increased pre-pubertal exposure to genistein is associated with early puberty. Post-weaning genistein exposure through diet or s.c. injections advanced age of vaginal opening, an early indicator of pubertal onset, in CD-1 mice [201, 202]. Mutli-generational exposure of genistein also advanced vagina opening in F1 and F2 generation by 500ppm diet, F3 generation by 5ppm diet [11]. Both delayed and advanced vagina opening were observed upon neonatal exposure of genistein varying with different stains, doses, treatment, etc. [178, 181, 203].

1.2.3 Body Fat

Pubertal development and adult reproductive activities require a significant increase of energy expenditure [204]. Therefore, adequate body mass and enough nutrition levels are pre-required for the maturation and functions of the reproductive system. A positive correlation between body weight and pubertal timing was found in rats [205], and neonatal underfed female mice also showed delayed puberty [206]. The critical fat mass hypothesis for female menstrual cycle in human was initiated in 1970s, and a clear correlation between increased Body Mass Index and advanced puberty in girls was also reported recently [207, 208]. The influences of fat tissues on puberty and reproduction depend on the interactions of a number of peripheral metabolic signals including leptin, ghrelin, glucose, insulin-like growth factor-1, insulin, etc., on the central

nervous system [209-211]. Among them, leptin and ghrelin are two well-studied peripheral metabolic signals.

Leptin is a peptide hormone synthesized and secreted by white adipose tissue (WAT) [212]. The level of leptin is proportional to the amount of body fat and leptin mainly acts as a satiation signal for food intake [213, 214]. Compelling evidence supported that leptin played a permissive role on pubertal onset. An increase of leptin level was observed in girls and female mice before puberty [215, 216]. One leptin injection without affecting body weight could advance puberty in normal female mice [217]. The decreased leptin signals caused by genetic mutation or growth disorder were correlated with delayed puberty in humans [218, 219]. Genetic mutations of leptin in *ob/ob* mice or leptin receptor in *db/db* mice prevented pubertal development, and leptin treatment could rescue the pubertal events and fertility in the ob/ob mice [220, 221]. Furthermore, leptin levels are increased during pregnancy and leptin receptors are expressed in the placenta and uterus, suggesting its roles at the peripheral reproductive system during pregnancy and delivery [222, 223].

Ghrelin is a gastrointestinal peptide that acts on the brain and modulate multiple activities including stimulation of appetite, sleep and behavior, glucose metabolism, etc. [224]. In contrast with leptin, ghrelin is inversely correlated with body mass index and decreased in human obesity [225, 226]. It transmits a signal of energy deficiency and acts as the counter balance of leptin. A decreased trend of ghrelin was observed from fetal to early adulthood, while an increased ghrelin level was found in humans with growth disorder [218, 227]. Repeated injections of ghrelin delayed pubertal onset in male rats but

not in female rats, and significantly decreased the release of GnRH and gonadotropins in adult female rats [228, 229].

More interestingly, cross-talk between these metabolic signals and circadian rhythm has also been observed. One of the major tasks of the circadian rhythm is to optimize the metabolism to sustain life [230]. In this context, metabolism is regulated by circadian rhythm [231]. Circadian control on metabolism is indicated by the cyclic changes of most metabolic hormones including leptin, insulin and ghrelin, etc. (reviewed in [232]). On the other hand, food is regarded as the dominant zeitgeber for peripheral circadian rhythm [233], and hypo- or hypercaloric diet could alter the master clock Suprachiasmatic nucleus (SCN) [234]. Leptin could indirectly alter SCN through medial hypothalamus [235]. Ghrelin receptor is expressed in the SCN [236], and knockout of this gene could alter the circadian rhythm [237]. In this case, the metabolic signals might also mediate some circadian rhythmic effects on female puberty and reproduction.

1.3 Olfaction and *Olfactomedin1* on female puberty and reproduction

1.3.1 Overview

Reproduction is critical for species survival and also a high energy-demanding activity. Suppression of reproduction without presence of male olfactory signals to save the energy, and stimulation of reproduction with presence of male olfactory signals to increase the pregnancy opportunity, is an optimal strategy. Correspondently, olfaction is essential for female puberty and reproduction, especially in rodents. Genetic mutations that disrupt the olfaction might also impair female puberty and reproduction. A global *Olfactomedin1* knockout mouse model was used to study the mechanism of a genetic factor on female puberty and reproduction.

1.3.2 Olfaction on puberty and reproduction

The mammalian olfaction system contains a diverse array of subsystems. The two major subsystems are Main Olfactory Systems (MOS) and Accessory Olfactory Systems (AOS) [238]. The main olfactory system consists of main olfactory epithelium that houses olfactory sensory neurons (OSNs), main olfactory bulb (MOB) that receives axons of OSNs and project to the central olfactory systems, and central olfactory systems including piriform cortex, anterior cortical amygdala, and entorhinal cortex, etc. The accessory olfactory system consists of vomeronasal organ (VNO) that houses vomeronasal sensory neurons (VSN), and accessory olfactory bulb (AOB) that receives axons of VSNs and projects to the central olfactory systems, and central olfactory systems including bed nucleus of stria terminalis, posteromedial cortical amygdala, and medial amygdala, etc. [238, 239]. Both MOS and AOS directly project to cortical and medial amygdala [240-242], where neurons could project to the preoptic area (POA) of hypothalamus [243]. Meanwhile, direct connections between olfactory bulb and GnRH neurons are also observed [244]. Therefore, the olfaction system might directly or indirectly act on the GnRH neurons to modulate the reproduction through HPG axis.

A large variety of chemosignals with distinct chemical structures and functions could be detected by the olfaction system and regarded as olfactory signals. There are two distinct groups: pheromones (chemical signals within the same species), and allelochemicals (chemical signals between different species) [245]. In mouse, pheromones are found in the urine, feces, tears, saliva and skin secretion and could convey the critical reproduction related information, i.e., sex, health state, sexual

receptivity, etc. They not only change the short term responses like mating behaviors, but also modulate the long term state of the reproductive system [246].

Olfaction is critical for female sexual behaviors. Destruction of the olfaction system reduces the sexual receptivity of the female mice [247, 248]. Crowded female mice unexposed to male odor for extended period have longer and irregular cycles [249], and male urine or the analogs stimulate them to enter the estrus stage and resume estrous cycle [250-252]. These effects could partially be explained by the facts that axons from accessory olfactory neurons projected to the mating neural circuits and might generate a permissive role (reviewed in [57]). Similar effects, also caller “ram effects”, are observed in sheep in which male odor stimulates females to enter into estrous cycle from anoestrus state [253].

Olfaction is also correlated with ovulation. The incidence of ovulation after copulation was lower after olfactory bulb removal in rats [254]. Lesions of the medial amygdala, an essential central olfactory system, impairs while electrical stimulation at the same region inhibits or activates ovulation in the rats [255-258]. Stimulation of olfactory bulb could inhibit or facilitate LH release in rats depending on distinct stimulated regions and animal models [259]. Besides, female puberty in rodents could also be accelerated by male odor stimulation [260].

1.3.3 *Olfactomedin 1*

Olfactomedin1 (Olfm1) is a protein encoding gene, first identified as a glycoprotein in the olfactory neuroepithelium of frog [261]. A further study found a distant relative of this protein in *C. elegans*, and 6 universally conserved motifs among invertebrates and vertebrates [262]. OLFM1 is also called neolin in chicken and *Xenopus*, pancortin in mice,

olfactomedin related protein in rats, and hOlfA in humans [263]. The highly conserve and widely distribution of OLFM1 imply its universal importance.

However, the function of OLFM1 is still largely unknown. It has been reported that *Olfm1* might promote the cell invasion during epithelial-mesenchymal transition of heart development in chickens [264], suppress the JAr spheroid (mimic embryo) attachment onto Ishikawa cells (mimic uterine endometrium) [265], affect neuronal generation and differentiation in *xenopus* [266, 267], inhibit axon elongation of optic nerve in zebrafish [268, 269], mediate ischemia induced neuron death in mouse cortex [270], and modulate cortical cell migration in mouse [271]. Furthermore, changed expression of *Olfm1* was related with the competence of follicle development in bovine ovary [272], as well as puromycin aminonucleoside nephrosis in rats [273].

In mice, there are four structurally different mRNA transcripts, *Pancortin 1-4* (see Fig. 1.2). They shared a central B part, with two variants A1 or A2 at N terminal transcribed by different promoters, and C1 or C2 at C terminal generated from alternative splicing [274]. There is another set of terminology used to describe these segments, in which the central part was named as M, two variants at N terminal was B and A, and at C terminal Y and Z. Therefore, *Pancortin 1* is composed of A1BC1 also named as *BMZ*, *Pancortin 2* is composed of A1BC2 also named as *BMY*, *Pancortin 3* is composed of A2BC1 also named as *AMZ*, *Pancortin 4* is composed of A2BC2 also named as *AMY*.

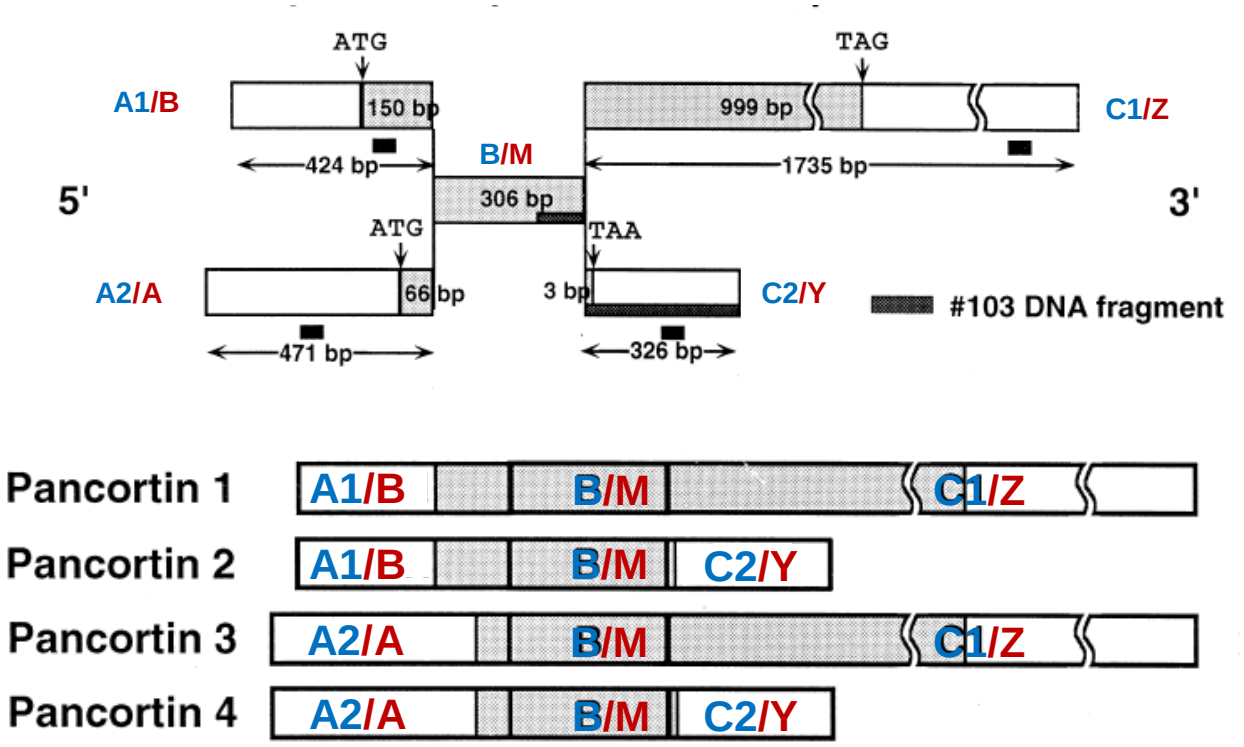

Figure 1.2. Different transcription patterns of *Olfactomedine 1* (*Olfm1*) in mouse. Modified from references [274, 275].

The 3D structure of OLFM1 is still undefined. Sequence analysis and biochemical studies indicated dimer and oligomer formation through disulfide bodes of cysteine residues in the central part, multiple glycosylated sites, and symmetric carbohydrate attachment site [276]. Secreted OLFM1 was identified in extra cellular matrix to bind with proteins, including receptors and co-regulators to modify multiple signaling pathways [264, 268, 269, 271, 277]. In the cytoplasma, OLFM1 was observed in endoplasmic reticulum (ER) of mouse brain [275], interacting with mitochondria proteins in rodent brain [270], and Golgi apparatus of glomerulus podocytes in rat kidney [278]. *Pancortin 1 and 3* have a SDEL sequence at the terminal, which is similar to the KDEL sequence that determines protein retention in ER [279].

Olfm1 is highly expressed in the main olfactory neuronal epithelium, main and accessory olfactory bulb, developing and adult brain in mice [275, 276, 280, 281]. Deletion of part of the middle part B/M and C2/Y of *Olfm1* in *Olfm1*$^{-/-}$mice led to reduced cerebral infarct size in males, reduced body weight, reduced activity and anxiety, and defective olfaction without affecting coordination locomotive activity or life span in both females and males [270, 282]. Although the fertility problem was mentioned in the original paper of the *Olfm1*$^{-/-}$mice, no systematic studies had been done.

1.4 Major hypothesis and specific aim

The working hypothesis of this dissertation is that environmental factors, such as genistein, and genetic factors, such as *Bscl2*, *Olfm1*, can affect female puberty and reproduction (see Fig. 1.3). This hypothesis has been tested in different mouse models. The specific aims include:

1) Determine the effects of postweaning dietary genistein exposure on female pubertal development and adult reproduction in C57Bl/6 mice;

2) Determine the interactive effects of genistein and body fat on female pubertal development using lipodystropic *Bscl2*$^{-/-}$female mice;

3) Determine the functions and mechanism of OLFM1 in female pubertal development and reproduction using *Olfm1*$^{-/-}$ mouse model.

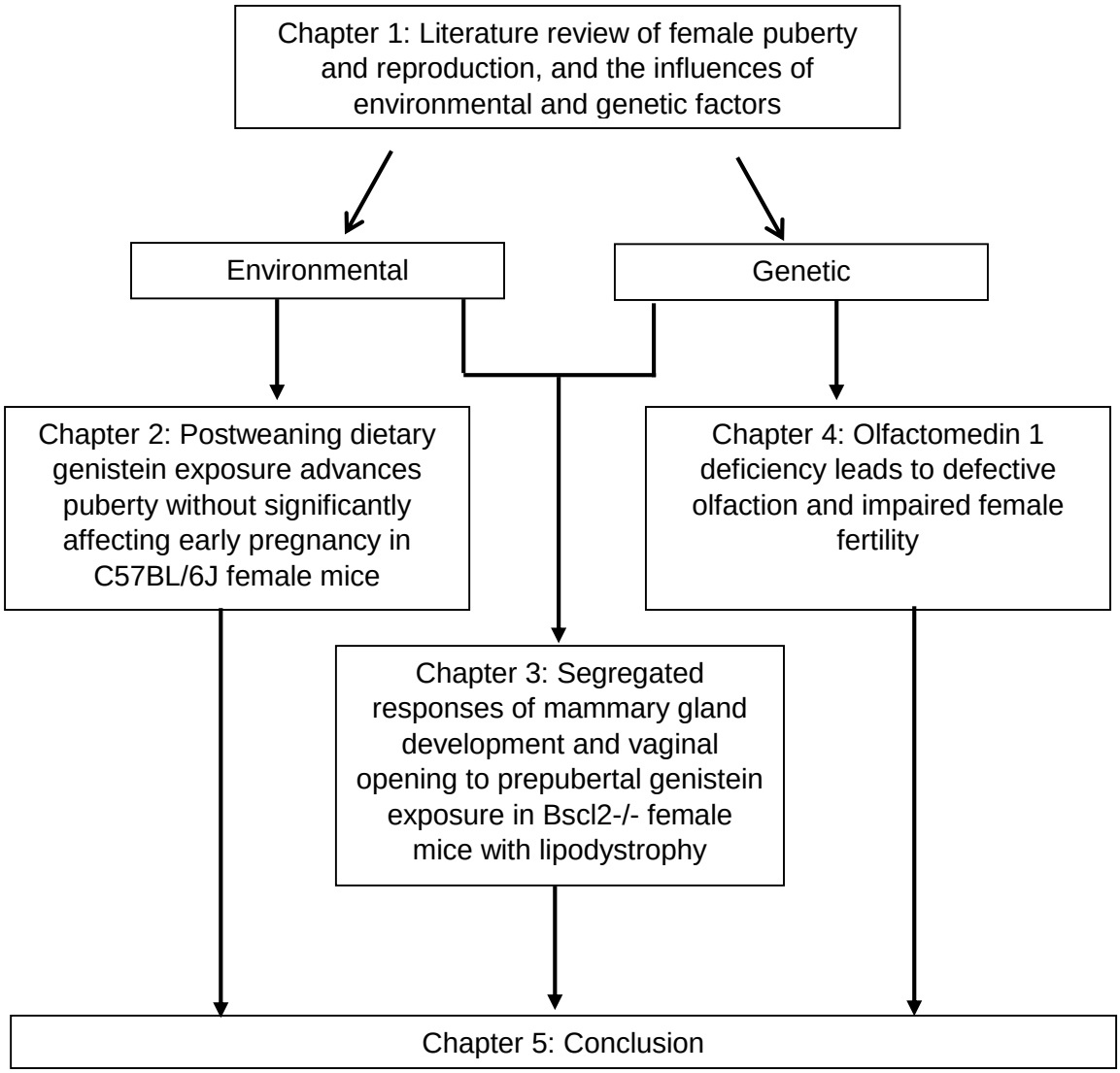

Figure 1.3. Outline of the dissertation

CHAPTER 2

POSTWEANING DIETARY GENISTEIN EXPOSURE ADVANCES PUBERTY WIHTOUT SIGNIFICANTLY AFFECTINNG EARLY PREGNANCY IN C57BL/6J FEMALE MICE

Rong Li, Ahmed E. El Zowalaty, Weiqin Chen, Elizabeth A. Dudley, and Xiaoqin Ye.

2014, *Reproductive Toxicology*; 54:76-83. Reprinted here with permission of publisher.

2.1 Abstract

An epidemiological study indicates higher plasma level of genistein in girls with earlier puberty. This study tests the hypothesis in C57BL/6J mice that postweaning (peripubertal) dietary genistein exposure could result in earlier puberty in females assessed by vaginal opening, estrous cyclicity, corpus luteum and mammary gland development. Newly weaned female mice were fed with 0, 5, 100, or 500 ppm genistein diets. Decreased age at vaginal opening, increased length on estrus stage, and accelerated mammary gland development were detected in 100 and 500 ppm genistein-treated groups. Increased presence of corpus luteum was found in 5 ppm genistein-treated group at 6 weeks old only. Increased expression of epithelial-specific genes but not that of ERα and ERβ was detected in 500 ppm genistein-treated mammary glands at 5 weeks old. No significant adverse effect on embryo implantation was observed. These data demonstrate causal effect of dietary genistein on earlier puberty in female mice.

2.2 Introduction

Genistein is a phytoestrogen abundant in soy [121]. High levels of genistein are found in traditional soy food, such as soy milk, tofu, miso, etc., as well as a variety of processed food, such as meatless burger, energy bar and soy yogurt, etc. [122]. The estimated daily intake of genistein in US adults is ~0.6 mg/day based on National Health and Nutrition Examination Survey 1999-2002 data [123], and ~6-19 mg/day in Asian people [124-126]. Since US FDA approved the health claims of soy diet on reducing coronary disease in 1999 [127], soy consumption in US has been steadily increasing [128].

Genistein could have different effects. The beneficial effects of genistein include relieving menopausal symptom, protecting cardiovascular system, preventing breast

cancer, etc. [146-148, 283]. Since genistein is a weak estrogen [117, 145], its potential endocrine disruptive effects have also been identified in many studies and recognized in the NTP-CERHR Expert Panel Report [150]. For example, genistein has been widely regarded as a contributing agent for a trend of earlier puberty in US and European girls [284-288]. Puberty is the physical development process of an immature body to an adult body capable of reproducing under the regulation of sexual hormones, such as estrogen [289]. A longitudinal study in UK including 1920 girls shows a positive correlation between soy formula intake during infancy and earlier menarche age [197]. Since menarche is an indicator of puberty [198] and genistein is the major phytoestrogen in the infant plasma after soy formulate consumption [199], it is most likely that genistein contributes to the puberty advancement upon infant soy formulate consumption. A case-control study of 150 6-12 years old precocious girls and 90 age-matched control girls in Korea reveals a significantly higher plasma level of genistein in the precocious group [200], implying that increased prepubertal exposure to genistein is associated with early puberty.

The majority of the human population is mainly exposed to genistein from food after infancy when non-milk food is added to the diet, equivalent to postweaning dietary exposure in rodents. We hypothesized that postweaning exposure to genistein in the diet could lead to earlier puberty in females. This hypothesis was tested in C57BL/6J female mice using human relevant exposure levels (5 ppm, 100 ppm, and 500 ppm genistein diets). It was reported that rats fed with 5 ppm and 100 ppm genistein diets could produce plasma levels of genistein similar to that in Western and Asian people, respectively [142], while 500 ppm genistein diet could be found in soy products, e.g., soy bacon [122]. These doses were also used in the multi-generational studies of genistein by the National

Toxicology Programs (NTP) [11]. Vaginal opening, estrous cyclicity, ovulation initiation, and mammary gland development were monitored as indicators for puberty development in this study.

2.3 Materials and Methods

2.3.1 Animals

C57BL/6J is a sensitive mouse strain to endocrine disruptors [290-292] and was selected as an in vivo model in this study. C57BL/6J mice were obtained from Jackson Laboratory (Bar Harbor, ME, USA) and maintained on phytoestrogen-free AIN-93G diet (Bio-Serv, Frenchtown, NJ) in Coverdell animal facility at the University of Georgia. The mice were housed in polypropylene cages with free access to food and water on a 12 h light/dark cycle (0600–1800) at 23±1 °C with 30–50% relative humidity. All methods used in this study were approved by the University of Georgia IACUC Committee (Institutional Animal Care and Use Committee) and conform to National Institutes of Health guidelines and public law.

2.3.2 Treatment

The genistein diets were prepared following the similar procedure as described previously [292]. Briefly, 0 g, 0.0025 g, 0.05 g, or 0.25 g genistein were dissolved in 150 ml 70% ethanol. Each solution was well mixed with 500 g AIN-93G diet in a glass bowl to attain 0 ppm (control), 5 ppm, 100 ppm, and 500 ppm genistein diets, respectively. Food pellets were hand squeezed, air dried at room temperature, and kept at 4°C in the dark. Fresh diets were prepared every two weeks. Breeding females were on phytoestrogen-free AIN-93G diet ad libitum throughout pregnancy and lactation. Newly weaned (postnatal day 21) female pups were randomly assigned into four groups and fed with 0

ppm, 5 ppm, 100 ppm, or 500 ppm genistein diet, respectively, until sacrificed for tissue collection / determination of pregnancy status. Food and water consumption were monitored weekly. The numbers of mice included in different experiments were indicated under each experiment. Newly weaning males were sacrificed without further study.

2.3.3 Vaginal opening and estrous cycle

Vaginal opening was evaluated daily from weaning until detection of vaginal opening (N=35 per group). Estrous cycle was monitored daily during two periods: from the day of vaginal opening for 10 days and from 5 to 8 weeks old (N=6 per group). Some overlaps of dates were seen during these two periods, especially for 0 and 5 ppm genistein groups. Vaginal smear was collected at 0800 h. The stages of estrous cycle were determined according to the composition of nucleated, cornified cells, and leukocytes as described [292, 293].

2.3.4 Tissue collection

All mice were dissected at estrus stage, which was determined by vaginal smear prior to dissection, by CO_2 inhalation and cervical dislocation. Only the mice on estrus stage at the selected time points (5, 6, 7, or 10 weeks old) ± 1 day were included. One side of the mammary glands was frozen, the other side of the mammary glands was used for whole mount staining or fixed for immunohistochemistry, and an ovary was fixed for histology.

2.3.5 Ovary histology

After fixation in formalin for 24 h, the ovaries were washed in 50%, 70%, 80%, 90%, and 95% ethanol for 30 min each, 100% ethanol for 30 min twice, and xylene for 5 min twice, then embedded in paraffin. Paraffin sections were cut at 5 μm. Serial sections of

the ovaries in all four groups at 6 weeks old (N=5-6 per group), in 0 and 500 ppm genistein-treated groups at 5 weeks old (N=3 per group) and 7 weeks old (N=6 per group), and in 5 ppm and 10 ppm genistein-treated groups at 7 weeks old (N=3 per group) were evaluated. Consecutive sections were separated by 50 μm.

2.3.6 Mammary gland whole mount and quantification of mammary gland development

The dissected whole inguinal (the 4th) mammary gland was flattened on a slide (Fisher scientific, Pittsburgh, PA) with weight for 24 h, then fixed in Carnoy' solution, stained by carmine alum, dehydrated through alcohol, cleared in xylene and mounted, as described [294]. Pictures were taken with an Olympus microscope BX41 with DP70 digital camera. The morphology of the mammary glands from 0 ppm, 5 ppm, 100 ppm, and 500 ppm genistein-treated groups (N=6-10 per group) at 5, 6, 7, or 10 weeks old, respectively, was analyzed by Image J (National Institutes of Health, Bethesda, MD, USA). The duct length of each mammary gland was indicated by the length of the longest duct. The occupied area of each mammary gland was approximated by a polygon area that covered all the ducts.

2.3.7 Realtime PCR

The whole inguinal mammary gland was dissected from 5 weeks old mice in 0 and 500 ppm genistein-treated groups (N=6-7 per group) and the lymph node was removed. Each lymph node-free mammary gland was homogenized in Trizol for total RNA isolation and cDNA synthesis using random primers (Invitrogen, Carlsbad, CA, USA) as previously described [295, 296]. Realtime PCR was performed in 384-well plates using Sybr-Green I intercalating dye on ABI 7900 (Applied Biosystems, Carlsbad, CA, USA). The mRNA expression levels of amphiregulin (*Areg*), cytokeratin 5 (*CK5*), *CK8*, *CK14*, *CK18*,

estrogen receptor α (*Esr1*) and *Esr2*, progesterone receptor (*PR*), and wingless-related MMTV Integration Site 4 (*Wnt4*) were determined using gene-specific primers from different exons (Integrated DNA Technology, San Diego, CA, USA) The mRNA expression levels were normalized by the expression of *Gapdh* (glyceraldehyde-3-phosphate dehydrogenase). *Hprt1* (hypoxanthine phosphoribosyltransferase 1) served as the second house-keeping gene (Suppl Table S1).

2.3.8 Immunohistochemistry

Paraffin sections (5 μm) of the inguinal mammary glands from 5 weeks old mice (N=3 per group) were used for immunohistochemistry. Sections from three mice each in 0 and 500 ppm genistein-treated groups were evaluated. After dewaxing, the slides were immunostained with rabbit anti-PR antibody (1:200, 6 μg/ml, Daco, Denmark), rabbit anti-ERα (ESR1) antibody (1:100, 5 μg/ml, Abcam), rabbit anti-phospho ERα (1:100, 10 μg/ml, Abcam), and anti-ERβ (ESR2) (1:50, 20 μg/ml, Abcam) as previously described [291].

2.3.9 Embryo implantation

Female mice from 0 and 500 ppm groups (N=8-27 per group) were mated with stud males starting at three time points: right after vaginal opening, at 5 weeks old, or at 7 weeks old, respectively. The morning of a detected copulation plug was defined as gestation day 0.5 (D0.5). All the mice were sacrificed on D4.5 to determine embryo implantation using blue dye reaction as described previously [297]. If no implantation sites were detected, the uterine horns and oviducts would be flushed with 1XPBS to determine the presence of oocyte or embryos in the reproductive tract. Pregnancy status was determined by the presence of embryos and/or implantation sites in the reproductive tract.

2.3.10 Statistical analysis

One way ANOVA followed by *Post-hoc* Tukey's test for data with equal variance homology, or followed by Dunnett's T3 tests for data with unequal variance homology, were used to compare the age of vaginal opening and quantitative data from whole mount mammary glands. Kruskal-Wallis equality-of-populations rank test was used to compare the % of time in estrus stage. Fisher's exact test was used to determine the distribution of mice with estrous cyclicity and mice with extended estrus stage. Student's t test with two tails and unequal variance was used to compare gene expression between 0 and 500 ppm genistein-treated groups. The significance level was set at $p<0.05$.

2.4 Results

2.4.1 Promoted vaginal opening

No significant differences among different groups in body weight or diet consumption were observed during the entire treatment duration (data not shown). Based on the food consumption, the estimated average doses in 0 ppm, 5 ppm, 100 ppm, or 500 ppm genistein groups were 0, 0.5, 10, or 50 mg/kg body weight per day, respectively.

Figure 2.1 shows the average ages at vaginal opening upon different doses of genistein treatment. Comparable ages were observed between 0 ppm control group and 5 ppm genistein-treated group ($p=0.078$). Compared to the control and 5 ppm genistein-treated groups, significant younger ages at vaginal opening were observed in both 100 ppm ($p<0.001$) and 500 ppm ($p<0.001$) genistein-treated groups. There was also significant difference between 100 and 500 genistein-treated groups ($p<0.001$). In the 500 ppm genistein-treated group, the average vaginal opening occurred within 3 days of treatment.

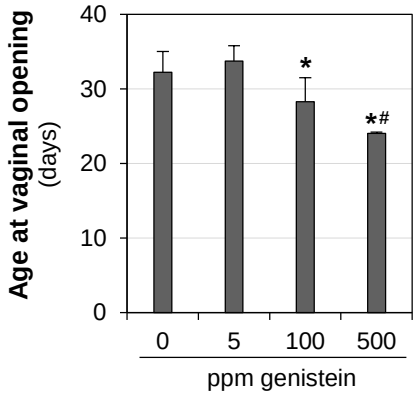

Figure 2.1. Effect of genistein on vaginal opening. N=35 per group; error bar, standard deviation; * $p<0.05$, compared to control (0 ppm); # $p<0.05$, compared to 100 ppm genistein-treated group.

2.4.2 Disrupted estrous cycle

Estrous cyclicity is established after puberty onset. There was a dose-dependent increase of time in estrus stage during the 10 days following vaginal opening. Compared to the control group, the average time (% of 10 days) in the estrus stage was marginally higher in 5 ppm ($p=0.055$) genistein-treated group, and significantly higher in 100 ppm ($p<0.001$) and 500 ppm ($p<0.001$) genistein-treated groups (Fig. 2.2A and S2.1). Significant differences were also observed in 100 ppm and 500 ppm genistein-treated groups compared to 5 ppm genistein-treated group ($p<0.05$). Most mice in the 0 or 5 ppm dose groups (5/6 each) demonstrated progression through their estrous cycles, however, only 50% (3/6) and 0% (0/6, $p=0.015$) of the animals in the 100 and 500 ppm exposure groups demonstrated normal estrous cycles, respectively (Figs. 2.2B, S2.1).

Since genistein treatment accelerated vaginal opening (Fig. 2.1), the ages during these 10 days following vaginal opening were different and those in the 500 ppm genistein-treated group were the youngest. To eliminate age as a contributing factor for

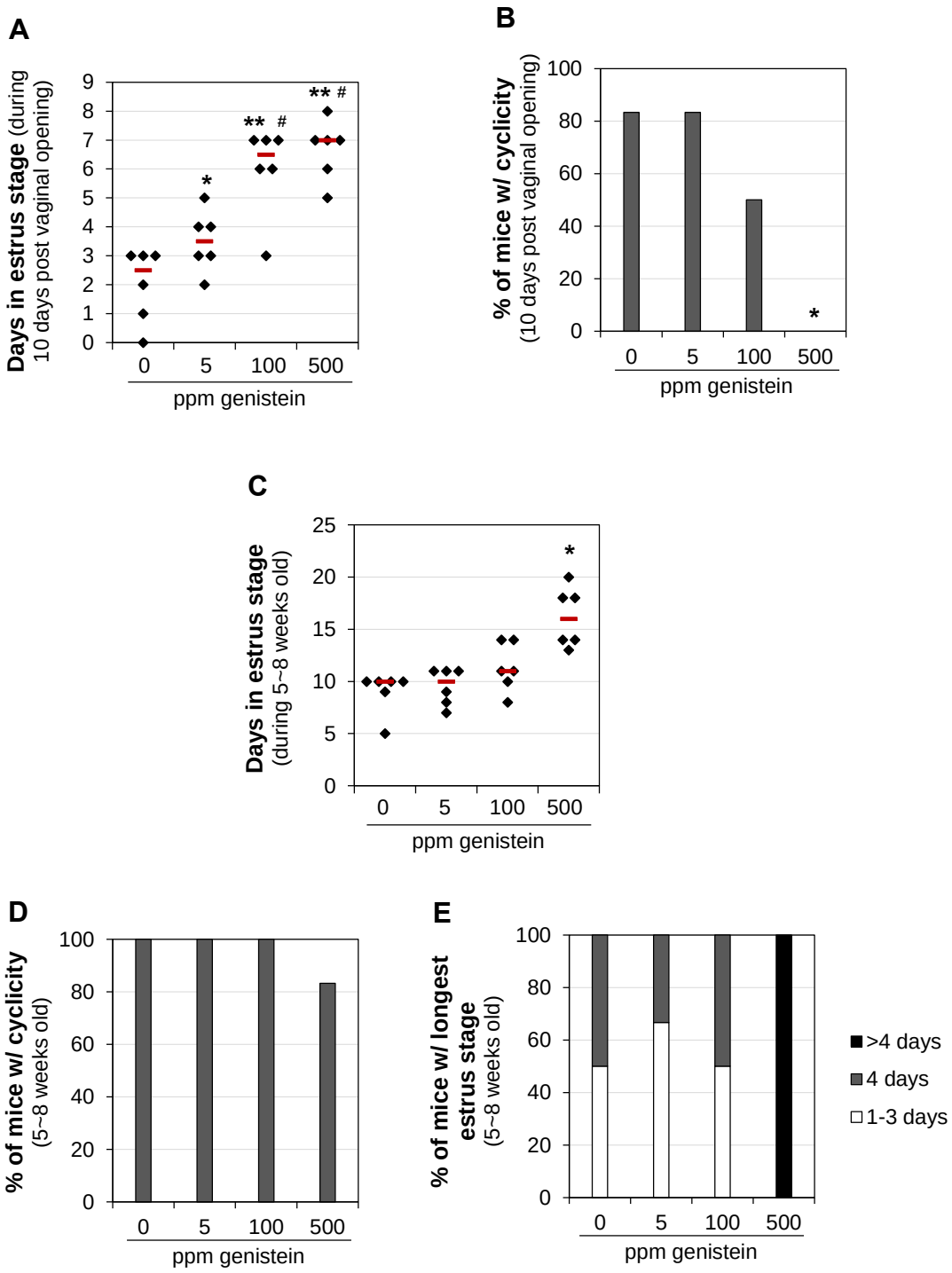

Figure 2.2. Effect of genistein on estrous cycle. A. Time (days) in estrus stage during the 10 days following vaginal opening. * p=0.055, ** p<0.001, compared to control (0 ppm); # p<0.05, compared to 5 ppm genistein-treated group. B. Percentage of mice with estrous

cyclicity during the 10 days following vaginal opening. C. Time (days) in estrus stage during 5~8 weeks old. D. Percentage of mice with estrous cyclicity during 5~8 weeks old. E. Distribution of mice with the longest estrus stage during 5~8 weeks old. A~E. N=6; error bar, standard deviation; * $p<0.05$, compared to 0, 5, and 100 ppm genistein-treated groups. A & C. black diamonds indicating data from individual mice; red lines indicating median in each group.

the disrupted estrous cyclicity in the genistein-treated groups (Figs. 2.2, S2.1), the same set of mice was examined for estrous cyclicity until 8 weeks old and the data during the 21 days from 5 to 8 weeks old in all four groups were analyzed. Prolonged estrus stage was still present in the 500 ppm genistein-treated group (Fig. 2.2C). Estrous cyclicity was observed in all mice except one in the 500 ppm genistein-treated group but those with estrous cyclicity had very irregular estrous cycle(s) during the observed period (Figs. 2.2D, S2.2). Extended length of estrus stage (>4 days) was only found in all the mice in the 500 ppm genistein-treated group (Fig. 2.2E), with two of them (33%) having persistent estrusstage for more than 10 days (Fig. S2.2). These data demonstrate that postweaning exposure to a high level of dietary genistein can disrupt estrous cyclicity.

2.4.3 Altered ovulation timing

Ovulation follows puberty onset and can be indicated by the presence of corpus luteum in the ovary [16, 298]. Primary, secondary, antral, and pre-ovulatory follicles were present in all the ovaries from different groups (Figs. 3.3A, 3.3B and data not shown). At 5 weeks old, none of the mice in 0 ppm (0/3) and 500 ppm (0/3) genistein-treated groups had corpus luteum (data not shown). At 6 weeks old, the percentages of mice with corpus

luteum were 0% (0/6), 100% (5/5, P=0.002), 50% (3/6, P=0.182), and 33% (2/6, P=0.455) in 0 ppm, 5 ppm, 100 ppm, and 500 ppm genistein-treated groups, respectively (Fig. 3C). At 7 weeks old, 67% (4/6) of the mice in the 0 ppm group and 100% of the mice in the 5 ppm (3/3), 100 ppm (3/3), and 500 ppm (6/6) genistein-treated groups had corpus luteum (P>0.05, data not shown).

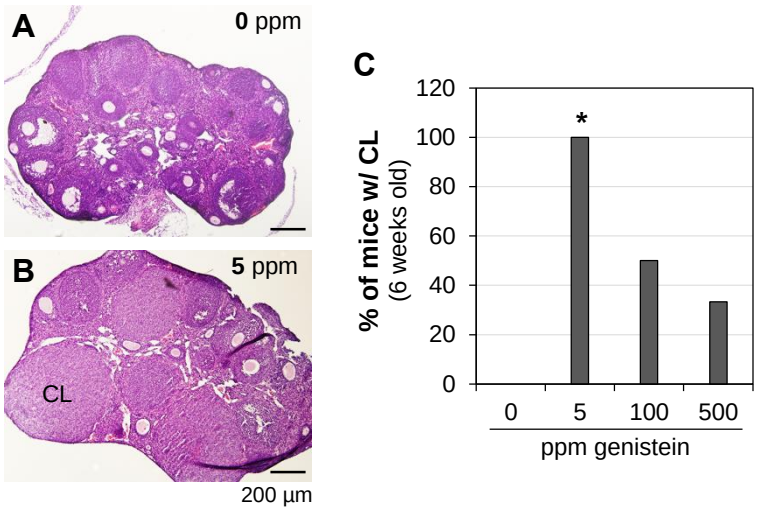

Figure 2.3. Effect of genistein on ovulation at 6 weeks old. A. A representative image of ovarian histology from control group. B. A representative image of ovarian histology from 5 ppm genistein-treated group. A & B. H & E stain; CL: corpus luteum; scale bar: 200 µm. C. Percentage of mice with corpus luteum. N=5-6; * p<0.05 compared to control (0 ppm).

2.4.4 Accelerated mammary gland development

During pubertal development, the mammary gland ducts grow towards the lymph node, therefore, mammary gland development can be evaluated based on the length of ducts and the area occupied by the ducts in whole mount mammary glands [299]. At 5 weeks old the frontier mammary gland ducts were halfway towards the lymph node in 0

and 5 ppm genistein-treated groups (Figs. 2.4A, 2.4B), but had reached or passed the lymph node in 100 ppm (Fig. 2.4C) and 500 ppm (Fig. 2.4D) genistein-treated groups, respectively. At 6 weeks old, the frontier mammary gland ducts had reached the lymph To confirm the accelerated development of mammary gland, the mRNA expression levels of several epithelial specific genes, CK5, CK8, CK14, and CK18, PR, Areg, and Wnt4,

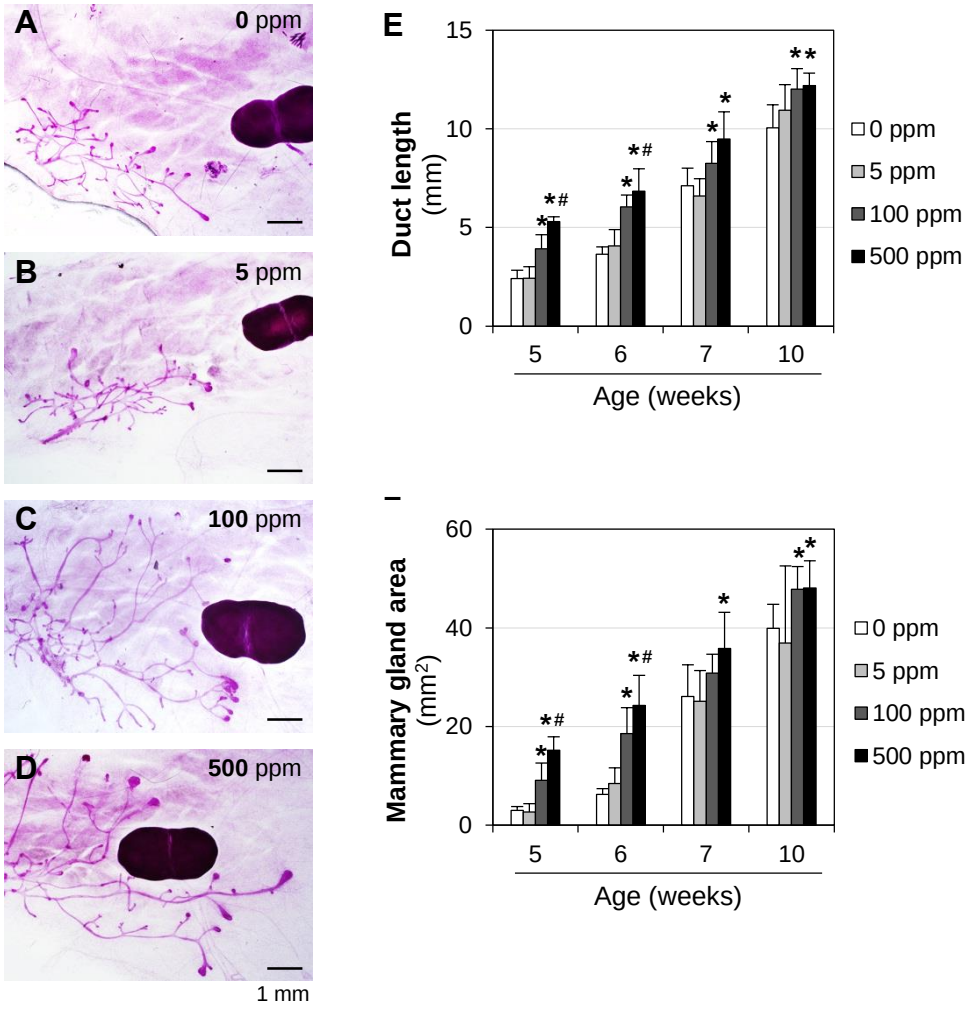

Figure 2.4. Effects of genistein on mammary gland development. A~D. Representative images of whole mount mammary glands in 0 ppm (A), 5 ppm (B), 100 ppm (C) and 500 ppm (D) genistein-treated groups at 5 weeks old. Pink lines, mammary gland ducts; LN:

lymph node. E. Length of the longest mammary gland duct. F. Area occupied by mammary gland ducts. N=6-10; error bar, standard deviation; * $p<0.05$, compared to control (0 ppm); # $p<0.05$, compared to 100 ppm genistein-treated group.

were examined in mammary glands from 5 weeks old mice treated with 0 or 500 ppm genistein diets. Significant upregulation of these genes was detected in the 500 ppm genistein-treated group (Fig. 2.5A). However, no significant difference was observed for Esr1 (ERα) and Esr2 (ERβ), as well as the house-keeping gene Hprt1 between these two groups (Fig. 2.5A). Immunohistochemistry results indicated that ERα mammary gland epithelial cells, and no obvious difference in signal intensity was observed between the two groups (Figs. 2.5B, 2.5C, 2.5F, 2.5G), which could explain why no difference was observed in Esr1 and Esr2 in the whole mammary gland (Fig. 2.5A). ERα and ERβ were detected in both nucleus and cytoplasm, while phosphor-ERα was mainly detected in the nucleus and no obvious difference was observed between these two groups (Figs. 2.5B~2.5G). PR was mainly detected in the nuclei of mammary gland epithelial cells and no obvious difference in signal intensity was observed between the two groups (Figs. 2.5H, 2.5I). The difference in mRNA levels for the epithelial specific genes most likely correlates with the difference in the abundance of mammary gland ducts thus epithelial cells (Figs. 2.4, 2.5A).

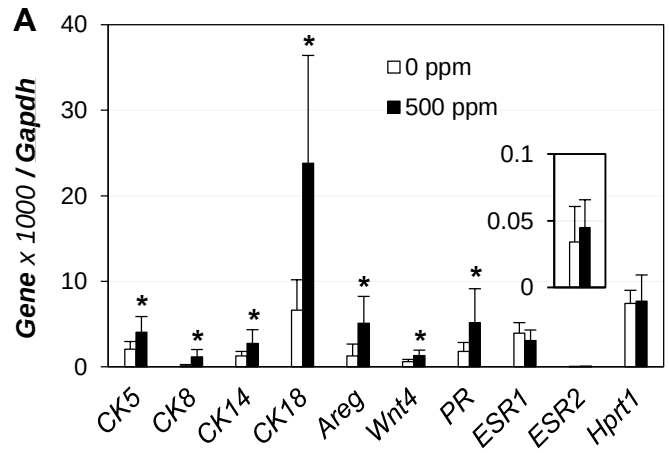
A
Gene x 1000 / Gapdh
40
30
20
10
0
0 ppm
500 ppm
0.1
0.05
0
*
CK5
CK8
CK14
CK18
Areg
Wnt4
PR
ESR1
ESR2
Hprt1

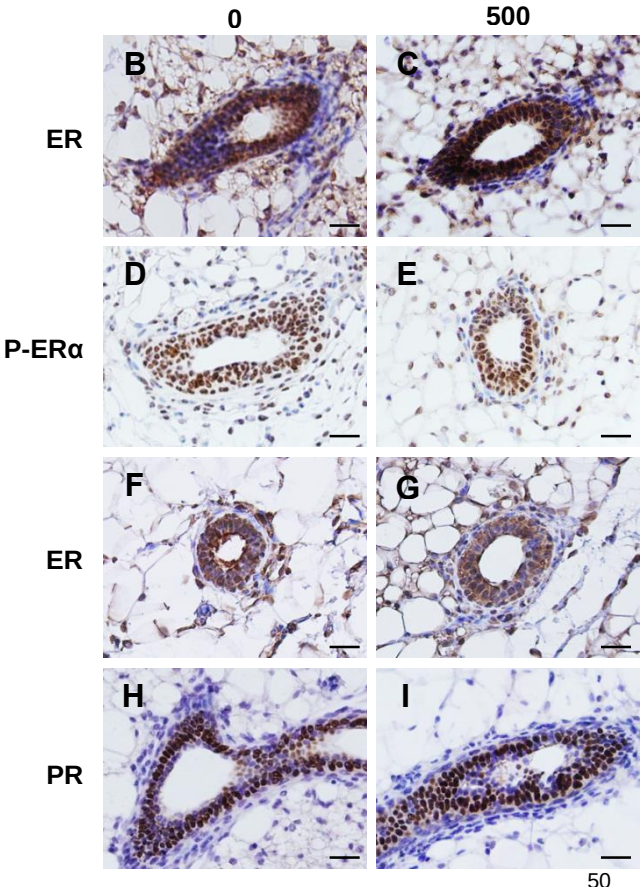
0
500
ER
P-ERα
ER
PR
B
C
D
E
F
G
H
I

50

Figure 2.5. Effects of 500 ppm genistein diet on gene expression in mammary gland at 5 weeks old. A. Real-time PCR. N=6-7; error bar, standard deviation; * $p<0.05$. B~I. Representative images of gene expression by immunohistochemistry in control (0 ppm) and 500 ppm genistein-treated groups. B. ERα, 0 ppm. C. ERα, 500 ppm. D. Phosphor-ERα, 0 ppm. E. Phosphor-ERα, 500 ppm. F. ERβ, 0 ppm. G. ERβ, 500 ppm. H. PR, 0 ppm. I. PR, 500 ppm. N=3; dark brown, immunostaining; purple-blue, counter staining with Harris hematoxylin; no specific immunostaining in negative controls (data not shown).

2.4.5 No significant adverse effects on early pregnancy

Figure 6A shows the average ages at the first copulation from each cohabitation period, right after vaginal opening, at 5 weeks old, and at 7 weeks old. Since 500 ppm genistein significantly advanced the age of vaginal opening, the average age of first copulation right after vaginal opening was significantly younger in the 500 ppm genistein-treated group. Although the average ages of first copulation after 5 weeks or 7 weeks showed no significant difference between 0 and 500 ppm genistein-treated groups, there were significant differences among the three examined times (Fig. 2.6A). First copulation right after vaginal opening yielded 0% implantation rate (Fig. 2.6B) in both groups, and 11% (1/9) and 0% (0/9) pregnancy rate in the control and 500 ppm genistein-treated groups, respectively. The first copulation after 5 weeks old yielded 40.7% (11/27) implantation rate and 55.6% (15/27) pregnancy rate in the control group, with 14.8% (4/27) of the mice having embryos but no implantation sites in the reproductive tract; as well as 48.0% (12/25) implantation rate and 64.0% (16/25) pregnancy rate in the 500 ppm genistein-treated group, with 16.0% (4/25) of the mice having embryos but no

implantation sites in the reproductive tract (Figs. 2.6B, 2.6C). The first copulation after 7 weeks old resulted in 100% (8/8) implantation rate and pregnancy rate in the control group; as well as 80.0% (8/10) implantation rate and 90.0% (9/10) pregnancy rate in the 500 ppm genistein-treated group, with 10.0% (1/10) of the mice having blastocysts but no implantation sites in the uterus (Figs. 2.2.6B, 6C). For those mice with implantation sites from mating after 5 weeks old or 7 weeks old, the ages at first copulation were not significantly different between the two groups at each time point (Fig. 2.6A and data not shown) and the average numbers of implantation sites were comparable between the two groups at each time point (Fig. 2.6D). These data indicate that 500 ppm genistein diet did not have a dramatic adverse effect on early pregnancy because comparable embryo implantation reflects no significant adverse effects on ovulation, fertilization, embryo transport and preimplantation embryo development, the early pregnancy events leading to successful embryo implantation [30]. However, we noticed that in the 500 ppm genistein-treated group at 5 weeks old time point, two of the 12 mice with implantation sites had 3 faint blue bands (data not shown), an indication of delayed embryo implantation [39], and two of the 13 mice without implantation sites had swollen appearance of uterus (data not shown), an indication of estrogenic effect [30]. Since no significant difference was observed compared to the control group and no faint blue bands or distended uteri were observed at 7 weeks old time point, these observations suggested that 500 ppm genistein diet might still have some minor effects on embryo implantation before the females are fully mature.

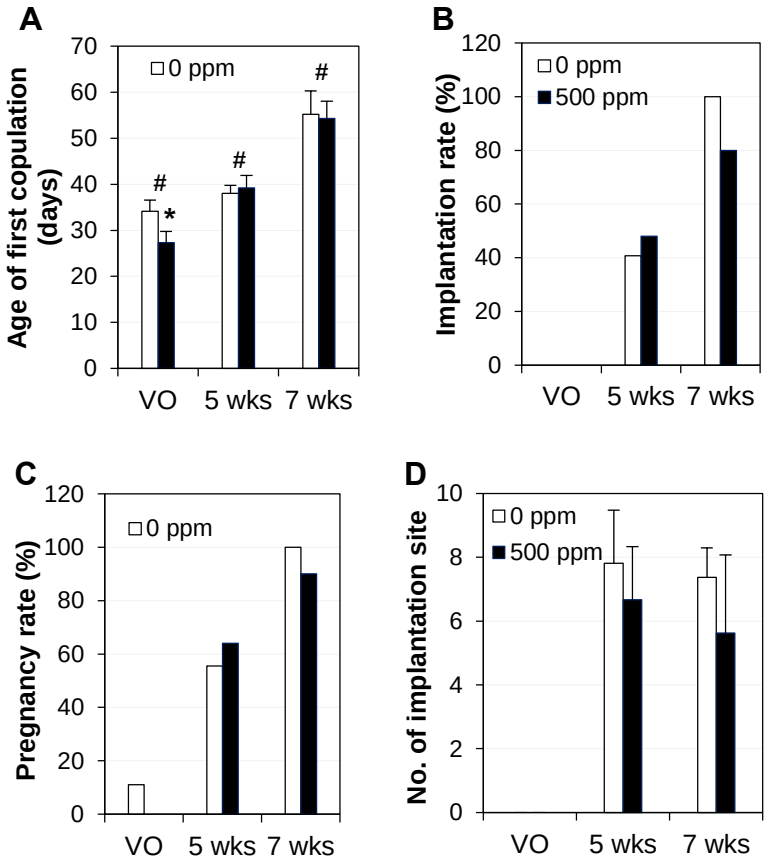

Figure 2.6. Effects of 500 ppm genistein on first copulation and early pregnancy. A. Age of first copulation upon mating at vaginal opening (VO), 5 weeks (wks) or 7 wks old. * $p<0.05$ compared to control at VO; # $p<0.05$ indicating differences among three mating periods. B. Implantation rate (% of mice with implantation sites on gestation day 4.5 / mice with a vaginal plug). C. Pregnancy rate (% of mice with implantation sites and/or embryos on gestation day 4.5 / mice with a vaginal plug). D. Number of implantation sites from mice with implantation sites. N=8-27; error bar, standard deviation.

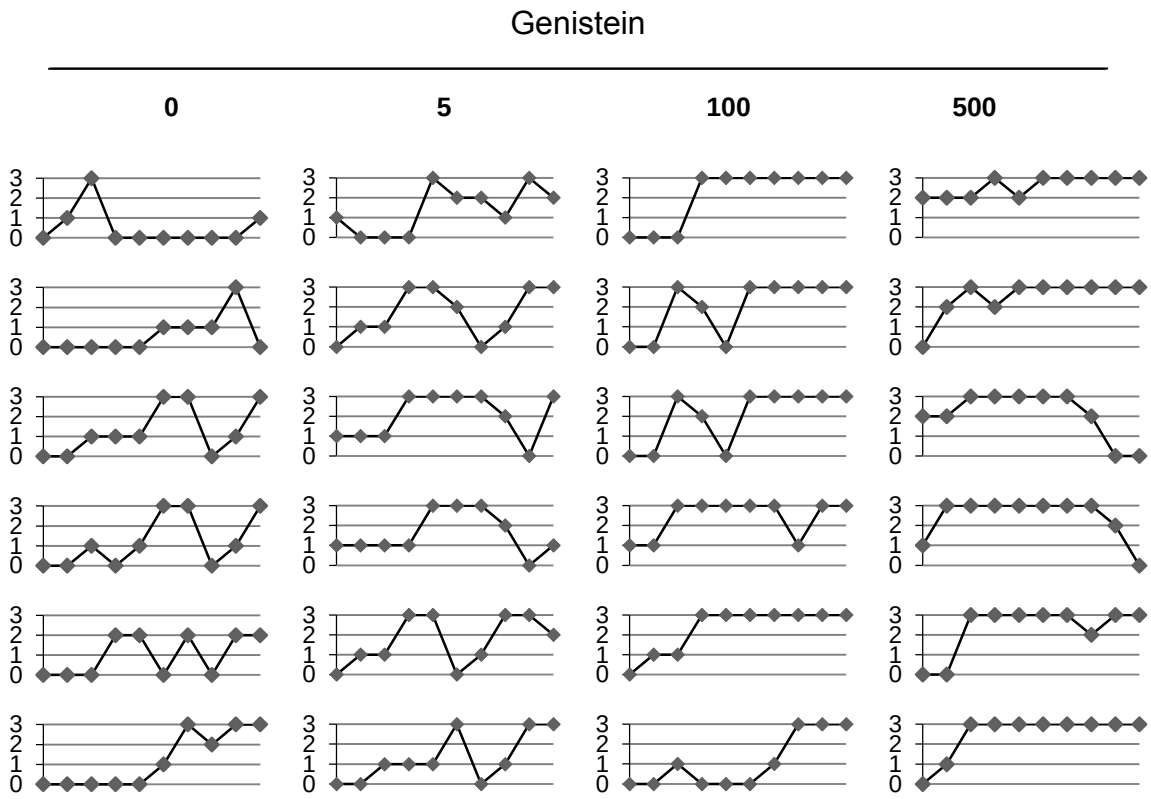

Figure S2.1. Effects of genistein on the estrous cycle of individual mice during the 10 days following vaginal opening. 0, diestrus; 1, proestrus; 2, metestrus; 3, estrus.

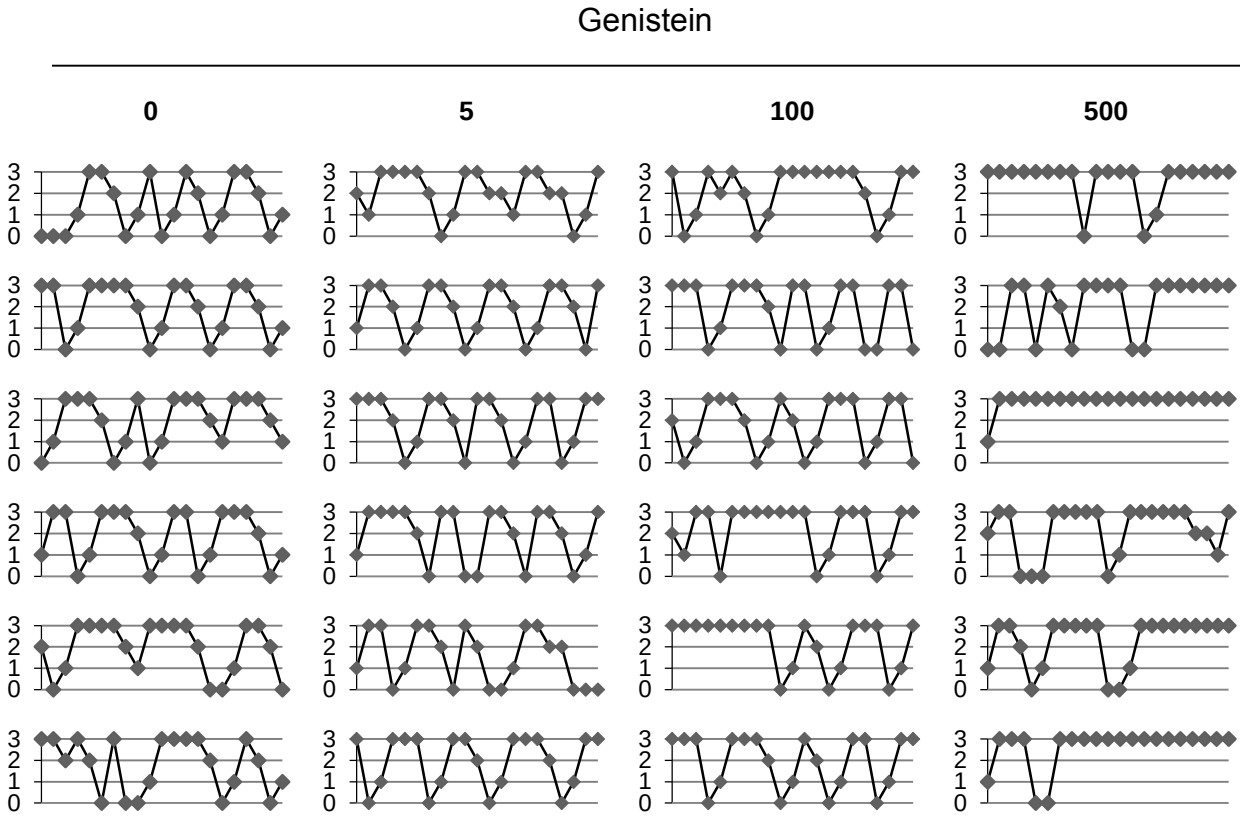

Figure S2.2. Effect of genistein on the estrous cycle of individual mice during 5~8 weeks old. 0, diestrus; 1, proestrus; 2, metestrus; 3, estrus.

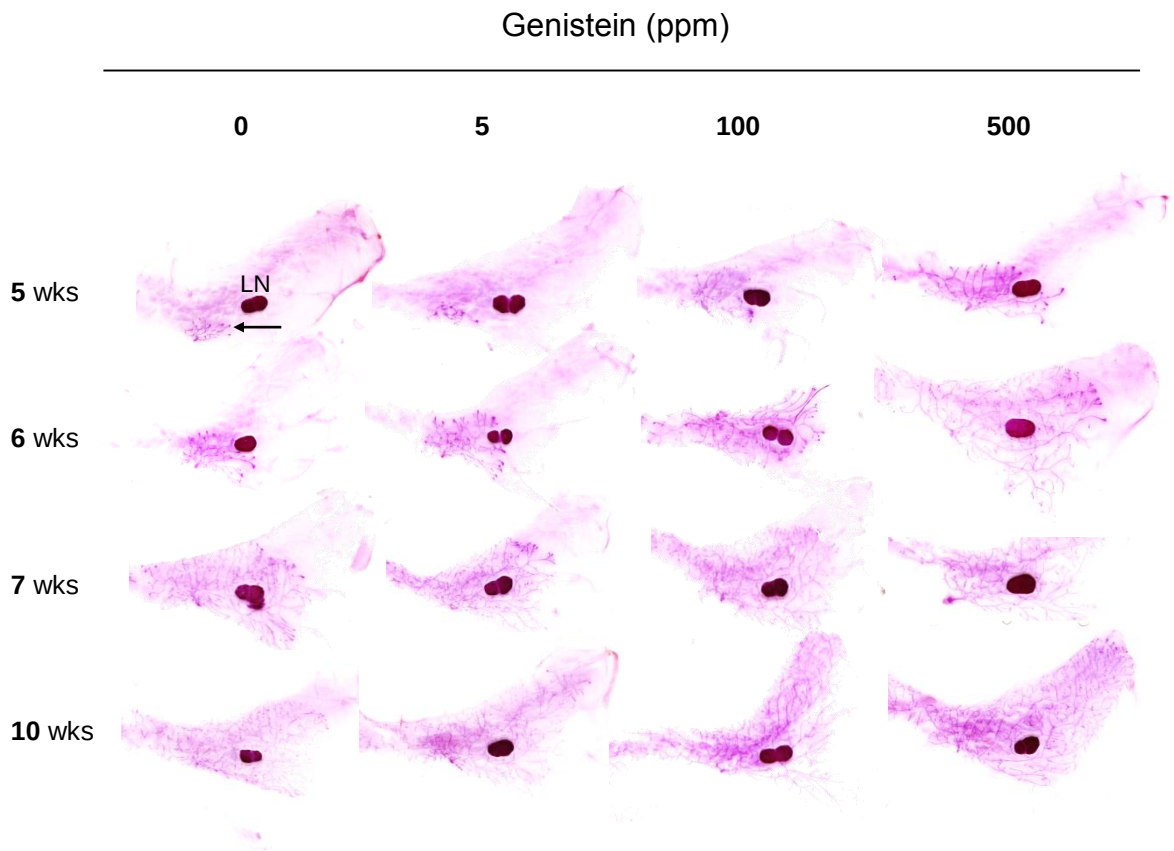

Figure S2.3. Representative images of whole mount mammary glands from each group at 5, 6, 7, and 10 weeks (wks) old upon postweaning genistein treatment. Arrow, mammary gland duct; LN, lymph node.

Table S2.1. Gene sequence for Real-time PCR

Gene	Primer sequence	PCR product size (bp)
CK5	F: GGATATCCTACAGTTCTGGCG R: GTGGTACGCTTGTTGATCTC	574
CK8	F: CCTACAAGATGTCCACCTCC R: CGCTTGTTGATCTCATCCTC	550
CK14	F: AAGACTACAGCCCCTACTTC R: CAGAAATCTCACTCTTGCCG	519
CK18	F: CTAGACAAGGTGAAGAGCCT R: GACAACTGTGGTACTCTCCT	567
Areg	F: GAACCAATGAGAACTCCGC R: CCTCTGAGTAGTCGTAGTCC	241
Wnt4	F: TTGAGGTGATGGACTCAGTG R: GCCTCGTTGTTGTGAAGATT	397
PR	F: ATCCCACAGGAGTTTGTCA R: GCAGCAATAACTTCAGACATCA	335
Esr1	F: GTGCCCTATACCTGGAGAA R: GCACAGTAGCGAGTCTCCTT	176
Esr2	F: GAAGCATTAAGGACATAATGA R: CATGGAGGCCTCGGTGAA	359
Gapdh	F: GCCGAGAATGGGAAGCTTGTCAT R: GTGGTTCACACCCATCACAAACAT	230
Hprt1	F: GCTGACCTGCTGGATTACAT R: CAATCAAGACATTCTTTCCAGT	172

2.5 Discussion

This study verifies our hypothesis that postweaning exposure to dietary genistein at human relevant levels can promote puberty in C57BL/6J female mice. All three doses examined have some effects on one or multiple parameters for puberty, including vaginal opening, estrous cyclicity, ovulation, and mammary gland development.

Dose-response is seen in all parameters but ovulation at 6 weeks old when significantly higher percentage of mice with corpus luteum, an indication of ovulation, is observed only in the lowest dose 5 ppm genistein-treated group (Fig. 2.3C). A reasonable explanation for this phenomenon is that genistein at all these three doses can promote ovulation. However, since ovulation is dependent on regular estrous cycle and estrous cyclicity is disrupted in the 100 and 500 ppm genistein-treated groups (Suppl Figs. S2.1, S2.2), the promotion effect of genistein on ovulation is counteracted by the disrupted estrous cyclicity in these two groups. None dose-response effect upon genistein treatment was also observed in other studies [13, 181]. For example, significantly increased number of oocytes from superovulation on postnatal day 22-23 was observed in CD-1 female mice subcutaneously treated with 0.5 mg/kg genistein but not 5 mg/kg or 50 mg/kg genistein during neonatal day 1-5 [181]; at 4 months old, same neonatal treatment regimen led to significantly increased number of corpora lutea in 5 mg/kg genistein group but significantly decreased number of corpora lutea in 50 mg/kg genistein group [13].

Although no corpus luteum was observed in the control group at 6 weeks old (Fig. 2.3C), 55.6% of mice were pregnant and 40.7% had implantation sites from the first copulation upon mating at 5 weeks old (Figs. 2.6B, 2.6C). These seemingly inconsistent

observations could most likely be explained by the different experiment settings. The later, but not the former, had cohabitation with males. Male odor could accelerate the puberty onset of female mice [300] and male seminal plasma has an ovulation-inducing factor to induce the ovulation in prepubertal mice [301]. Therefore, cohabitation could induce ovulation and subsequent pregnancy at an earlier age.

Sexually immature females seem to be more sensitive to genistein treatment from the following observations. First, the extended estrus stage was observed in 100 and 500 ppm groups right after vaginal opening (~28-38 days old), but only observed in 500 ppm group from 5 to 8 weeks old; second, the difference in the percentages of mice with corpus luteum was only seen at 6 weeks old but not 7 weeks old; third, although no significant differences in implantation rate and number of implantation sites were observed between control and 500 ppm genistein-treated groups from both 5 weeks old and 7 weeks old mating ages, some minor effects, such as distended uteri and faint implantation sites were observed in a small fraction of 500 ppm genistein-treated group at 5 weeks old mating age only.

However, the treatment timing and route, and possibly different strains of mice during different sexually immature periods could also make some differences. For example, neonatal day 1-5 subcutaneous injection with 50 mg/kg (a dose equivalent to 500 ppm genistein diet in this study) in CD-1 mice led to a general delayed vaginal opening although no statistical difference was found [13]. Such treatment also led to disrupted uterine receptivity for embryo implantation, indicated by lower implantation rate and smaller implantation sites from embryo transfer of untreated embryo to treated pseudopregnant females [179]. However, postnatal treatment of 500 ppm genistein diet

in this study significantly advanced vaginal opening in C57BL/6J mice (Fig. 1). The treatment in this study didn't have significantly adverse effect on all events, including uterine receptivity, that are required for successful embryo implantation (Figs. 6B, 6D), although we did observe 3 out of total 80 implantation sites in the 5 weeks mating group showing faint blue bands, indicating delayed implantation. It is possible that the days prior to puberty onset is a sensitive window to exogenous estrogenic endocrine disruptors for pubertal development and neonatal day 1-5 is likely a more sensitive window than postweaning period for uterine development leading to the establishment of uterine receptivity for embryo implantation.

The mechanism of genistein on pubertal development is largely unknown. Previous studies on endocrine disruptors showed that both central regulation hypothalamus-pituitary-gonads (HPG) axis and peripheral target tissues could be involved [302]. Genistein seems to regulate both HPG axis and peripheral target tissues. For example, genistein could excite GnRH neurons in the hypothalamus of juvenile mice [187]; it could inhibit steroidogenesis in the follicles from immature rats and human granulosa-luteal cells [189, 190]; it could induce vaginal cornification in ovariectomized rats [303]. Although our study could not specify the mechanism of regulation by genistein, vaginal opening, estrous cyclicity, mammary gland development are estrogen dependent events, and ovulation is highly orchestrated by HPG axis, supporting the notion that genistein regulates both HPG axis and peripheral target tissues.

At molecular level, estrogen signaling is expected to play an important role in genistein-promoted puberty. Although significantly increased mammary gland duct growth was observed in the 500 ppm genistein-treated group at 5 weeks old (Fig. 2.4),

comparable expression of ERα and ERβ was observed in the 5 weeks old mammary gland between 0 and 500 ppm genistein-treated groups (Fig. 2.5). First, since ERα and ERβ are highly expressed in both epithelial and stromal compartments in the mammary gland during puberty (Figs. 2.5B-2.5G) [304, 305], any local changes, e.g., at terminal end bud where duct epithelial proliferation leads mammary gland growth, could be obscured or missed in whole mammary gland real-time PCR (Fig. 2.5A) or immunohistochemistry (Figs. 2.5B-2.5G). Second, estrogen signaling might be regulated by ER coregulators without altered ER expression levels. Third, it is also possible that the ligand level is maintained at a higher level for longer time indicated by extended estrus stage (Suppl Figs. S2.1, S2.2) to increase the overall estrogen signaling. Fourth, it could act through ER downstream signaling, such as Areg (Fig. 2.5A), the only epidermal growth factor receptor ligand that is abundantly expressed in the mammary gland epithelial cells during puberty and an essential mediator for estrogen promoted mammary gland duct growth [306-308].

In summary, postweaning exposure to human relevant genistein diets accelerates pubertal development in female mice. The effect of genistein on puberty does not seem to have significant negative consequence on early pregnancy in young female mice.

Acknowledgments

The authors thank Dr. Suzanne Fenton at NIEHS for technical guidance and insightful suggestions on the manuscript, Department of Pathology at University of Georgia for the access to the imaging system, Dr. James N. Moore in the Department of Large Animal Medicine at University of Georgia for the access to the ABI 7900 Realtime PCR machine, and the Office of the Vice President for Research, Interdisciplinary Toxicology Program,

Graduate School, and Department of Physiology & Pharmacology at University of Georgia, and National Institutes of Health (NIH R15HD066301 and NIH R01HD065939 to X.Y.) for financial support.

CHAPTER 3

SEGREGATED RESPONSES OF MAMMARY GLAND DEVELOPMENT AND VAGINAL OPENING TO PREPUBERTALL GENISTEIN EXPOSURE IN *BSCL2*$^{-/-}$ FEMALE MICE WITH LIPODYSTROPHY

Rong Li, Ahmed E. El Zowalaty, Weiqin Chen, Elizabeth A. Dudley, and Xiaoqin Ye. 2014, *Reproductive Toxicology*; 54:76-83. Reprinted here with permission of publisher.

3.1 Abstract

Berardinelli-Seip congenital lipodystrophy 2-deficient (*Bscl2*$^{-/-}$) mice recapitulate human BSCL2 disease with lipodystrophy. *Bscl2*-encoded seipin is detected in adipocytes and epithelium of mammary gland. Postnatal mammary gland growth spurt and vaginal opening signify pubertal onset in female mice. *Bscl2*$^{-/-}$ females have longer and dilated mammary gland ducts at 5-week old and delayed vaginal opening. Prepubertal exposure to 500 ppm genistein diet increases mammary gland area and accelerates vaginal opening in both control and *Bscl2*$^{-/-}$ females. However, genistein treatment increases ductal length in control but not *Bscl2*$^{-/-}$ females. Neither prepubertal genistein treatment nor *Bscl2*-deficiency affects phospho-estrogen receptor α or progesterone receptor expression patterns in 5-week old mammary gland. Interestingly, *Bscl2*-deficiency specifically reduces estrogen receptor β expression in mammary gland ductal epithelium. In summary, *Bscl2*$^{-/-}$ females have accelerated postnatal mammary ductal development but delayed vaginal opening; they display segregated responses in mammary gland development and vaginal opening to prepubertal genistein treatment.

Key words: *Bscl2*/Seipin, lipodystrophy, mammary gland, vaginal opening, puberty, genistein.

3.2 Introduction

Mammary gland development and vaginal opening are estrogen-dependent processes and markers for pubertal onset in mice [17, 292, 309-311]. Mammary gland development is also an indicator of pubertal onset in most girls [5]. Pubertal mammary gland growth is characterized by branching morphogenesis to form a ductal tree filling the fat pad [312-314]. Estrogen receptor alpha (ERα)-deficiency leads to failed mammary

gland development beyond prepubertal stage [314]; ERβ$^{-/-}$ nulliparous mammary glands appear to have normal ductal growth but decreased side branching [315-317]. Estrogenic endocrine disruptors can affect both pubertal mammary gland development [183, 309] and vaginal opening, which is used as an external biomarker for pubertal onset in rodents [15, 292, 309, 318, 319].

Epidemiological studies have suggested that obesity may be causally related to earlier puberty in girls (reviewed in [320]). One study involving 135,223 girls (born between 1930 and 1969) indicates that heavier girls at age seven had earlier puberty; it also suggests that obesity epidemic is not solely responsible for the trend of younger age at puberty and that endocrine disruptors could contribute to this trend [321]. Indeed, we have demonstrated in mice that prepubertal exposure to endocrine disruptors accelerates pubertal onset [292, 309, 322, 323].

We hypothesized that both body fat and endocrine disruptors could affect pubertal onset and that body fat could influence the effect of endocrine disruptors on pubertal onset. This hypothesis was tested in *Bscl2*$^{-/-}$ mice [324] that recapitulate human Beinardinalli-Seipin Congenital Lipodystrophy type 2 (BSCL2) disease. *BSCL2*/*Bscl2* gene encodes seipin, an integral endoplasmic reticulum membrane protein that plays an essential role in adipose tissue development [324-330]. Seipin is highly expressed in the adipose tissue, brain and testis of both human and mouse [325, 331-333]. Mutations or deletion of *BSCL2*/*Bscl2* are associated with generalized lipodystrophy characterized by a near complete absence of adipose tissue and associated metabolic complications [324, 325, 328-330]. Although it was reported that among 45 patients (27 boys and 18 girls) with *BSCL2* mutations, one girl had precocious puberty [334], it is unknown whether

seipin deficiency and related lipodystrophy affect pubertal onset. It is also unknown whether lipodystrophy affects the responsiveness to prepubertal exposure of endocrine disruptors. These two aspects were investigated in this study. Genistein was used as a testing endocrine disruptor. A dose of 500 ppm in the diet was chosen because it was found in some soy products, such as soy bacon [122], and it was previously demonstrated to be an effective dose to influence pubertal onset in mice [309]. Pubertal mammary gland development and vaginal opening were two end points for determining pubertal onset in this study.

3.3 Materials and Methods

3.3.1 Animals

Bscl2-deficient mice (*Bscl2*$^{-/-}$) on C57BL/6J background were derived from a colony at Georgia Regents University, which was originally derived from a colony at Baylor College of Medicine [324]. Mice with different genotypes were from *Bscl2*$^{+/-}$ (Het) females X *Bscl2*$^{+/-}$ (Het) males. They were genotyped as previously described [324]. All mice were maintained on PicoLab mouse diet 20 with soybean as a main protein source. They were housed in polypropylene cages with free access to food and water on a 12 h light/dark cycle (0700–1900) at 23±1°C with 30–50% relative humidity at the College of Veterinary Medicine animal facility at the University of Georgia. All methods used in this study were approved by the University of Georgia IACUC Committee and conform to National Institutes of Health guidelines and public law.

3.3.2 Treatment

Bscl2$^{+/+}$ (WT) and *Bscl2*$^{+/-}$ (Het) mice had no difference in phenotypes and were both included in the genotype control for *Bscl2*$^{-/-}$ (Hom) mice. At weaning (3 weeks old), control females and their *Bscl2*$^{-/-}$ female littermates were randomly assigned into 0 ppm

(vehicle control) or 500 ppm genistein diet groups, resulting in four groups: control mice, 0 ppm; control mice, 500 ppm; *Bscl2*$^{-/-}$ mice, 0 ppm; and *Bscl2*$^{-/-}$ mice, 500 ppm. The 0 ppm and 500 ppm genistein diets were prepared as described previously [309, 335]. Briefly, 0 g or 0.25 g genistein (LC Laboratories, Woburn, MA) was dissolved in 150 ml 70% ethanol, then mixed well with 500 g phytoestrogen-free AIN-93G diet (Bio-Serv, Frenchtown, NJ) in different glass bowls to obtain 0 ppm and 500 ppm genistein diets, respectively. Food pellets were hand squeezed, air dried at room temperature, and kept at 4°C. Fresh diets were prepared every two weeks. Body weight was measured at 3, 4, and 5 weeks old. At least 6 mice were included in each study group. Vaginal opening was evaluated daily from weaning until detection [309].

3.3.3 Tissue collection

All mice at 5 weeks old ± 1 day were dissected at estrus stage, which was determined by vaginal smear prior to dissection [309], except in *Bscl2*$^{-/-}$, 0 ppm group, in which 6 out of the 7 mice had vaginal opening on PND34 or 35, and they were dissected on the day of vaginal opening detection. Both vaginal opening and estrus stage occur after an estrogen increase [319, 336-338]. The day at vaginal opening and the day at estrus stage were chosen as relatively comparable stages ~5 weeks old between control and *Bscl2*$^{-/-}$ females. The 4th inguinal mammary glands on both sides were collected, one was saved for whole mount analysis and the other was fixed in 10% formalin for histology and immunohistochemistry.

3.3.4 Mammary gland whole mount and quantification of mammary gland development

Mammary gland whole mount and quantification were done as previously described [294, 309]. ImageJ (National Institutes of Health, Bethesda, MD, USA) was

used to quantify the size of each lymph node, the length of the longest duct from the nipple, the diameter of the widest mammary gland duct at the position near each lymph node, the occupied area of each mammary gland (approximated by a polygon area that covered all the ducts), the width of the ductal tree passing the lymph node, and the number of terminal end buds (TEB) with diameters larger than 70 mm.

3.3.5 Histology

Mammary gland histology was done as previously described [309].

3.3.6 Immunohistochemistry

Paraffin sections (5 μm) of the 4th inguinal mammary glands were used in immunohistochemistry as previously described [291, 309]. Seipin expression was detected in 5 weeks old *Bscl2*$^{+/+}$ and *Bscl2*$^{-/-}$ mammary glands as well as 3 months old *Bscl2*$^{+/+}$ and *Bscl2*$^{-/-}$ testes using our customized rabbit polyclonal anti-seipin antibody (1:1,000, 2.21 μg/ml, Thermo Scientific), which was raised against the C-terminal 17 amino acids of mouse seipin. *Bscl2*$^{+/+}$ mammary gland sections and testis sections without primary antibody were also included. To determine the effects of *Bscl2*-deficiency and genistein treatment on the expression of phospho-estrogen receptor α (P-ESR1/P-ERα), estrogen receptor β (ESR2/ERβ), and progesterone receptor (PR) in the mammary gland, mammary gland sections from three mice in each of the four groups (control mice, 0 ppm; control mice, 500 ppm; *Bscl2*$^{-/-}$ mice, 0 ppm; and *Bscl2*$^{-/-}$ mice, 500 ppm) were evaluated using immunohistochemistry for P-ERα (rabbit anti-phospho-ERα antibody, 1:100, 10 μg/ml, Abcam), ERβ (anti-ERβ antibody, 1:50, 20 μg/ml, Abcam), and PR (rabbit anti-PR antibody, 1:200, 6 μg/ml, Daco, Denmark) as previously described [69, 291, 309]. Sections were counterstained with Harris Hematoxylin.

3.3.7 Statistical analysis

Nonparametric Two-Sample Kolmogorov-Smirnov test was used to compare the ages at vaginal opening, the sizes of lymph nodes, the ductal lengths and the areas of mammary glands, the diameters of mammary gland ducts, the widths of ductal trees passing the lymph nodes, and the numbers of TEB. Two-tail unequal variance student's t-test was used to compare the weaning body weight. ANOVA with repeated measure was used to compare the body weight from 3 to 5 weeks old in different genotypes and treatments. Error bars represented standard deviation. The significance level was set at $p<0.05$.

3.4 Results and Discussion

3.4.1 Body weight

Bscl2$^{-/-}$ females had significantly lower body weight than the control mice only at weaning (3 weeks old) but not at 4 or 5 weeks old (Fig. 3.1A), in agreement with our previous report [324]. The average weaning weights were 10.87±1.18 g (N=23) for control females and 9.69±0.85 g (N=13, P<0.01) for *Bscl2*$^{-/-}$ females.

Interestingly, we noticed a dramatic difference in the weaning body weight of the control C57BL/6J females (10.87±1.18 g, N=23) in this study compared to that of the control C57BL/6J females in our previous study, which was 7.22±1.05 g (N=111, P<0.001, two-tailed unequal variance t-test) [309]. The main difference in these two studies was the diet. In the previous study, our C57BL/6J colony was maintained on phytoestrogen-free AIN-93G diet (3.8 kcal/g), and the ancestors of the females used in the previous study were already on this diet for at least 2 generations. In this current study, all the female pups were from parents maintained on PicoLab mouse diet 20 (4.6 kcal/g).

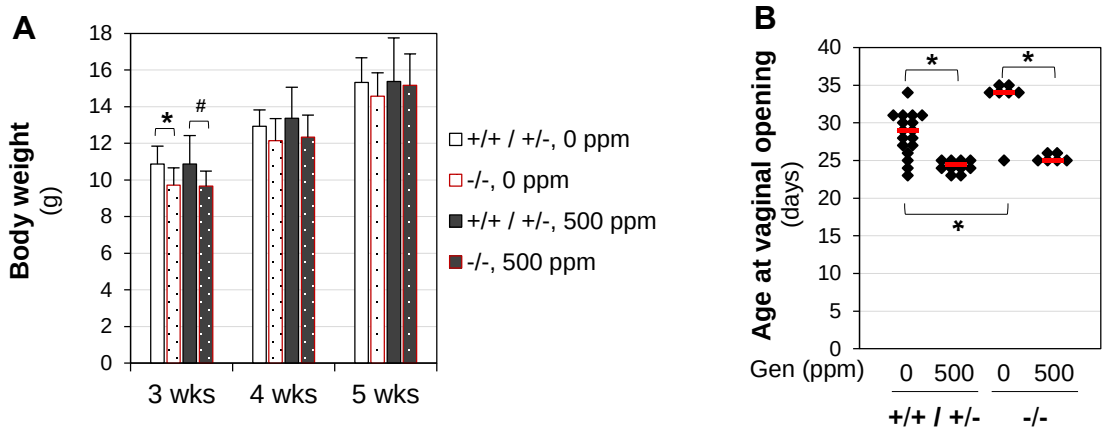

Figure 3.1. Body weight and age at vaginal opening. A. Body weight from weaning (3 weeks old, 3wks) to dissection (5 wks). Body weight at weaning: two-tail unequal variance t-test; * P=0.022; # P=0.086. Body weight from 3 to 5 weeks old: ANOVO repeated measures; no treatment related difference (P=0.645). Error bars, standard deviations. N=6-15. B. Age at vaginal opening. * p<0.05; nonparametric Two-Sample Kolmogorov-Smirnov test. Black diamonds indicate data from individual mice; red lines indicate median in each group. N=6-17. +/+ / +/-, *Bscl2*$^{+/+}$ (WT) and *Bscl2*$^{+/-}$ (Het) mice as the genotype control for *Bscl2*$^{-/-}$ (Hom) mice; -/-, *Bscl2*$^{-/-}$ mice. Genistein (Gen) diets: 0 ppm or 500 ppm.

3.4.2 Vaginal opening

Although it has been debated for its accuracy as a biomarker for puberty [16], vaginal opening has been used as a standard endpoint for assessing pubertal development by U.S. Environmental Protection Agency (EPA) (http://www.epa.gov/endo/pubs/pubertal_protocol_2007_v7.2c.pdf) and it has been used in many rodent studies to indicate pubertal onset [11-15]. Analyses of the original data from our previous study [309] revealed a significant correlation between age at vaginal

opening and age at first copulation following vaginal opening. In addition, other biomarkers for puberty, such as vaginal estrus, vaginal plug, and ovulation, also showed a consistent sequential pattern following vaginal opening [15, 16]. Therefore, vaginal opening can be used as an easily obtainable noninvasive biomarker for pubertal onset in rodents [15].

Genistein treatment significantly advanced vaginal opening in both control and *Bscl2*$^{-/-}$ mice (Fig. 3.1B). Interestingly, without genistein treatment, *Bscl2*$^{-/-}$ mice had significantly delayed vaginal opening compared to the control mice (Fig. 3.1B). The lower body weight in the newly-weaned *Bscl2*$^{-/-}$ mice (Fig. 3.1A) might contribute to the delayed vaginal opening. This difference seemed to be erased by 500 ppm genistein treatment because no significant difference in the ages at vaginal opening was observed between genistein-treated control and *Bscl2*$^{-/-}$ mice (Fig. 3.1B). These results indicated that although *Bscl2* deficiency delayed vaginal opening, it did not seem to affect the responsiveness to genistein treatment.

In our previous study [309], the age at vaginal opening in the vehicle control group was 32.2±2.8 days old (N=35). It was significantly younger in the vehicle control mice (28.5±2.9 days old, N=17, $P<0.001$) in this study. There could be two related potential explanations: body weight and diet. The body weight in the previous study [309] was significantly lower than that in the current study (Fig. 3.1A). Normally, higher body weight is correlated with earlier pubertal development (reviewed in [339]). Females in the previous study were not exposed to phytoestrogen-containing diet directly or indirectly from gestation to weaning because they were from a colony maintained on phytoestrogen-free AIN-93G diet [309]. Females in the current study were indirectly

exposed to PicoLab mouse diet 20 from gestation to weaning. Soybean was a main protein source in this diet, and it contained phytoestrogens genistein and daidzein [340-342]. It has been reported that *in utero* and lactational exposure to phytoestrogens could promote pubertal onset [343, 344] and the phytoestrogen content in the diet could affect the age at vaginal opening [345].

3.4.3 Mammary gland

Since seipin-deficiency is associated with generalized lipodystrophy characterized by a near complete absence of adipose tissue [324, 325, 328-330], it was expected that adipocyte-rich mammary gland would have abnormalities in the *Bscl2*$^{-/-}$ female mice. Indeed, several obvious differences were observed. Whole mount mammary glands showed enlarged lymph nodes (1.23±0.24 mm^2 (N=7) vs. 0.54±0.22 mm^2 (N=9) in the control, P<0.001), and longer and wider mammary gland ducts in the 5 weeks old *Bscl2*$^{-/-}$ female mice (Figs. 3.2A, 3.2B). Histology of mammary gland confirmed enlarged ductal lumen and smaller adipocytes in these mice (Figs. 3.2C, 3.2D). The average diameters of the widest mammary gland ducts near the lymph nodes were 0.027±0.006 mm (N=9) for the control females and 0.063±0.007 mm (N=7, P<0.001) for the *Bscl2*$^{-/-}$ females. Interestingly, cells and patches of cells were often seen in the *Bscl2*$^{-/-}$ mammary gland ductal lumen (Fig. 3.2D). It was possible that they were sloughed ductal epithelial cells.

Upon postweaning 500 ppm genistein treatment, the control mice had significantly increased ductal length and area of mammary gland at 5 weeks old (Figs. 3.3A, 3.3B, 3.3E, 3.3F). This effect was consistent with our previous study in C57BL/6J females derived from a colony maintained on phytoestrogen-free AIN-93G diet [309]. In *Bscl2*$^{-/-}$ mammary glands, segregated responses upon 500 ppm genistein treatment were observed. Significantly increased mammary gland area but not mammary gland ductal

length was observed in the 500 ppm genistein-treated *Bscl2*$^{-/-}$ females (Figs. 3.3C-3.3F). This could be attributed to the accelerated ductal growth in the *Bscl2*$^{-/-}$ females, which had significantly longer duct than the control females on either 0 or 500 ppm genistein diet (Figs. 3.3A-3.3E). It was possible that the ductal lengths in the *Bscl2*$^{-/-}$ females had reached the maximum and 500 ppm genistein treatment could not further extend the ductal lengths. In support of this speculation, we found that the number of TEB (highly proliferative structures located at the tips of the invading ducts) in the *Bscl2*$^{-/-}$ females on 0 ppm genistein diet was comparable to those in the control females and the *Bscl2*$^{-/-}$ females on 500 ppm genistein diet (Fig. 3.3G).

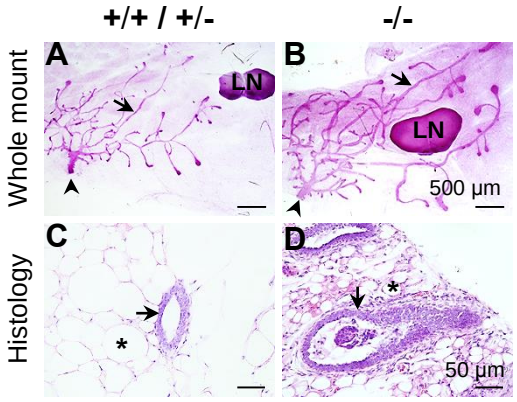

Figure 3.2. Representative images of whole mount and histology of mammary gland of females at 5 weeks old on vehicle control diet. A. Whole mount of *Bscl2*$^{+/+}$ / *Bscl2*$^{+/-}$ control mammary gland. B. Whole mount of *Bscl2*$^{-/-}$ mammary gland. Scale bars in A & B, 500 µm. C. Histology of *Bscl2*$^{+/+}$ / *Bscl2*$^{+/-}$ control mammary gland. D. Histology of *Bscl2*$^{-/-}$ mammary gland. H & E stain. Scale bars in C & D, 50 µm. A~D: arrows, mammary gland ducts; arrowheads, nipples; *, mammary gland adipocyte; LN, lymph node.

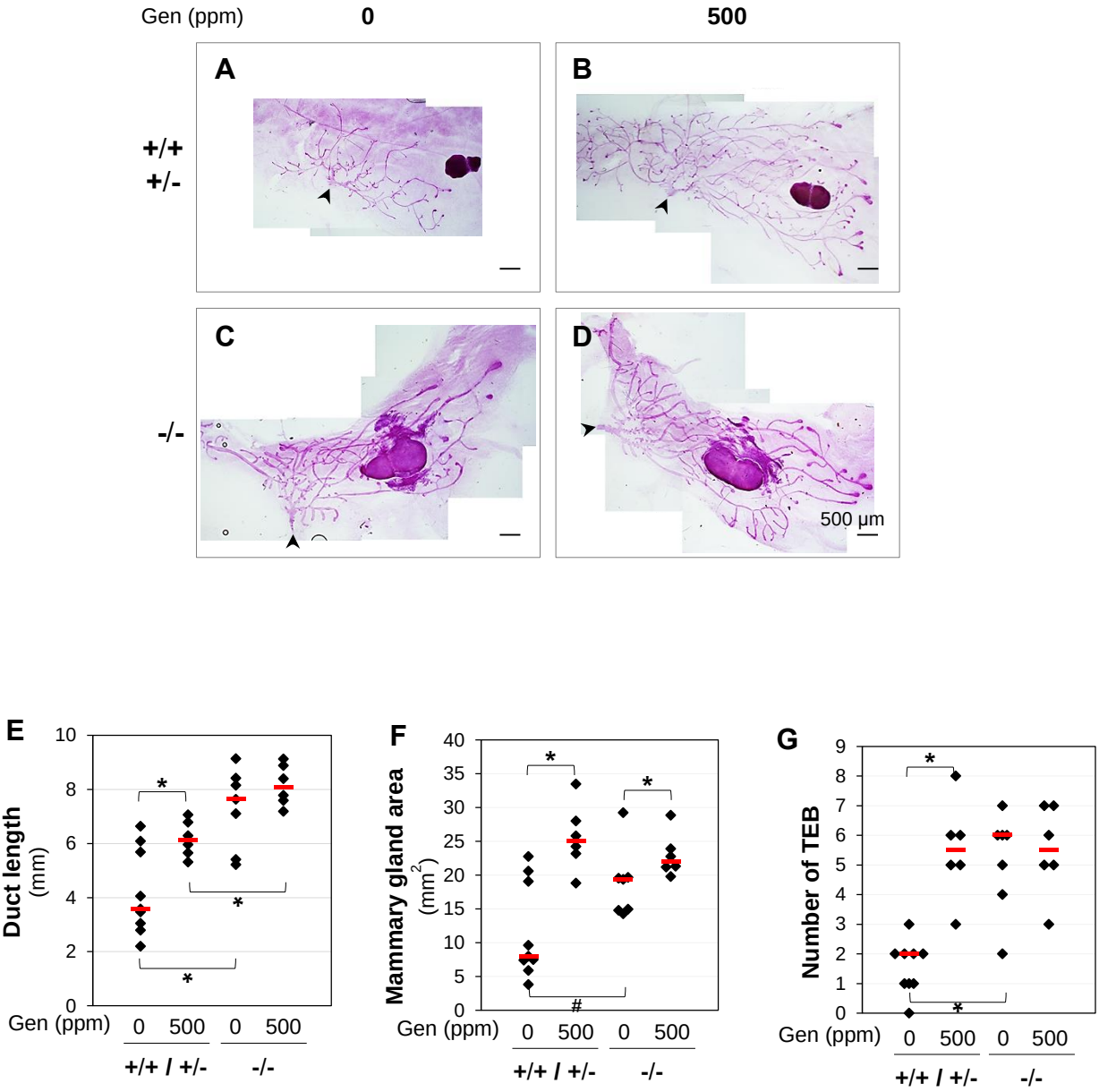

Figure 3.3. Effects of *Bscl2*/seipin and genistein on mammary gland development. A~D. Representative images of whole mount mammary glands in *Bscl2*$^{+/+}$ / *Bscl2*$^{+/-}$, 0 ppm genistein group (A), *Bscl2*$^{+/+}$ / *Bscl2*$^{+/-}$, 500 ppm genistein group (B), *Bscl2*$^{-/-}$, 0 ppm genistein group (C), and *Bscl2*$^{-/-}$, 500 ppm genistein group (D) at 5 weeks old. E. Lengths of the longest mammary gland ducts. * P<0.05. F. Areas occupied by mammary gland ducts. * P<0.05; # P=0.092. G. Numbers of terminal end buds (TEB). * P<0.05. E-G:

nonparametric Two-Sample Kolmogorov-Smirnov test. Black diamonds indicate data from individual mice; red lines indicate median in each group. N=6-9. +/+ / +/-, *Bscl2*$^{+/+}$ and *Bscl2*$^{+/-}$ control mice; -/-, *Bscl2*$^{-/-}$ mice; Genistein (Gen) diets, 0 ppm or 500 ppm. A-D: scale bars, 500 µm; arrowheads, nipples.

However, there was still limited room to expand the mammary gland area in the *Bscl2*$^{-/-}$ females. In the control females, the average increase of mammary gland area was ~200% upon genistein treatment; while in the *Bscl2*$^{-/-}$ females, it was ~15% in response to 500 ppm genistein treatment (Figs. 3.3A~3.3D, 3.3F). Although the mammary gland ductal tree was supported by the surrounding fat tissue, which was not well developed in the *Bscl2*$^{-/-}$ females (Fig. 3.2D), it did not seem to limit the ductal growth. However, the width of ductal tree passing the lymph node was narrower in the 500 ppm genistein-treated *Bscl2*$^{-/-}$ females (2.91±0.46 mm (N=6), Fig. 3.3D) compared to 500 ppm genistein-treated control mice (3.99±0.37 mm (N=6), P=0.026, Fig. 3.3B). This observation could be supported by the longer ductal length in the *Bscl2*$^{-/-}$ mammary gland (Fig. 3.3E) but comparable area of mammary gland between control and *Bscl2*$^{-/-}$ mammary glands upon 500 ppm genistein treatment (Fig. 3.3F).

3.4.4 Expression of seipin in 5 weeks old mammary gland

Seipin has been demonstrated to be highly expressed in adipose tissue, brain and testis [325, 331, 332, 346]. Its expression in the mammary gland had not been previously reported. Immunohistochemistry showed seipin expression in the adipocytes and the ductal epithelial cells of 5 weeks old Bscl2+/+ mammary gland (Fig. 3.4A). However, there were still lower levels of staining in the Bscl2-/- mammary gland (Fig. 3.4B) but no staining

in the mammary gland without the primary antibody (Fig. 3.4C). Seipin was highly detected in the *Bscl2*$^{+/+}$ spermatids but not in the *Bscl2*$^{-/-}$ spermatids (Figs. 3.4D, 3.4E) as previously reported [332, 346]. However, compared to the testis section without the primary antibody (Fig. 3.4F), the *Bscl2*$^{-/-}$ testis had background immunostaining throughout all the cell types (Fig. 3.4E). The expression of seipin in the mammary gland supported its potential role in mammary gland development and/or function.

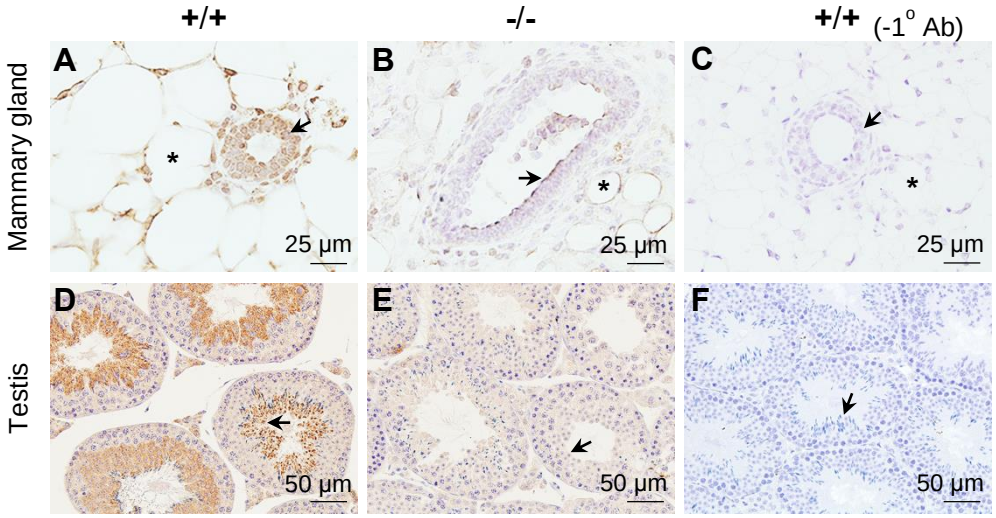

Figure 3.4. Immunohistochemistry detection of seipin expression in 5 weeks old mammary glands and 3 month old testes. A. Wild type (+/+) mammary gland with anti-seipin antibody. B. *Bscl2*$^{-/-}$ mammary gland with anti-seipin antibody. C. Wild type (+/+) mammary gland without primary antibody (-1º Ab). A~C: arrows, mammary gland ductal luminal epithelial cells; *, mammary gland adipocytes; scale bars, 25 µm. D. Wild type (+/+) testis with anti-seipin antibody. E. *Bscl2*$^{-/-}$ testis with anti-seipin antibody. F. Wild type (+/+) testis without primary antibody (-1º Ab). D~F: arrows, spermatids; scale bars, 50 µm. Brown signal, positive staining.

3.4.5 ER and PR expression

ERα is critical for pubertal mammary gland development [314]. ERβ seems to be important for side branching [315], presumably through its involvement in progesterone production from corpora lutea [315-317] because PR-mediated progesterone signaling is critical for side branching [347, 348]. It was previously demonstrated that postweaning genistein treatment did not influence P-ERα, ERβ, and PR expression in C57BL/6 mammary gland at 5 weeks old [309]. Here we further examined P-ERα, ERβ, and PR expression in 5 weeks old mammary gland to determine if any of these receptors had altered expression in the *Bscl2*$^{-/-}$ mammary glands treated with 0 or 500 ppm genistein diets.

P-ERα was mainly detected in the nuclei of epithelial cells and adipocytes; there was no obvious difference in the P-ERα expression patterns among all four groups (Figs. 3.5A-3.5D). ERβ was comparably highly expressed in the epithelial cells and adipocytes of the control mammary glands (both 0 and 500 ppm genistein-treated) (Figs. 3.5E, 3.5F). However, its expression was lower in the epithelial cells compared to that in the surrounding adipocytes of the *Bscl2*$^{-/-}$ mammary glands (both 0 and 500 ppm genistein-treated) (Figs. 3.5G, 3.5H). The expression levels of ERβ in the adipocytes of the control mammary gland and of the *Bscl2*$^{-/-}$ mammary gland seemed to be comparable (Figs. 3.5E-3.5H). PR was mainly detected in the nuclei of mammary gland epithelial cells, and no obvious difference in the epithelial PR expression pattern was observed among all four groups (Figs. 3.5I-3.5L).

The mechanism of ERβ downregulation in the *Bscl2*$^{-/-}$ ductal epithelium and the consequence of such cell-type specific downregulation are unclear. It was demonstrated that glucocorticoid receptor (GR) deficiency (*GR*$^{-/-}$) could lead to accelerated pubertal

mammary ductal growth and distention [349], similar to what was seen in the *Bscl2*$^{-/-}$ mammary gland (Figs. 3.2, 3.3). Based on a mammary gland transplant study, the driving force for the *GR*$^{-/-}$ mammary gland duct phenotypes was from the transplanted *GR*$^{-/-}$ duct itself and not the host wild type fat pad [349]. ERβ has an antiproliferative function in the uterus [313, 350]. It may also have an antiproliferative function in the mammary gland. With this assumption, reduced ERβ expression specifically in the *Bscl2*$^{-/-}$ ductal epithelium could lead to increased proliferation of the ductal epithelium, leading to longer and dilated *Bscl2*$^{-/-}$ mammary gland duct (Figs. 3.2, 3.3).

3.4.6 Leptin and genistein on puberty

There is a leptin surge during the second postnatal week, preceding the developmental estrogen increase in the female mice [215]. Leptin might promote puberty by indirectly stimulating gonadotropin-releasing hormone (GnRH) production [351]. Leptin is synthesized in the adipocytes and leptin levels are positvely correlated with fat mass [214]. Therefore, lipodystrophy is often accompanied with reduced leptin levels [352]. Indeed, our *Bscl2*$^{-/-}$ mice were previously demonstrated to have greatly reduced leptin levels [324], which might cause the delayed pubertal onset indicated by delayed vaginal opening (Fig. 3.1B). However, prepubertal exposure to 500 ppm genistein significantly accelerated vaginal opening in the *Bscl2*$^{-/-}$ females to a level comparable to that in the genistein-treated control females (Fig. 3.1B).

Genistein can induce GnRH pulsatile production in the prepubertal mice [187]. It advances pubertal onset possibly via suppressing inhibitory and activating stimulatory components of the GnRH network [195]. Leptin administration could restore pubertal onset in the leptin-deficient mice [353]. However, *in vitro* studies showed that genistein

could decrease leptin production in adipocytes [354, 355], while an *in vivo* study on adult ovariectomized C57BL/6 mice treated with 1500 ppm genistein diet for 21 days did not show any effect of genistein on blood leptin levels [356]. These observations suggested that genistein advanced pubertal onset in the *Bscl2*$^{-/-}$ females but it might not act through increasing leptin levels. It could possibly enhance leptin sensitivity in the brain in a way similar to what estrogen does [357]. It is also possible that genistein could circumvent the defect(s) leading to delayed pubertal onset in *Bscl2*$^{-/-}$ females via an unknown pathway.

3.4.7 Fat and pubertal mammary gland development

Pubertal mammary gland growth is characterized by ductal morphogenesis with extensive epithelial cell proliferation, a process that is believed to be regulated by paracrine signaling [312-314, 358]. Adipocytes play a key role in this paracrine regulation of pubertal mammary gland development [359]. Ablation of adipocytes during puberty could inhibit pubertal mammary gland growth, and restoration of adipocytes could rescue it to a considerable extent [360]. A-ZIP/F1 transgenic mice without white adipose tissue have short and dilated mammary gland ducts and lack normal pubertal mammary gland growth, resulting from the lack of adipose tissue but not any defects in the ductal epithelial cells [361]. Although the *Bscl2*$^{-/-}$ females also lack well-developed fat tissue [324], they have long and dilated mammary gland ducts at 5 weeks old (Figs. 3.3A-3.3E). It is possible that the longer mammary gland ducts in the *Bscl2*$^{-/-}$ females (Fig. 3.3E) are caused by the local loss of seipin in the ductal epithelium (Fig. 3.4A), potentially involving downregulation of ERβ in the ductal epithelium (Fig. 3.5G, 3.5H).

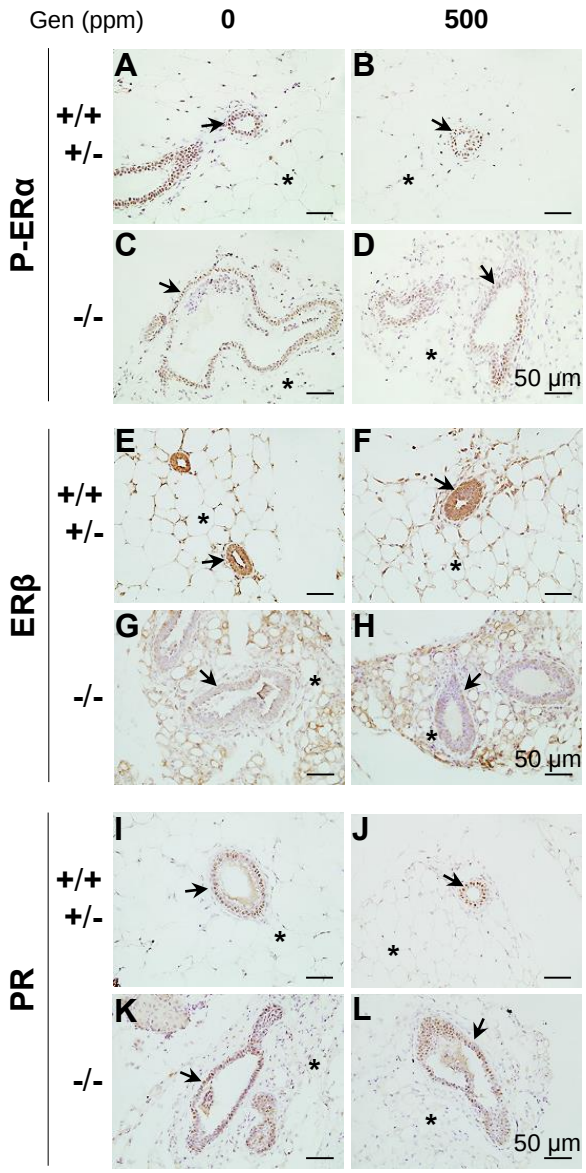

Figure 3.5. Expression of phospho-estrogen receptor alpha (P-ERα/P-ESR1), estrogen receptor beta (ERβ/ESR2), and progesterone receptor (PR) in 5 weeks old mammary gland. Sections from 3 mice in each group were examined and representative images were shown. A. P-ERα, *Bscl2*$^{+/+}$ / *Bscl2*$^{+/-}$, 0 ppm genistein group. B. P-ERα, *Bscl2*$^{+/+}$ /

Bscl2$^{+/-}$, 500 ppm genistein group. C. P-ERα, *Bscl2*$^{-/-}$, 0 ppm genistein group. D. P-ERα, *Bscl2*$^{-/-}$, 500 ppm genistein group. E. ERβ, *Bscl2*$^{+/+}$ / *Bscl2*$^{+/-}$, 0 ppm genistein group. F. ERβ, *Bscl2*$^{+/+}$ / *Bscl2*$^{+/-}$, 500 ppm genistein group. G. ERβ, *Bscl2*$^{-/-}$, 0 ppm genistein group. H. ERβ, *Bscl2*$^{-/-}$, 500 ppm genistein group. I. PR, *Bscl2*$^{+/+}$ / *Bscl2*$^{+/-}$, 0 ppm genistein group. J. PR, *Bscl2*$^{+/+}$ / *Bscl2*$^{+/-}$, 500 ppm genistein group. K. PR, *Bscl2*$^{-/-}$, 0 ppm genistein group. L. PR, *Bscl2*$^{-/-}$, 500 ppm genistein group. Dark brown, immunostaining; purple-blue, counter staining with Harris Hematoxylin; no specific immunostaining in the minus primary antibody negative control (Fig. 3.4C). Arrows, mammary gland ducts; *, mammary gland adipocytes.

3.5 Summary

Both mammary gland development and vaginal opening are markers for pubertal onset in mice. These two processes are segregated in the *Bscl2*$^{-/-}$ female mice with lipodystrophy, indicated by accelerated mammary gland ductal growth but delayed vaginal opening. *Bscl2*$^{-/-}$ females are responsive to genistein treatment, indicated by accelerated vaginal opening and increased mammary gland area. Mammary gland development is not as responsive as vaginal opening upon genistein treatment in the *Bscl2*$^{-/-}$ females. This can be explained by accelerated pubertal mammary gland ductal growth but limited mammary fat pad in the *Bscl2*$^{-/-}$ females. Reduced expression of ERβ may contribute to the phenotypes in the *Bscl2*$^{-/-}$ mammary gland ducts.

Acknowledgements

The authors thank the Department of Pathology in the College of Veterinary Medicine, University of Georgia for access to the imaging system; the Office of the Vice President for Research, Interdisciplinary Toxicology Program, and Department of Physiology and

Pharmacology at the University of Georgia, and the National Institutes of Health (NIH R15HD066301 and NIH R01HD065939 (co-funded by ORWH and NICHD) to X.Y.) for financial support

CHAPTER 4

OLFACTOMEDIN 1 DEFICIENCY LEADS TO DEFECTIVE OLFACTION AND IMPARIED FEMAEL FERTILITY

Rong Li, Honglu Diao, Fei Zhao, Shuo Xiao, Ahmed E. El Zowalaty, Elizabeth A. Dudley, Mark P. Mattson, and Xiaoqin Ye. 2015 *Endocrinology*; 156 (9): 3344-57.

4.1 Abstract

Olfactomedin 1 (OLFM1) is a glycoprotein highly expressed in the brain. *Olfm1*$^{-/-}$ female mice were previously reported to have reduced fertility. Previous microarray analysis revealed *Olfm1* among the most highly upregulated genes in the uterine luminal epithelium (LE) upon embryo implantation, which was confirmed by *in situ* hybridization. We hypothesized that *Olfm1* deficiency led to defective embryo implantation and thus impaired fertility. Indeed, *Olfm1*$^{-/-}$ females had defective embryo implantation. However, *Olfm1*$^{-/-}$ females rarely mated and those that mated rarely became pregnant. Ovarian histology indicated the absence of corpora lutea in *Olfm1*$^{-/-}$ females, indicating defective ovulation. Superovulation using eCG-hCG rescued mating, ovulation and pregnancy, and eCG alone rescued ovulation in *Olfm1*$^{-/-}$ females. *Olfm1*$^{-/-}$ females had a 13% reduction of hypothalamic GnRH neurons, but comparable basal serum luteinizing hormone (LH) levels and GnRH-induced LH levels compared to wild type controls. These results indicated no obvious local defects in the female reproductive system and a functional HPG axis. *Olfm1*$^{-/-}$ females were unresponsive to the effects of male bedding stimulation on pubertal development and estrous cycle. There were 41% fewer cFos positive cells in the mitral cell layer of accessory olfactory bulb upon male urine stimulation for 90 minutes. OLFM1 was expressed in the main and accessory olfactory systems including main olfactory epithelium, vomeronasal organ, main olfactory bulb and accessory olfactory bulb, with the highest expression detected in the axon bundles of olfactory sensory neurons. These data demonstrate that defective fertility in *Olfm1*$^{-/-}$ females is most likely a secondary effect of defective olfaction.

4.2 Introduction

Olfactomedin1 (OLFM1) is a highly conserved glycoprotein that was originally identified in the frog olfactory neuroepithelium [261, 362]. It belongs to subfamily I of the olfactomedin protein family, which has 8 subfamilies [363-365]. Olfactomedin proteins can interact with other proteins and play roles in cell adhesion, cell invasion, and differentiation [264, 364, 366]. OLFM1 is also known as Noelin in chicken and *xenopus*, pancortin in mice, olfactomedin-related glycoprotein in rats and hOlfA in humans [263]. There are four mouse *Olfm1* mRNA transcripts that share a central B part, with 5' variants A1 or A2 by different promoters, and 3' variants C1 or C2 by alternative splicing [281, 367]. *Olfm1* is highly expressed in the nervous system including the cerebral cortex and olfactory bulb [280, 281, 367]. OLFM1 regulates neural development, migration and apoptosis [271, 368, 369]. It can interact with the Nogo A receptor (NgR1) complex to promote axon growth [366] and can be co-precipitated with many other proteins [282].

Deletion of the middle part (B and part of C1) of *Olfm1* (*Olfm1*$^{-/-}$) in mice led to reduced cerebral infarct size in males, reduced body weight, reduced activity and anxiety, and defective olfaction without affecting coordination of locomotive activity or life span in both females and males [282, 369]. It was reported that *Olfm1*$^{-/-}$ breeding pairs did not breed well, but the colony could be maintained by breeding *Olfm1*$^{-/-}$ males with *Olfm1*$^{+/-}$ females [369], indicating defective fertility in the *Olfm1*$^{-/-}$ females but the cause(s) for defective fertility has not been previously investigated.

Our microarray analysis of mouse periimplantation uterine luminal epithelium (LE) demonstrated that *Olfm1* was one of the most upregulated genes in the LE upon embryo implantation [370]. LE is the first layer of contact for an implanting embryo and is

considered essential for uterine receptive sensitivity [371, 372]. A receptive uterus is a prerequisite for embryo implantation. LE is involved in all three initial stages of embryo implantation: embryo apposition to the LE, embryo adhesion to the LE, and embryo penetration through the LE [68, 373-375]. The upregulation of *Olfm1* in the LE upon embryo implantation [370], the potential role of OLFM1 in cell adhesion and invasion [264, 364], as well as the defective fertility in the *Olfm1*$^{-/-}$ females [369] led us to hypothesize that LE OLFM1 was involved in uterine preparation for embryo implantation and that the defective fertility in the *Olfm1*$^{-/-}$ females [369] was caused by defective embryo implantation. This hypothesis was tested in the *Olfm1*$^{-/-}$ females. Systematic analyses of *Olfm1*$^{-/-}$ females indeed revealed defective embryo implantation in the *Olfm1*$^{-/-}$ females, but follow-up experiments testing responsivity to male odor stimulation indicated that it was most likely a secondary effect of defective olfaction in the *Olfm1*$^{-/-}$ females.

4.3 Materials and Methods

4.3.1 Animals

Olfm1$^{-/-}$ mice (129/SvEvBrd background) were derived from a colony at the National Institutes of Health [369]. Heterozygous females and males were mated to obtain females (newly-weaned at PND21 or 2-3 months old young virgin females) used in this study and genotyped as described previously [369]. They were housed in polypropylene cages with free access to food and water on a 12 h light/dark cycle (0600–1800) at 23±1°C with 30–50% relative humidity. All methods used in this study were approved by the University of Georgia IACUC Committee and conform to National Institutes of Health guidelines.

4.3.2 Fertility and mating activity

The female fertility test lasted from 2 to 8 months old. There were 8 cages, with one *Olfm1*$^{+/+}$ female, one *Olfm1*$^{-/-}$ female, and one *Olfm1*$^{+/+}$ stud male per cage. Pregnancy and litter size were recorded. In the first mating test, young virgin adult *Olfm1*$^{+/+}$ (N=12) and *Olfm1*$^{-/-}$ (N=15) females cohabitated with *Olfm1*$^{+/+}$ stud males. Copulation plug was checked every morning for 4 months. Plugging latency (the period from cohabitation to detection of the first copulation plug) and pregnancy from this first mating were recorded. In the second mating test, one young virgin female (*Olfm1*$^{+/+}$ or *Olfm1*$^{-/-}$, N=6) cohabitated with one *Olfm1*$^{+/+}$ stud male. Copulation plug was checked every morning for one month.

4.3.3 Vaginal opening

Vaginal opening was checked daily until its detection [309].

4.3.4 Embryo implantation

Young virgin *Olfm1*$^{+/+}$ and *Olfm1*$^{-/-}$ females were mated with stud *Olfm1*$^{+/+}$ males and checked for a copulation plug every morning. The day of copulation plug detection was defined as gestation day (D) 0.5. Plugged females (N=9) were examined for embryo implantation on D4.5 using blue dye injection as previously described [69, 297]. Females without implantation sites had their reproductive tracts flushed with PBS for the presence of embryos/oocytes.

4.3.5 Serum LH and FSH measurement

Young virgin adult *Olfm1*$^{+/+}$ and *Olfm1*$^{-/-}$ females in diestrus stage determined by vaginal smear [293] were anesthetized between 8:00 and 10:00 h for blood collection via orbital sinus. Serum was collected after clotting (1.5 h, RT) and centrifugation (2000 g, 10

min) and stored at -80°C. Serum LH and FSH were measured in the Ligand Assay and Analysis Core of the Center for Research in Reproduction at the University of Virginia (Charlottesville, Virginia). N=6-8.

4.3.6 Ovarian histology and mammary gland whole mount

After blood collection above, one ovary and one side of mammary gland were dissected from each female for ovarian histology and mammary gland whole mount as previously described [294, 309].

4.3.7 Superovulation

Superovulation using both eCG and hCG was induced in two sets of animals following a procedure described previously [376]. The first set was performed on newly-weaned *Olfm1*$^{+/+}$ (N=6) and *Olfm1*$^{-/-}$ (N=6) females, which were sacrificed for determining the number of cumulus oocyte complexes (COCs). The second set was performed on young virgin adult *Olfm1*$^{+/+}$ (N=7) and *Olfm1*$^{-/-}$ (N=8) females. After hCG injection, each superovulated female was cohabitated with one *Olfm1*$^{+/+}$ stud male for overnight, checked for a copulation plug next morning, and observed for 22 days. Pregnancy and litter size were recorded.

4.3.8 Superovulation with eCG alone

Newly-weaned control (*Olfm1*$^{+/+}$ and *Olfm1*$^{+/-}$, N=5) and *Olfm1*$^{-/-}$ (N=4) females were i.p. injected with 5 IU eCG at 16:00 h, and sacrificed 72 h later as described previously [377]. The COCs from both oviducts were counted.

4.3.9 GnRH stimulation assay

Young virgin adult *Olfm1*$^{+/+}$ and *Olfm1*$^{-/-}$ females were injected with 200 ng/kg GnRH peptide (Sigma-Aldrich) between 8:00 and 10:00 h. They were anesthetized 10

minutes later for blood collection from the orbital sinus as described previously [378]. Serum was collected and serum LH was measured as described in “Serum LH and FSH measurement” above. N=6-8.

4.3.10 GnRH neuron counting

Young virgin adult *Olfm1*$^{+/+}$ (N=5) and *Olfm1*$^{-/-}$ (N=5) females in diestrus were anesthetized under isoflurane and perfused transcardially with PBS followed by 4% paraformaldehyde (PFA). The brains were collected, post-fixed in 4% PFA, cryoprotected in 30% sucrose, and frozen for immunohistochemistry to label GnRH neurons as described previously [379], except that primary rabbit anti-GnRH (see Antibody Table) at 1:1000 and secondary goat anti-rabbit at 1:500 were used. Sections without the primary antibody served as the negative control. All the labeled GnRH neurons with cell bodies were counted.

4.3.11 Immunohistochemistry

D3.5 and D4.5 *Olfm1*$^{+/+}$ uteri, D13.5, D15.5, PND0, and 3 months old *Olfm1*$^{+/+}$ brains were collected and processed for detection of OLFM1 in the periimplantation uterus and olfactory systems, respectively, using primary mouse anti-mouse OLFM1/Noelin antibody (1:800, 1.25 µg/ml, S96-7, Novus biological) (see Antibody Table) and secondary antibody goat anti-mouse IgG-B (1:200, Santa Cruz Biotechnology, Dallas, Texas, USA). Adult *Olfm1*$^{-/-}$ olfactory bulb sections served as a negative control. D3.5 and D4.5 *Olfm1*$^{+/+}$ and *Olfm1*$^{-/-}$ uterine sections were immunostained for progesterone receptor (PR) (see Antibody Table) as described previously [69, 291, 380].

4.3.12 *In situ* hybridization

In situ hybridization in uterus and olfactory systems was done as described previously [69, 380]. The *Olfm1* antisense probe had a sequence complementary to a sequence shared by all four *Olfm1* mRNA transcripts [281, 367].

4.3.13 Male odor stimulation test *Male odor on estrous cyclicity*: Young virgin adult *Olfm1*$^{+/+}$ (N=14) and *Olfm1*$^{-/-}$ (N=20) females were checked for estrous cycle 5 days on regular bedding (RB) and then 5 days on male soiled bedding (MB), which was occupied by 3-5 adult *Olfm1*$^{+/+}$ males for at least 4 days. Females with different genotypes were placed in the same cages. *Male odor on vaginal opening and ovulation*: Newly weaned (PND21) control females (*Olfm1*$^{+/+}$ & *Olfm1*$^{+/-}$) and *Olfm1*$^{-/-}$ females (N=4-6) were randomly placed in cages with regular bedding or male soiled bedding, with control and *Olfm1*$^{-/-}$ females cohabitated in the same cages. Fresh male soiled bedding replaced old bedding every 3 days. Vaginal opening and subsequent estrus stages were determined daily at 8:00 h using vaginal smear [293]. All mice were sacrificed at 7 weeks old. Body weight was recorded. One ovary was frozen and weighed, and the other was fixed for histology.

4.3.13 Male urine-induced cFos expression in female olfactory systems

Urine was collected from 9 stud males, mixed together, and stored at -20°C until use. Young virgin adult *Olfm1*$^{+/+}$ (N=5) and *Olfm1*$^{-/-}$ (N=5) females cohabitated for at least two days before testing. Between 8:00 and 10:00 h of the testing day, 10 µl male urine was pipetted around their noses. After 90 minutes, the females were anesthetized by i.p injection of 2.5 ml/kg body weight euthasol® solution (Virbac, Fort Worth, TX) and perfused. Olfactory bulb was collected, post-fixed, and cryoprotected in 30% sucrose

overnight. From the first appearance of the accessory olfactory bulb every second 20 µm coronal section was collected. Immunohistochemistry of c-Fos (1:500, 0.4 µg/ml, SC-52, Santa Cruz, kindly provided by Dr. Jesse Schank) (see Antibody Table) was performed as described for detecting GnRH neurons, except with antigen retrieval and DAB staining for 2 min.

Table 4.1. Antibody table

Peptide/Protein Target	Antigen sequence (if known	Name of antibody	Manufacture. Catalog number and/or individual of providing the antibody	Species raised (Monoclonal or polyclonal)	Dilution used
Gonadontropin-releasing hormone (GnRH)	EHWSYGLRPG	Anti-GnRH	Pierces antibody, PA1-121	Rabbit, polyclonal	1:1000
cFOS	N terminal	Anti-cFOS	Santa cruz biotechnologies, sc-52	Rabbit, polyclonal	1:500
Olfactomedin 1	SLVGLNTTRLSAASGGTLDRS	Anti-OLFM1	Novus biologicals, S96-7	Mouse monoclonal	1:800
Progesterone receptor (PR)	GLPQVYPPYLNYLRP	Anti-PR	Dako, A0098	Rabbit, polyclonal	1:200

4.3.14 Statistical analyses

Fisher's exact test was used to compare different mating and pregnancy rates. ANOVA with repeated measures was used to compare body weights from 0-8 weeks of age. The rest of the data were tested for normality using Shapiro-wilk test. Two-sample Kolmogorov-Smirnov non-parametric analysis was used to compare data without normality, including age at vaginal opening, mating latency, number of litters, litter size and gestation period after superovulation, serum LH and FSH levels. Normally distributed data were further evaluated for homogeneity of variance using Levene's test. Two tail, unpaired, equal variance student's t-test was used for litter size, ovary weight, body

weight and age at vaginal opening upon male bedding exposure, numbers of cFos neurons and GnRH neurons, number of COCs after hCG+eCG treatment. Two tail, unpaired, unequal variance student's t-test was used for number of COCs after eCG treatment. P<0.05 was considered as significant.

4.4 Results

4.4.1 Fertility is severely reduced in *Olfm1*$^{-/-}$ females

It was previously reported that *Olfm1*$^{-/-}$ females did not breed well [369]. We found that *Olfm1*$^{-/-}$ females had significantly lower body weight from birth to adults compared to both *Olfm1*$^{+/-}$ females and *Olfm1*$^{+/+}$ females (Fig. S4.1A). *Olfm1*$^{-/-}$ females had ~5% less (P=0.04) body weight at birth and ~17%-25% less body weight from 1 to 8 weeks old compared to age-matched *Olfm1*$^{+/+}$ females (Fig. 4.S1A). They had ~4 days of delay (29.4±3.8 days old, P<0.05) in vaginal opening compared to both *Olfm1*$^{+/-}$ females (25.9±2.8 days old) and *Olfm1*$^{+/+}$ females (25.4±2.8 days old) (Fig. S4.1B). No differences in body weight or age at vaginal opening were observed between *Olfm1*$^{+/-}$ females and *Olfm1*$^{+/+}$ females (Fig. S4.1). Fertility test indicated that all *Olfm1*$^{+/+}$ females (8/8=100%) had pups, with an average of 5.9±1.0 litters per female and 5.1±0.9

Table 4.2. 6 months fertility test

	Olfm1(+/+)	**Olfm1(+/+)**	**P value**
Pregnancy rate %	100 (8/8)	12.5 (1/8)	.001
Litters/pregnant female	5.9±1.0 (n=8)	4 (n=1)	<.001
littersize	5.1±0.9 (n=47)	3.3±1.5 (n=4)	0.0602

pups per litter during the 6 months of cohabitation. However, only 1 out of 8 (12.5%, P=0.001) *Olfm1*$^{-/-}$ females ever delivered pups, with a total of 4 litters and an average litter size of 3.3±1.5 per litter (P= 0.0602) (Table 4.2). These data demonstrated severely impaired fertility in the *Olfm1*$^{-/-}$ females.

4.4.2 *Olfm1* expression in periimplantation uterus

Our previous microarray analysis revealed dramatic upregulation of *Olfm1* in the uterine luminal epithelium (LE) upon embryo implantation [370]. *In situ* hybridization confirmed this upregulation in gestation day 4.5 (D4.5) *Olfm1*$^{+/+}$ LE and *Olfm1* was undetectable in D4.5 *Olfm1*$^{-/-}$ LE (Figs. S4.2A, S4.2B, 4.1F, 4.1G). *Olfm1* was occasionally detected in a few *Olfm1*$^{+/+}$ glandular epithelial cells but undetectable in other uterine cellular compartments (Fig. S4.2C). Both OLFM1 protein and *Olfm1* mRNA were localized in LE (Fig. 4.1A, 4.1B, S4.2D~S4.2H). OLFM1 protein was mainly detected in the apical side of D4.5 LE (Fig. 4.1B). Since the uterine lumen was closed at D4.5 [380] and *Olfm1* mRNA was highly expressed in D4.5 LE (Fig. 4.1F), it was difficult to distinguish its presence in the apical side of LE cytoplasm or the LE surface. However, based on the comparable IHC images in D4.5 LE of OLFM1 (Fig. 4.1B) and transthyretin [381], which is a protein synthesized in the GE and secreted to uterine lumen, it is reasonable to speculate that OLFM1 is present in the LE surface.

4.4.3 Olfactomedin deficiency impairs embryo implantation

Significant upregulation of *Olfm1* in D4.5 LE (Figs. 4.1, S4.2) and severely impaired fertility in *Olfm1*$^{-/-}$ females (Table 4.2) led us to hypothesize that OLFM1 was critical for embryo implantation and deletion of *Olfm1* would lead to impaired embryo implantation and thus impaired fertility. Embryo implantation was determined in D4.5

females. *Olfm1*$^{+/+}$ females were easily plugged and 8 out of 9 plugged females had on-time implantation indicated by the presence of clear implantation sites (Fig. 4.1C, 4.1D).

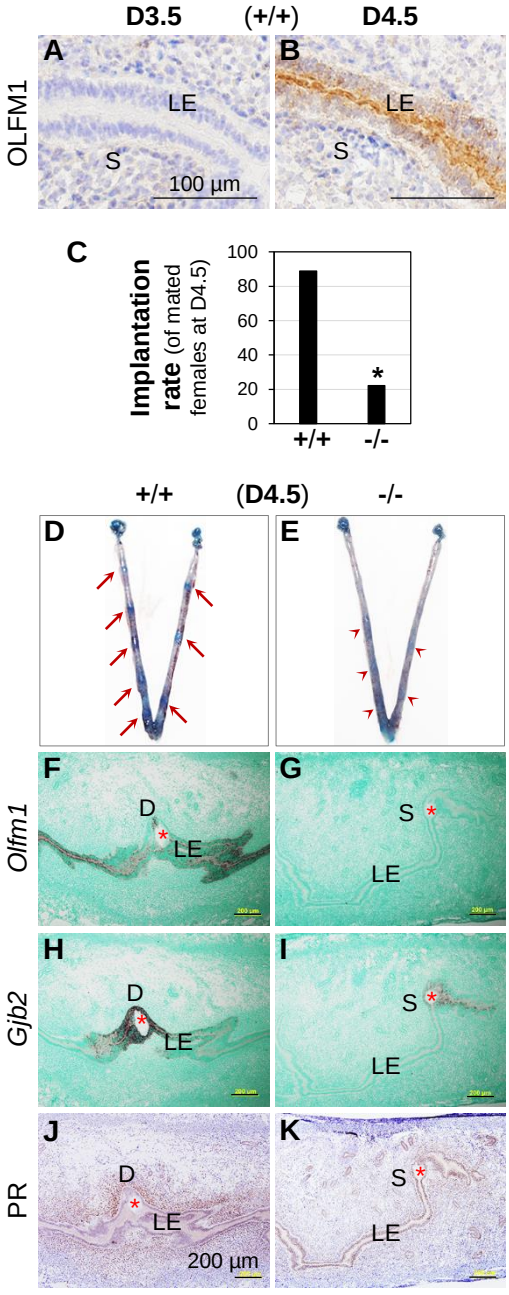

Figure 4.1. Expression of OLFM1 in periimplantation mouse uterus and impaired embryo implantation in *Olfm1*$^{-/-}$ female mice. A & B. Detection of OLFM1 protein in gestation day 3.5 (D3.5) (A) and D4.5 (B) *Olfm1*$^{+/+}$ female (+/+) mouse uterus by immunohistochemistry. Scale bar, 100 µm. C. Implantation rate of plugged *Olfm1*$^{+/+}$ (+/+) and *Olfm1*$^{-/-}$ (-/-) females. N=9; * P=0.015, Fisher's exact test. D. Representative D4.5 *Olfm1*$^{+/+}$ uterus. Red arrows, on-time implantation sites (clear blue bands). E. One *Olfm1*$^{-/-}$ uterus with implantation sites. Red arrowheads, delayed implantation sites (faint blue bands). F, H, and J, serial sections from an implantation site in D; G, I, and K, serial sections from an implantation site in E. F~I, *in situ* hybridization; J & K, immunohistochemistry. F. *Olfm1*, +/+. G. *Olfm1*, -/- tissue served as a second negative control in addition to sense probe negative control (data not shown). H. *Gjb2* (gap junction protein, beta 2), +/+. I. *Gjb2*, -/-. J. PR (progesterone receptor), +/+. K. PR, -/-. F~K scale bars, 200 µm. LE, uterine luminal epithelium; S, stroma; D, decidual zone; red star, embryo.

In comparison, Olfm1-/- females were rarely plugged. Among the 9 Olfm1-/- females that did get plugged after an extended cohabitation period, only two of them exhibited faint implantation sites on D4.5 (P=0.015, Fig. 4.1C, 4.1E), indicating delayed embryo implantation [69, 291]. The delayed embryo implantation in the Olfm1-/- females was also confirmed by the expression of marker genes Gjb2 (gap junction protein, beta 2) (Fig. 4.1H, 4.1I), which is expressed at the implantation site upon embryo attachment [380], and PR (progesterone receptor) (Fig. 4.1J, 4.1K), which disappears from the LE and thenis highly expressed in the decidual cells upon decidualization [69]. Among the 7 *Olfm1*$^{-/-}$ females without implantation sites, 3 had no oocytes nor embryos flushed from

the reproductive tract, one had one oocyte flushed from the uterus, and the rest 3 *Olfm1*$^{-/-}$ females had one to three oocytes flushed from the oviduct. These observations suggested that although embryo implantation was abnormal, more severe issues leading to severely impaired *Olfm1*$^{-/-}$ female fertility occurred in earlier processes, especially mating and ovulation.

4.4.4 Olfactomedin deficiency results in impaired mating activity

To determine the mating activity of *Olfm1*$^{-/-}$ females, 12 *Olfm1*$^{+/+}$ females and 15 *Olfm1*$^{-/-}$ females cohabitated with *Olfm1*$^{+/+}$ stud males were checked daily for the presence of a copulation plug for 4 months. The mating rate was 100% (12/12) for *Olfm1*$^{+/+}$ females and 46.7% (7/15) for *Olfm1*$^{-/-}$ females (P=0.0031) during these 4 months (Fig. 4.2A). The mating latency was dramatically prolonged in the 7 *Olfm1*$^{-/-}$ females that did get plugged (Fig. 4.2B). While the majority of the plugged *Olfm1*$^{+/+}$ females (11/12) mated within 4 days of cohabitation with a median of 2 days, the majority of the plugged *Olfm1*$^{-/-}$ females (5/7) mated over a greatly protracted time period after cohabitation with a median of 49 days (P<0.001) (Fig. 4.2B). Considering both mating rate (Fig. 4.2A) and first plug latency (Fig. 4.2B), the mating activity of young *Olfm1*$^{-/-}$ females decreased over 50-fold (1/0.467 x 49/2=52.5) compared to young *Olfm1*$^{+/+}$ females. Consistent with the 6 month fertility test, 83.3% (10/12) plugged *Olfm1*$^{+/+}$ females while only 14.3% (1/7) plugged *Olfm1*$^{-/-}$ females delivered pups (P=0.0063) (Fig. 4.2C).

Since *Olfm1*$^{-/-}$ females were smaller (Fig. S4.1A) and less active than *Olfm1*$^{+/+}$ females, it was possible that the stud males might prefer *Olfm1*$^{+/+}$ females for mating. To eliminate any potential influence of the *Olfm1*$^{+/+}$ females on the mating activity of the *Olfm1*$^{-/-}$ females, a one month mating test with only one female and one *Olfm1*$^{+/+}$ stud

male per cage was performed. All 6 Olfm1+/+ females were plugged, but none of the 6 Olfm1-/- females was plugged during the one month period (P=0.002). These data demonstrated that Olfm1-/- females had severely impaired mating activity.

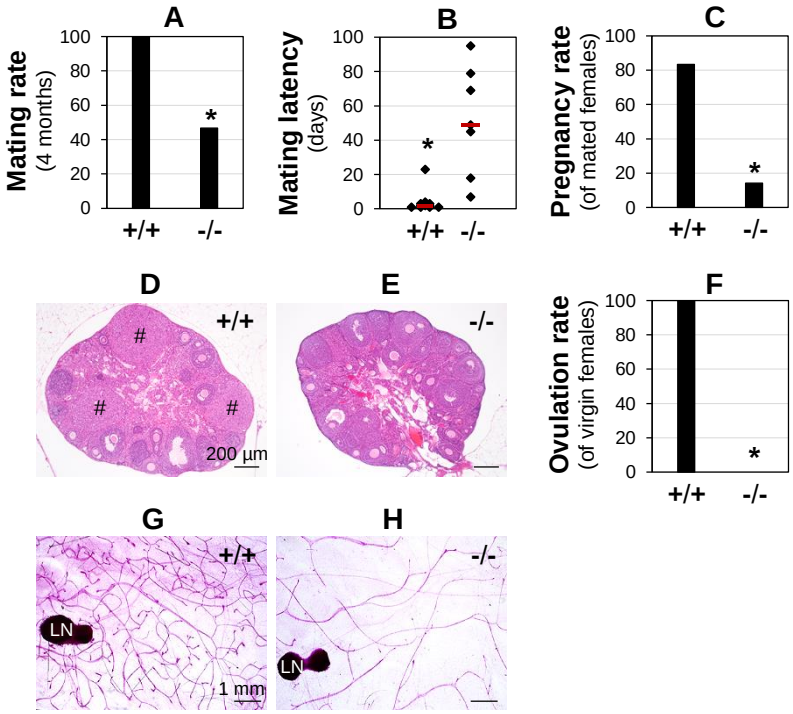

Figure 4.2. Mating activity and ovulation. A. Mating rate of young adult females during 4 months of cohabitation. N=12 for *Olfm1*$^{+/+}$ (+/+) and N=15 for *Olfm1*$^{-/-}$ (-/-) females. * P= 0.0031. B. Mating latency of the mated females in A. Black diamonds, data from individual mice; red lines, median in each group; N=12 (+/+) and 7 (-/-); * P<0.001; two-sample Kolmogorov-Smirnov non-parametric test. C. Pregnancy rate of mated females. N=12 (+/+) and 7 (-/-); * P=0.0063. D~F, data from young adult virgin females. D. Representative ovarian histology from *Olfm1*$^{+/+}$ (+/+) females. #, corpus luteum. E. Representative ovarian histology from *Olfm1*$^{-/-}$ (-/-) females. Scale bar (in D & E), 200 µm.

F. Ovulation rate. N=6; * P=0.0022. A, C, & F: Fisher's exact test. G & H. Representative whole mount mammary gland from *Olfm1*$^{+/+}$ (+/+) females (G) and *Olfm1*$^{-/-}$ (-/-) females (H). N=5 (+/+) and 9 (-/-); LN, lymph node; pink lines, mammary ducts; scale bar, 1 mm.

4.4.5 Ovulation is reduced in *Olfm1*$^{-/-}$ mice

To evaluate ovulation, ovaries from 2-4 month old virgin females were examined. Histology of one ovary from each of 6 virgin *Olfm1*$^{+/+}$ females showed corpora lutea in all of them (Fig. 4.2D). *Olfm1*$^{-/-}$ ovaries revealed no obvious abnormality of follicle development, with primary, secondary, antral, and peri-ovulatory follicles present in all 6 *Olfm1*$^{-/-}$ females. However, no corpora lutea were observed in any of these females (P= 0.0022) (Fig. 4.2E). The ovulation rate was significantly decreased in the *Olfm1*$^{-/-}$ females (Fig. 4.2F). Corpora lutea produce high levels of progesterone, which is critical for mammary duct side branching [382]. Indeed, side branching of the mammary ducts was severely underdeveloped in the *Olfm1*$^{-/-}$ females (Fig. 4.2G, 4.2H). These data indicated that accompanying the defective mating activity, there was defective ovulation in the *Olfm1*$^{-/-}$ females also (Fig. 4.2). Defective mating activity and ovulation (Fig. 4.2) suggested disrupted function of the hypothalamic–pituitary–gonadal (HPG) axis.

4.4.6 Superovulation rescues mating activity and fertility in *Olfm1*$^{-/-}$ females

To evaluate the function of the HPG axis, superovulation was performed. Superovulation has been widely used to induce estrus stage and ovulation in many species. Superovulation completely rescued mating activity in all *Olfm1*$^{-/-}$ females. All superovulated *Olfm1*$^{+/+}$ (N=7) and *Olfm1*$^{-/-}$ (N=8) females had a copulation plug the first night of cohabitation (Fig. 4.3A). The rate of delivering pups in Olfm1+/+ females

(3/7=42.9%) and Olfm1-/- females (4/8=50%) were comparable (Fig. 4.3B), so were the litter sizes (Fig. 4.3C) and gestation periods (Fig. 4.3D). Interestingly, both groups had very small litter sizes, average 1.5-2 pups per litter (Fig. 4.3C). Further study indicated that superovulated females in both groups had on-time implantation and limited embryo resorption on D7.5 (Fig. 4.3E, 4.3F), but extensive embryo resorption on D15.5 (Fig. 4.3G, 4.3H). These data demonstrated that: 1) superovulation not only rescued mating activity

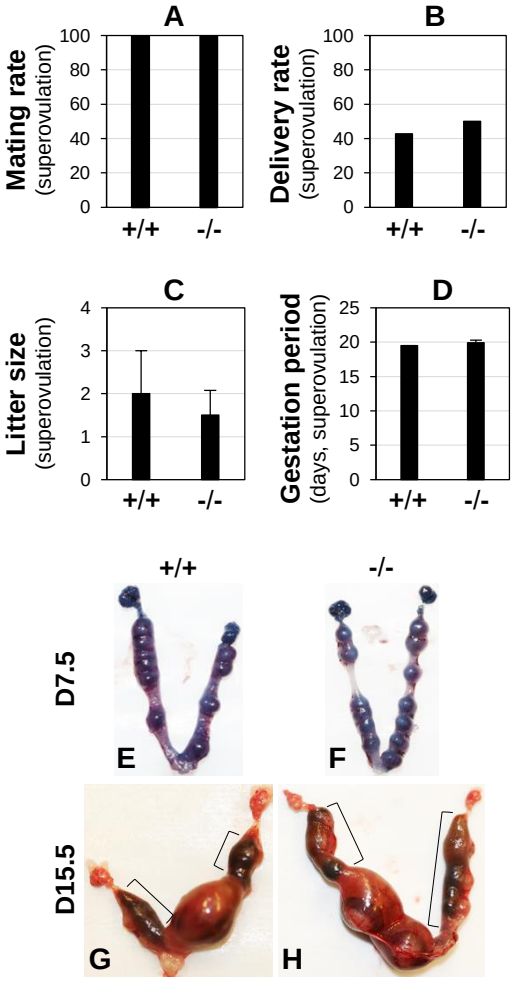

Figure 4.3. Mating activity and fertility upon superovulation with eCG and hCG in 2-4 months old *Olfm1*$^{+/+}$ (+/+) and *Olfm1*$^{-/-}$ (-/-) females. A. Mating rate. B. Delivery rate. A & B: N=7 (+/+) and 8 (-/-); Fisher's exact test. C. Litter size. D. Gestation period. C & D: Error bars, standard deviation; N=3 (+/+) and 4 (-/-); two-sample Kolmogorov-Smirnov non-parametric test. E. Gestation day 7.5 (D7.5) *Olfm1*$^{+/+}$ uterus. F. D7.5 *Olfm1*$^{-/-}$ uterus. G. D15.5 *Olfm1*$^{+/+}$ uterus. H. D15.5 *Olfm1*$^{-/-}$ uterus. Bracket, reabsorbed embryo(s).

but also fertility in *Olfm1*$^{-/-}$ females; 2) defective embryo implantation (Fig. 4.1C-1K) and ovulation (Fig. 4.2D-2F) in the *Olfm1*$^{-/-}$ females were not due to local uterine defect or ovarian defect, but neuroendocrine defect(s). When newly weaned females (3 weeks old) were superovulated with eCG + hCG, the average number of COCs from *Olfm1*$^{+/+}$ females was 47.5±8.1 (N=6) and from *Olfm1*$^{-/-}$ females was 34.5±8.8 (N=6, P=0.024). Superovulation demonstrated functional ovaries although the number of superovulated COCs was reduced in the juvenile *Olfm1*$^{-/-}$ females.

4.4.7 Olfactomedin deficiency does not compromise basal LH level and GnRH-induced LH surge

Because the ovaries were functional in *Olfm1*$^{-/-}$ mice (Fig. 4.3), we turned our attention to the next upstream regulator in the HPG axis, the pituitary gland. The pituitary releases gonadotropins FSH and LH to regulate ovarian development and functions. *Olfm1*$^{-/-}$ females had a significantly increased basal level of FSH compared to *Olfm1*$^{+/+}$ females (N=8, P=0.002, Fig. 4.4A). The basal LH levels were comparable between *Olfm1*$^{+/+}$ females and *Olfm1*$^{-/-}$ females (Fig. 4.4B). An LH surge is induced by GnRH from the hypothalamus and is a prerequisite for ovulation. Both *Olfm1*$^{+/+}$ females and *Olfm1*$^{-/-}$

females had significantly increased LH levels upon exogenous GnRH administration (N=6-8, P=0.023 (+/+) and 0.009 (-/-), Fig. 4.4B). These results indicated that the pituitary in the HPG axis was functional in the *Olfm1*$^{-/-}$ females.

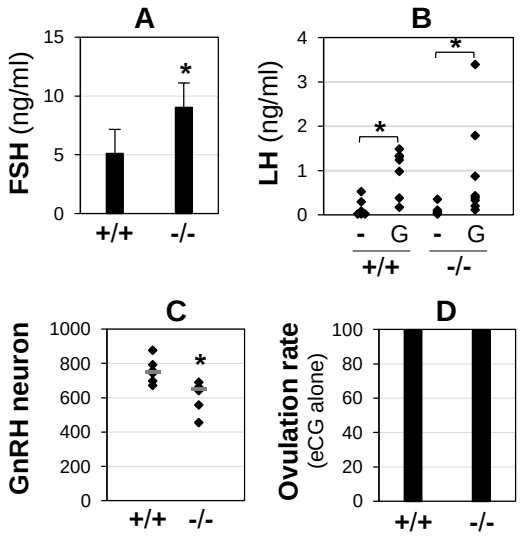

Figure 4.4. Determination of pituitary and hypothalamic functions in *Olfm1*$^{+/+}$ (+/+) and *Olfm1*$^{-/-}$ (-/-) females. A. Basal levels of follicle-stimulating hormone (FSH) in 3 months old females at diestrus stage. Error bars, standard deviation; N=8; * P=0.002. B. Basal levels (-) and GnRH-stimulated levels (G) of luteinizing hormone (LH) in 3 months old females at diestrus stage. Black diamonds, data from individual mice; N=6 for basal levels and N=8 for GnRH-stimulated levels; * (+/+) P=0.023; * (-/-) P=0.009. A & B: Two-sample Kolmogorov-Smirnov non-parametric test. C. Total number of GnRH neurons in anteroventral periventricular nucleus (AVPV) in 2-4 months old females at diestrus. Black diamonds, data from individual mice; N=5; * P=0.026; two tail, unpaired, equal variance

student's t-test. D. Ovulation rate from eCG-treated juvenile females (21-23 days old). N=5 (+/+) and 4 (-/-); Fisher's exact test.

4.4.8 Olfactomedin deficiency does not compromise hypothalamic function

GnRH release from the hypothalamus is a proximal event in activation of the HPG axis. GnRH positive neurons were labeled by immunohistochemistry (Fig. S4.3A, S4.3B). Most GnRH neurons are fusiform with thin cell bodies and two processes, and some are multipolar with triangular or rounded cell bodies [383] (Fig. S4.3C). There was a small ~13% ($P<0.05$) but significant decrease in the total number of GnRH neurons from all sections covering the preoptic area and anterior hypothalamus in *Olfm1*$^{-/-}$ females compared to *Olfm1*$^{+/+}$ females (Fig. 4.4C). Since GnRH neurons receive feedback from steroid hormones, superovulation with eCG alone was performed to determine such feedback function of GnRH neurons in the hypothalamus. It has been demonstrated that eCG alone can stimulate the development of follicles into antral follicles [377, 384], which produce a large amount of estrogen to induce estrogen positive feedback on GnRH release in the hypothalamus, resulting in an LH surge from the pituitary to induce ovulation [385]. All eCG-treated juvenile females (21-23 days old) exhibited ovulation (Fig. 4.4D), indicated by the presence of COCs in the oviducts. The average number of COCs from the control (*Olfm1*$^{+/+}$ & *Olfm1*$^{+/-}$) females was 33.4±3.4 (N=5) and from *Olfm1*$^{-/-}$ females was 21.3±10.8 (N=4, P=0.108). These data (Figs. 4.3, 4.4) demonstrated that *Olfm1*$^{-/-}$ females had a functional HPG axis.

4.4.9 Olfactomedin deficient females are unresponsive to male odor stimulation

It has been reported that multiple female mice housed in the same cage develop longer and irregular estrous cycle [249] and the odor of male mice could stimulate the female mice into estrus stage within a few days to facilitate the mating activities [386]. Young adult virgin females were used in this study. Among the 14 *Olfm1*$^{+/+}$ females

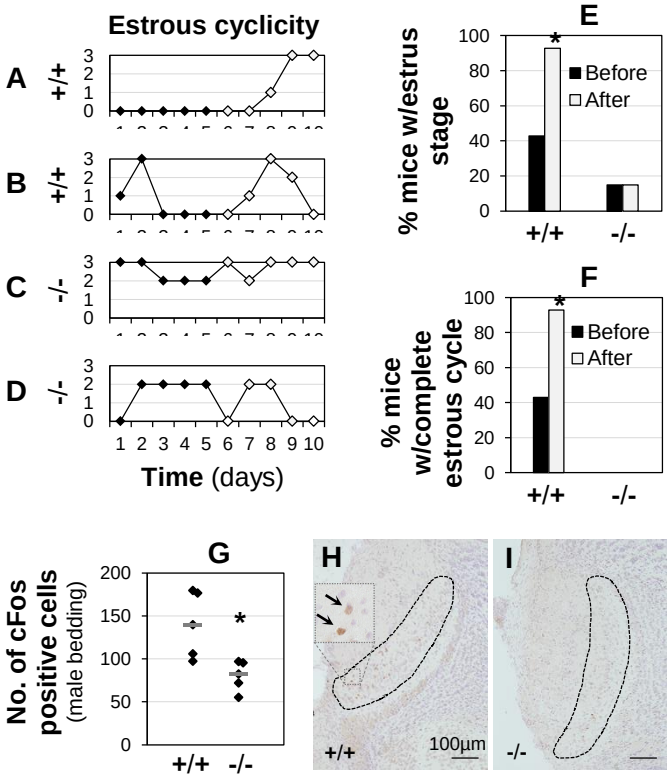

Figure 4.5. Effects of male odor on estrous cyclicity and cFos neuron activation in accessory olfactory bulb in *Olfm1*$^{+/+}$ (+/+) and *Olfm1*$^{-/-}$ (-/-) young adult virgin females. A~D. Representative estrous cyclicity during the 5 days before (black dots) and 5 days after (grey dots) exposure to male bedding. Number assignments: 0, diestrus; 1, proestrus; 2, metestrus; 3, estrus. A. An *Olfm1*$^{+/+}$ female with a complete estrous cycle after exposure to male bedding. B. An *Olfm1*$^{+/+}$ female with complete estrous cycles

before and after exposure to male bedding. C. An *Olfm1*$^{-/-}$ female with estrus stage but without a complete estrous cycle. D. An *Olfm1*$^{-/-}$ female without estrus stage. E. Percentage of mice with estrus stage before and after exposure to male bedding. F. Percentage of mice with a complete estrous cycle before and after exposure to male bedding. E & F: N=14-20; * P=0.0128; Fisher's exact test. G. Male urine on cFos positive neurons in accessory olfactory bulb. N=5; * P=0.014; two tail, unpaired, equal bulb; scale bar, 100 µm; negative control, no specific brown staining (data not shown).

examined, 42% (6/14) had estrus stage and a complete estrous cycle during the 5 days before exposure to male bedding, and 92.8% (13/14, P=0.0128) had estrus stage and a complete estrous cycle during the 5 days after placed on male bedding (Fig. 4.5A, 4.5B, 4.5E, 4.5F). One *Olfm1*$^{+/+}$ female remained in diestrus stage during the entire 10 days of examination. However, among the 20 *Olfm1*$^{-/-}$ females examined, 20% (4/20) had estrus stage, but none of them had a complete estrous cycle during the 5 days before or after exposure to male bedding (Fig. 4.5C, 4.5D, 4.5E, 4.5F). The 4 *Olfm1*$^{-/-}$ females with estrus stage either remained in estrus stage or only had estrus stage and metestrus stage (Fig. 4.5C). These data demonstrated that young adult *Olfm1*$^{-/-}$ females did not respond to male odor stimulation on estrous cyclicity.

cFos is a widely used marker for neuronal activity [387]. cFos positive cells were found in the mitral cell layer of accessory olfactory bulb 90 min after male urine stimulation in both young virgin adult *Olfm1*$^{+/+}$ and *Olfm1*$^{-/-}$ females. There was a significant reduction of cFos positive cells in the *Olfm1*$^{-/-}$ females (140.1±38.5 vs. 80.5±17.3, P=0.014) (Fig. 4.5G). There were no cFos positive cells in the unstimulated *Olfm1*$^{+/+}$ and *Olfm1*$^{-/-}$

accessory olfactory bulb (data not shown). These data are consistent with the blunted response to male odor stimulation in the young adult *Olfm1*$^{-/-}$ females.

To further confirm the defective response of *Olfm1*$^{-/-}$ females to male odor [243], newly weaned control and *Olfm1*$^{-/-}$ females (3 weeks old) were cohabitated in cages with regular bedding (RB) or male soiled bedding (MB). Parameters indicative of female pubertal development were examined, including age at vaginal opening, body weight and estrous cycle. Vaginal opening was an early indicator of puberty onset. Male bedding significantly accelerated vaginal opening in control females but not *Olfm1*$^{-/-}$ females (Fig. 4.6A). The appearance of estrus stage is another indicator of pubertal development. During the 4 weeks of study (3-7 weeks old), 5 out of 6 control females had estrus stage in male bedding compared to 1 out 6 in regular bedding (P=0.08); while in *Olfm1*$^{-/-}$ females, it was 1/4 in male bedding and 0/4 in regular bedding with estrus stage (Fig. 4.6B). These two parameters indicated accelerated pubertal development in control but not *Olfm1*$^{-/-}$ females upon exposure to male bedding. Accordingly, the body weight of control females at 7 weeks old was significantly increased in the male bedding group, whereas no such change was observed in the *Olfm1*$^{-/-}$ females (Fig. 4.6C). Both absolute and relative ovary weights were significantly increased in the control females in the male bedding group, but there was no change in the *Olfm1*$^{-/-}$ females upon exposure to male bedding (Fig. 4.6D, 4.6E). Ovarian histology indicated that 2 out of 6 control females in the male bedding group had corpora lutea, whereas none of the control females in the regular bedding and no *Olfm1*$^{-/-}$ females in both beddings had corpora lutea (data not shown). The results (Figs. 4.5, 4.6) demonstrated that there was defective olfaction in the *Olfm1*$^{-/-}$ females that impaired pubertal development and sexual maturation, resulting in impaired fertility.

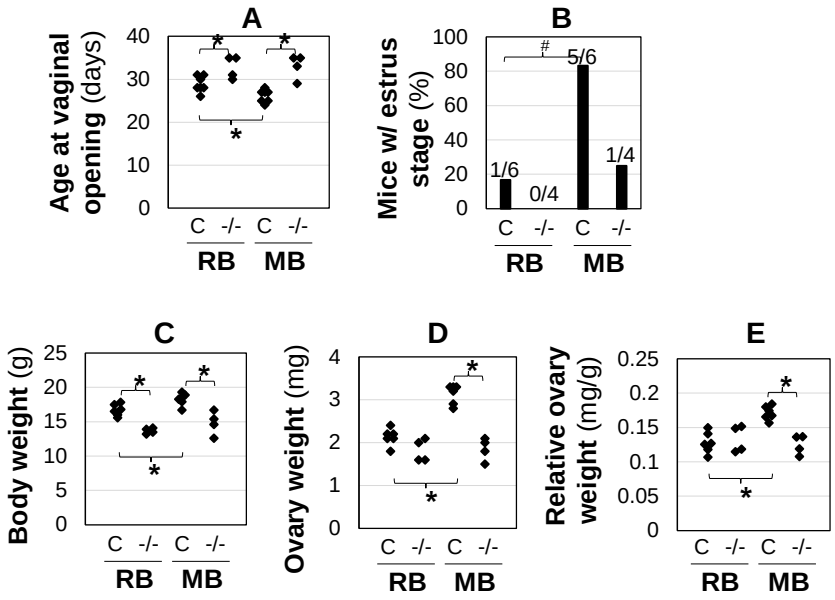

Figure 4.6. Effects of male bedding on pubertal development and gene expression in forebrain. C, control females (*Olfm1*$^{+/+}$ & *Olfm1*$^{+/-}$, N=6)); -/-, *Olfm1*$^{-/-}$ (N=4); RB, regular bedding; MB, male bedding. A. Age at vaginal opening. #, P=0.065; * P=0.014 (control MB vs control RB), P<0.001 (-/- MB vs control MB), and P=0.015 (-/- RB vs control RB). B. Percentage of mice with estrus stage during 3-7 weeks old. #, P=0.0801; Fisher's exact test; the fraction on top of each column, number of mice with estrus stage over total number of mice in each group. C. Body weight. * P=0.011 (control MB vs control RB), P=0.003 (control MB vs -/- MB), and P<0.001 (control RB vs -/- RB). D. Ovary weight. * P<0.001. E. Relative ovary weight. * P<0.001. A, C, D, & E: two tail, unpaired, equal variance student's t-test.

4.4.10 Cellular localization of OLFM1 in the olfactory system

The *Olfm1*$^{-/-}$ females had a functional HPG axis (Figs 4.3, 4.4) but defective olfaction (Figs. 4.5, 4.6). To support the function of OLFM1 in olfaction, the

spatiotemporal expression of OLFM1 in the *Olfm1*$^{+/+}$ female olfactory systems was determined by immunohistochemistry. There are two olfactory systems, the main olfactory system with the main olfactory epithelium and main olfactory bulb and the accessory olfactory system with vomeronasal organ and accessory olfactory bulb. On D13.5, OLFM1 was not detected in olfactory epithelium (Fig. S4.4A). On D15.5, OLFM1 was not detected in the olfactory epithelium at main olfactory epithelium or vomeronasal organ; it was detected in the outer rim of the forebrain in the region of the mitral cell layer of the main olfactory bulb (Fig. S4.4B). On PND0, OLFM1 was highly expressed in the olfactory epithelium of main olfactory epithelium and vomeronasal neuroepithelium of vomeronasal organ, and axon bundles of sensory neurons in main olfactory epithelium (Figs. 4.7A, 4.7G, S4.4D). It was also highly expressed in both main olfactory epithelium and accessory olfactory bulb, especially the glomerulus layer and mitral cell layer in the main olfactory bulb (Fig. 4.7B) and lateral olfactory tract in the accessory olfactory bulb (Fig. 4.7H). In young adult females, OLFM1 was barely detectable in the olfactory epithelium but highly expressed in the axon bundles of sensory neurons of main olfactory epithelium (Fig. 4.7D). It remained expressed in the vomeronasal neuroepithelium of vomeronasal organ and was detectable in the axon bundles of sensory neurons of vomeronasal organ (Fig. 4.7J). OLFM1 had moderate levels of staining in the glomerulus layer and high levels of staining in some scattered cells in the external plexiform layer and mitral cell layer of main olfactory bulb (Figs. 4.7E, S4.4F). There was also OLFM1 immunoreactivity in the mitral cell layer of accessory olfactory bulb (Fig. 4.7K). Negative controls using no primary antibody in *Olfm1*$^{+/+}$ sections (Fig. S4.4C, S4.4E) or using an *Olfm1*$^{-/-}$ section (Fig. S4.4G) confirmed the specificity of the immunostaining. *Olfm1*

mRNA was detected in the mitral cell layer but not the glomerulus layer (Fig. 4.7C, 4.7F, 4.7I, 4.7L).

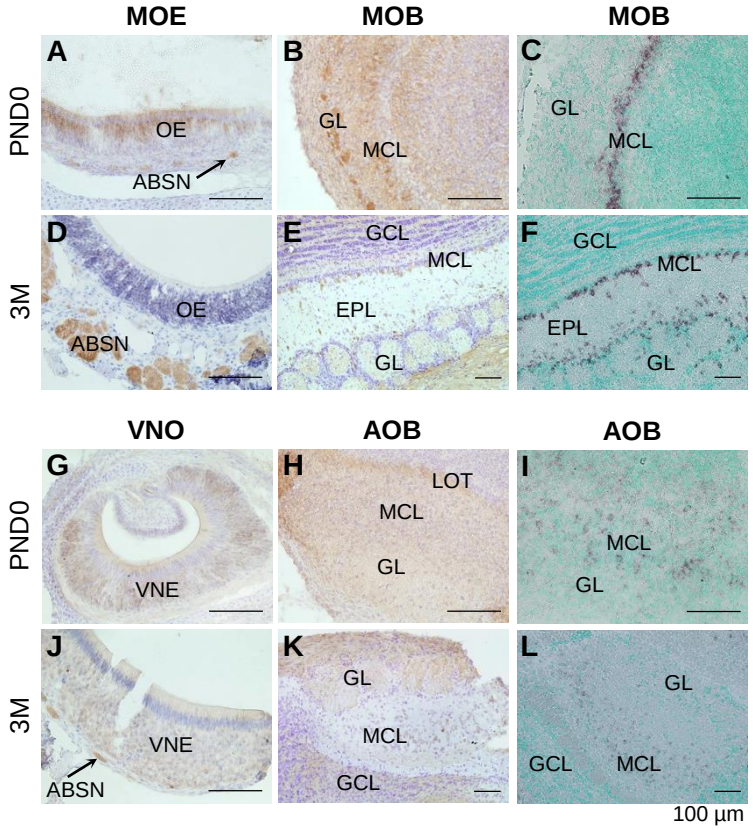

Figure 4.7. Expression of OLFM1 in *Olfm1*$^{+/+}$ female main olfactory system (A~F) and accessory olfactory system (G~L) by immunohistochemistry (A, B, D, E, G, H, J, K) and *in situ* hybridization (C, F, I, L). MOE, main olfactory epithelium; MOB, main olfactory bulb; VNO, vomeronasal organ; AOB, accessory olfactory bulb; PND0, postnatal day 0; 3M, 3 months old. A. PND0 MOE. B & C. PND0 MOB. D. 3M MOE. E & F. 3M MOB. G. PND0 VNO. H & I. PND0 AOB. J. 3M VNO. K & L. 3M AOB. ABSN, axon bundles of sensory neurons; EPL, external plexiform layer; GCL, granule cell layer; GL, glomerular layer; MCL, mitral cell layer; LOT, lateral olfactory tract; OE, olfactory epithelium; VNE, vomeronasal neuroepithelium; scale bar, 100 µm.

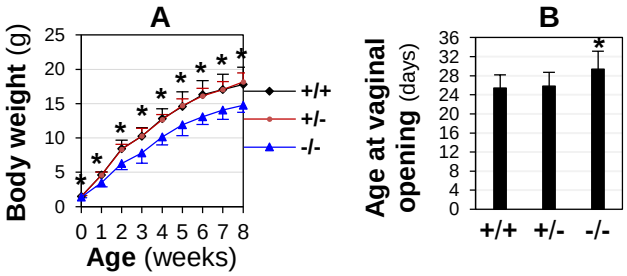

Figure S4.1. Growth curve and age at vaginal opening in *Olfm1*$^{+/+}$ (+/+), *Olfm1*$^{+/-}$ (+/-), and *Olfm1*$^{-/-}$ (-/-) females. A. Body weight from birth to 8 weeks old. N=24-37; * P<0.05 (-/- vs. +/+; -/- vs. +/-); ANOVA with repeated measures. B. Age at vaginal opening. N=35-82; * P<0.05; two-sample Kolmogorov-Smirnov non-parametric analysis. A & B: Error bar, standard deviation.

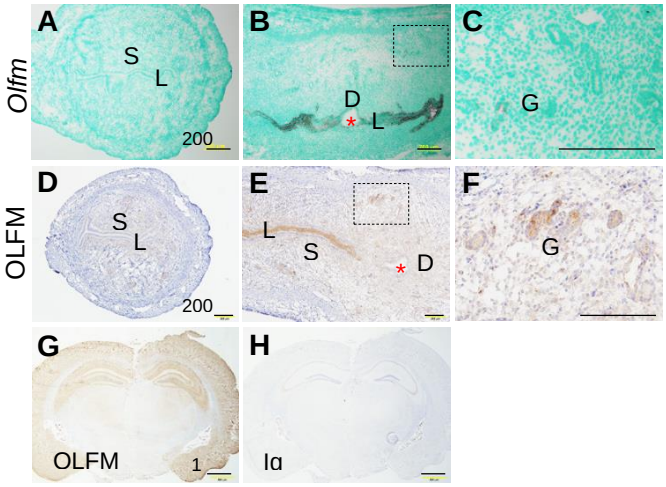

Figure S4.2. Expression of OLFM1 in periimplantation wild type mice. A~C, *in situ* hybridization; D~H, immunohistochemistry. A. Gestation day 3.5 (D3.5) uterus, cross section, *Olfm1* antisense probe. B. D4.5 uterus, longitudinal section, *Olfm1* antisense probe. C. Enlarged view of the rectangle in B to show *Olfm1* expression in glandular

epithelium. D. D3.5 uterus, cross section, anti-OLFM1 antibody. E. D4.5 uterus, longitudinal section, anti-OLFM1 antibody. F. Enlarged view of the rectangle in B to show OLFM1 expression in glandular epithelium. G. Brain, anti-OLFM1 antibody, positive control. H. Brain, anti-mouse IgG antibody, negative control. Scale bars, 200 μm for A~F and 1 mm for G & H. LE, uterine luminal epithelium; S, stroma; D, decidual zone; red star, embryo; G, glandular epithelium.

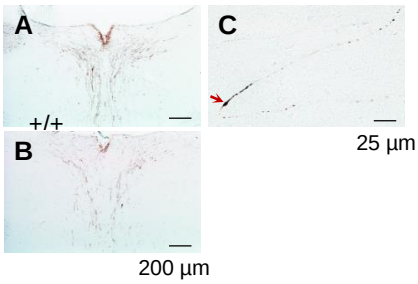

Figure S4.3. Immunohistochemistry of GnRH neurons. A & B. Representative sections of *Olfm1*$^{+/+}$ (+/+) (A) and *Olfm1*$^{-/-}$ (-/-) (B) forebrain anteroventral periventricular nucleus showing GnRH neurons and axons (brown). Scale bar, 200 μm. C. A GnRH neuron (arrow) with axon (dark brown). Scale bar, 25 μm.

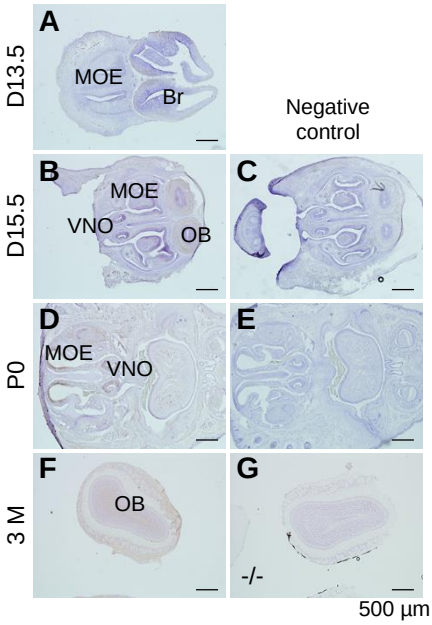

Figure S4.4. Spatiotemporal expression of OLFM1 in the *Olfm1*$^{+/+}$ olfactory systems. A. Gestation day 13.5 (D13.5) head. B. D15.5 head. C. D15.5 head negative control, no primary antibody. D. Postnatal day 0 (P0) head. E. P0 head negative control, no primary antibody. F. 3 month old (3M) olfactory bulb. F. 3M *Olfm1*$^{-/-}$ (-/-) olfactory bulb as a negative control. MOE: main olfactory epithelium; Br, brain; VNO, vomeronasal organ; OB, olfactory bulb; scale bar, 500 µm.

4.5 Discussion

The objective of this study was to determine the mechanism(s) responsible for the fertility defect in the *Olfm1*$^{-/-}$ females [369]. Although we hypothesized that defective embryo implantation was the cause for the defective fertility in the *Olfm1*$^{-/-}$ females, and indeed embryo implantation was abnormal in the *Olfm1*$^{-/-}$ females, defective mating and ovulation also contributed to the defective fertility. The fertility defects were demonstrated to be secondary effects with the proximal cause being defective regulation of the HPG

axis, apparently resulting from defective olfaction in the *Olfm1*$^{-/-}$ females. The loss of OLFM1 in the olfactory system is consistent with a role for impaired olfaction in the defective fertility of *Olfm1*$^{-/-}$ females.

The HPG axis is the central control system that regulates mating and ovulation. We found that superovulation with eCG and hCG rescued mating and pregnancy, as well as ovulation and embryo implantation, which eliminated any obvious local defects in the female reproductive system but pointed to neuroendocrine defects in the reduced fertility in the *Olfm1*$^{-/-}$ females. The main function of eCG in this regimen was to stimulate follicle growth and that of hCG was to induce ovulation and luteinization [377, 384]. It has been reported that eCG alone could not induce ovulation in hypogonadal mice with deficient GnRH neurons, or prepubertal C57 females treated with GnRH antagonists [388]. In addition, whereas only one out of nine *in vitro* perfused ovary which had been primed with eCG for two days ovulated one oocyte, all the nine ovaries ovulated multiple oocytes after one dose of LH stimulation [389]. A functional HPG axis is required for eCG to induce ovulation. When only eCG was used for superovulation, the maturing ovarian follicles produce a large amount of estrogen which mediates positive feedback on GnRH release in the hypothalamus, and an LH surge from the pituitary to induce ovulation. Since ovulation occurred in all eCG-treated *Olfm1*$^{-/-}$ females, these females had a functional HPG axis. However, there was a ~27% reduction of COCs in the eCG and hCG-treated juvenile *Olfm1*$^{-/-}$ females and ~36% reduction of COCs in the eCG alone-treated juvenile *Olfm1*$^{-/-}$ females. These reductions could be caused by the smaller size (~24% lighter at 3 weeks old) of the juvenile *Olfm1*$^{-/-}$ females. Interestingly, there were more COCs from eCG and hCG treatment than from eCG treatment in both control and *Olfm1*$^{-/-}$ juvenile

females, indicating that hCG further boosted ovulation in both control and *Olfm1*$^{-/-}$ juvenile females.

GnRH neurons converge on pathways for triggering ovulation, and GnRH is the first key player in the HPG axis to regulate reproduction [115, 390]. During development, GnRH neurons originate from the olfactory placodes and migrate across the nasal septum toward olfactory bulb and become dispersed in the forebrain [22]. Successful migration is critical for the survival of GnRH neurons. OLFM1 plays an important role in cortical neuron migration [271], and might therefore also be involved in GnRH neuron migration. However, the number of GnRH neurons in the hypothalamus of *Olfm1*$^{-/-}$ females was ~13% lower compared to controls, indicating that GnRH neuron migration was not obviously impaired in the *Olfm1*$^{-/-}$ females. In addition, such a small reduction of GnRH neurons should not pose any significant negative effect on female fertility because it was reported that as low as 34% GnRH neurons were sufficient to support the fertility of female mice [391]. The functional HPG axis was also supported by the observations that *Olfm1*$^{-/-}$ females had comparable serum basal and GnRH-induced LH levels with the control. Interestingly, basal serum FSH level was increased in the *Olfm1*$^{-/-}$ females. Since *Olfm1*$^{-/-}$ females had defective ovulation, it was possible that an increased FSH level was contributed by the reduced negative feedback from corpora lutea. However, such an increase was not observed for serum LH level in the *Olfm1*$^{-/-}$ females. Interestingly, a functional HPG axis was also reported in female mice overexpressing FGF21 that had delayed puberty, defective mating activity, and continuous diestrus stage [392]. Whether an olfactory deficit contributes to the reproductive abnormalities of FGF21 deficient mice is unknown.

The data from superovulation with eCG+hCG and eCG alone as well as GnRH neurons and LH and FSH levels suggested that the endogenous stimulation of HPG axis was insufficient to activate HPG axis in the *Olfm1*$^{-/-}$ females. Although different stages of follicles, including late stage follicles that produce a large amount of estrogen for positive estrogen feedback on GnRH neurons, were present in the *Olfm1*$^{-/-}$ ovaries, the positive estrogen feedback from ovarian follicles was insufficient to induce LH surge for ovulation. In addition to positive estradiol feedback from maturing ovarian follicles, there are other regulators of preovulatory GnRH surge, such as circadian rhythm [115] and metabolism [114, 393]. Since the HPG axis of *Olfm1*$^{-/-}$ females was functional in receiving positive feedback from eCG treatment, it is possible that impaired regulation by other regulators plays a role in the defective mating and ovulation in the *Olfm1*$^{-/-}$ females, although any deficiency in these regulators could be overcome by strong exogenous eCG or eCG+hCG stimulations to activate HPG axis for ovulation.

OLFM1 was originally identified in the frog olfactory neuroepithelium [261, 362]. A recent study demonstrated that *Olfm1*$^{-/-}$ mice had reduced volume of olfactory bulb and defective smelling, which was indicated by the reduced time in exploring different smells, including urine [282]. Olfaction can regulate suprachiasmatic nucleus [394-396], a key regulator of the preovulatory GnRH surge [115], potentially via kisspeptin to activate GnRH neurons [390, 397]. Defective olfaction is associated with defective GnRH function in the humans [398]. Although several mutant mice with mild olfactory defects could still maintain normal ovulation [399, 400], it has been reported that olfaction is important in guiding mating behaviors of mice [401-403]. Crowded females unexposed to male odor for extended period show anovulation, and male odor could stimulate them to resume the

estrous cycle [402]. These observations support the notion that olfaction defects in the *Olfm1*$^{-/-}$ mice contribute to the female fertility defects. Mating and ovulation are associated with the estrous cycle, therefore estrous cyclicity is critical for female fertility. *Olfm1*$^{-/-}$ females lacked estrous cyclicity and were nonresponsive to male odor stimulation, demonstrating that the olfaction defects in the *Olfm1*$^{-/-}$ females affected their estrous cyclicity and fertility.

Molecular evidence revealed a ~43% reduction of male urine-stimulated cFos positive cells in the mitral cell layer of *Olfm1*$^{-/-}$ female accessory olfactory bulb. cFos is a widely used neuron activity marker and has been correlated with multiple emotional and behavioral changes [387]. Male odor stimulates cFos expression in the olfactory system and promotes mating activity of female mice [243, 404, 405]. The reduction of male urine-stimulated cFos positive cells might result from the ~25% reduction of olfactory bulb volume and the reduced signal transduction from olfactory epithelium to olfactory bulb in the *Olfm1*$^{-/-}$ females [282].

Besides defective fertility, other endocrine-related issues, such as reduced postnatal growth rate, delayed vaginal opening, and severely underdeveloped mammary gland side branching were also observed in the *Olfm1*$^{-/-}$ females. Because olfaction is critical for suckling [406, 407], the reduced increase of body weight from newborn (~5% less than control) to one week old (~25% less than control) in the *Olfm1*$^{-/-}$ females was most likely due to defective olfaction leading to reduced milk intake [282]. Vaginal opening is a noninvasive biomarker for pubertal onset in rodents. Higher body weight is normally correlated with earlier pubertal development [339]. Delayed vaginal opening in the *Olfm1*$^{-/-}$ females might be caused by the lower body weight. Since the HPG axis is

central to pubertal development [408], vaginal opening, albeit delayed, indicated a functional HPG axis in the *Olfm1*$^{-/-}$ females. Interestingly, *Olfm1*$^{-/-}$ females exhibited normal main mammary duct growth, but severely underdeveloped side branches. Since the former is mainly stimulated by estrogen signaling and the latter is controlled by progesterone signaling [382], the development of mammary gland in the *Olfm1*$^{-/-}$ females suggests normal ovarian follicle development for estrogen secretion but defective ovulation and corpora lutea formation for progesterone secretion, which is consistent with the results of our histological analysis of the ovaries of *Olfm1*$^{-/-}$ females. However, because OLFM1 is expressed in mammary gland epithelium (data not shown), it can't be ruled out that the mammary gland defect in *Olfm1*$^{-/-}$ females is a primary genetic effect.

Although the majority of *Olfm1*$^{-/-}$ females were infertile, a small fraction of them could still reproduce. Such individual variations could potentially result from compensation from other olfactomedin proteins, such as OLFM2, which also plays a role in olfactory function in mice [409], and OLFM3 that shares similar expression patterns and structures with OLFM1 [263] and coprecipitates with OLFM1 [282]. In addition, there was a truncated C-terminus OLFM1 protein in the *Olfm1*$^{-/-}$ mice and the truncated C-terminus OLFM1 protein has different coprecipitation partners from the wild type OLFM1 protein [282], which could potentially add more complexity to the individual variations.

We observed that pregnancies from superovulation had reduced litter sizes. The small litter sizes could result from the high percentage of defective embryos from superovulation [410, 411]. Although many superovulated oocytes could be fertilized and implant, most implanted embryos had defective postimplantation embryonic development and eventually were reabsorbed.

Olfm1 was one of the most upregulated genes in the uterus upon embryo implantation [370]. *OLFM1* mRNA expression was decreased in the human endometrium upon the establishment of uterine receptivity in the secretory phase (reviewed in [412]), but increased in the human endometrium in women with unexplained recurrent spontaneous abortion [413]. The opposite expression patterns of *Olfm1* in the periimplantation mouse and human uterus is reminiscent of another glycoprotein, mucin 1, which exhibits reduced expression in mouse uterus, but increased expression in human uterus, upon establishment of uterine receptivity [414]. It was suggested that decreased expression of *OLFM1* during the secretory phase of the human endometrium may allow successful trophoblast attachment for implantation [265]. However, olfactomedin proteins are generally involved in cell adhesion [364, 415].

In summary, OLFM1 was detected in the uterus, HPG axis (data not shown), and olfactory systems. Deletion of *Olfm1* led to impaired embryo implantation, defective mating and ovulation that are under the control of HPG axis, as well as defective smelling. Defective olfaction was the main cause of defective fertility in the *Olfm1*$^{-/-}$ females because these females had a functional HPG axis and superovulation could rescue all the defects that contributed to the fertility issue. However, the defined level(s) of OLFM1 in regulating female fertility can be obtained from tissue selective *Olfm1*-deficient models.

Acknowledgements

The authors thank the Department of Pathology in the College of Veterinary Medicine, University of Georgia for access to the imaging system; Dr. Simonetta Camandola at National Institutes on Aging for preparing the founder mice; Dr. Jesse Schank at University of Georgia for providing anti-cFos antibody; Office of the Vice

President for Research, Interdisciplinary Toxicology Program, and Department of Physiology and Pharmacology at the University of Georgia, the National Institutes of Health (NIH R15HD066301 and NIH R01HD065939 (co-funded by ORWH and NICHD) to XY) for financial support. This work was also funded, in part, by the Intramural Research Program of the National Institute on Aging.

CHAPTER 5

CONCLUSION AND FUTURE DIRECTION

Puberty and reproduction are important aspects of human life. A trend of earlier puberty during the past decades has been found in US and European girls [284-288]. Disrupted pubertal timing has been correlated with higher risk of psychological and social problems, such as depression, anxiety, and aggression, etc., as well as chorionic diseases, such as diabetes, breast cancer, and cardiovascular diseases [416-419]. During the past decades, there is also a trend of more women with reproductive problems and decreased fertility [420, 421]. The overarching goal of my PhD study is to explore potential causes and underlying mechanism for the earlier puberty and increased infertility in females.

It is well known that female puberty and reproduction could be affected by both environmental and genetic factors. Genistein, an endocrine disruptor, has been regarded as one contributing factor for early puberty [284, 286, 287] based on a positive correlation between genistein/soy and earlier puberty. However, a causal effect of genistein on earlier puberty had not been established [197, 422]. Considering the high exposure of genistein due to the popularity of soy food, studying the effects of genistein on female puberty and reproduction is significant for human health.

The increased rate of population with overweight and obesity has become a health issue in the USA and most of the rest world [423]. In addition to its adverse effects on metabolism and cardiovascular system, increased Body Mass Index (BMI) is also

correlated with advanced puberty [207]. On the other hand, a very low percentage of body fat might also be related to disrupted female menstrual cycle [16]. Several genetic mutations in mice and humans are related to extremely low body fat [17-19]. *Bscl2*$^{(-/-)}$ mouse model recapitulates human congenital generalized lipodystrophy [424]. Exposed newly weaned *Bscl2*$^{(-/-)}$ female mice to genistein will potentially provide insight into the interplay between environmental (genistein) and genetic (*Bscl2*) factors on female pubertal development.

Female puberty and reproduction are under the control of HPG axis, which can be affected by other factors, such as olfaction. It was reported that *Olfm1*$^{(-/-)}$ female mice were not good breeders [369]. The functions of OLFM1 in female puberty and fertility and the mechanism involved had not been investigated. *Olfm1*$^{(-/-)}$ mouse model has been employed in my dissertation to study a genetic factor on female puberty and reproduction.

Accordingly, my first project indicated the effects of environmental factor, genistein, on promoting female puberty using C57BL/6 mouse model (Chapter 2); my second project found out female puberty was disrupted by the deletion of genetic factor, *Bscl2*, and the interplay effects between genetic factor, *Bscl2*, and environmental factor, genistein using *Bscl2*$^{(-/-)}$ mouse model (Chapter 3); my third project explored the functions and mechanism of OLFM1 in female puberty and reproduction using *Olfm1*$^{(-/-)}$ mouse model (Chapter 4). Several conclusions are drawn from these studies.

1) Environmental factor (genistein): 1) 5, 100 and 500 ppm postweaning dietary genistein exposure advanced the age of vaginal opening, increased the percentage of estrus stage, and accelerated mammary gland development at a dose dependent manner, and 5 ppm significantly advanced the age of ovulation. 2) 500 ppm genistein diet did not

pose any significant negative effects on early pregnancy in young female mice. 3) At 5 weeks old, 500 ppm genistein stimulated the mRNA levels of epithelial markers *CK 5*, *8*, *14*, *18*, *Areg*, *PR*, *wnt4*, but did not affect the mRNA or protein levels of *ERα* and *ERβ* in the mammary gland.

2) Interactive effects of environmental factor (genistein) and genetic factor (*Bscl2*): 1) *Bscl2*$^{(-/-)}$ female mice with lipodystropy had segregated pubertal development processes. Compared to the wildtype / heterozygous littermates, vaginal opening was delayed but mammary gland development was accelerated in *Bscl2*$^{(-/-)}$ female mice. 2) Postweaning 500 ppm genistein dietary exposure still accelerated vaginal opening and increased mammary gland area in *Bscl2*$^{(-/-)}$ mice. 3) Due to the accelerated mammary duct length elongation and limited fat pad in *Bscl2*$^{(-/-)}$ mammary gland, genistein had less effect on mammary gland growth in *Bscl2*$^{(-/-)}$ mammary gland compared to control. 4) Reduced expression of ERβ might contribute to the accelerated mammary gland growth in *Bscl2*$^{(-/-)}$ female mice.

3) Genetic factor (*Olfm1*): 1) OLFM1 is expressed in the peri-implantation uterus, HPG axis and olfaction system. 2) Deletion of OLFM1 caused delayed pubertal development and defective fertility. 3) Reduced mating activities, impaired embryo implantation, ovulation failure and reduced mammary duct branching might all contribute to the fertility defects. 4) Delayed vaginal opening indicated delayed pubertal development in *Olfm1*$^{(-/-)}$ female mice. 5) Superovulation rescued fertility, normal basal FSH and LH levels, GnRH induced LH levels and eCG alone stimulated ovulation suggested functional uterus and HPG axis in *Olfm1*$^{(-/-)}$ female mice. 6) Reduced cFOS positive cells in the mitral layer of AOB upon male urine stimulation, and

unresponsiveness to male bedding stimulation on estrous cycle and pubertal development suggested disrupted olfaction in *Olfm1*$^{(-/-)}$ females. 7) Disrupted olfaction contributed to defective puberty and fertility in *Olfm1*$^{(-/-)}$ females.

Based on these findings, more problems are unveiled and required in future studies.

My first project indicated that genistein could accelerate pubertal development in a dose dependent manner. How did this happen? There are still no direct evidence. Because vaginal opening, estrus stage and mammary gland development are mainly controlled by estrogen, and genistein is a phytoestrogen, it is highly possible that 100 and 500 ppm genistein diet had direct effects on these target organs. In contrast, 5 ppm genistein diet had minimal effects on these indicators but advanced ovulation. Because ovulation is initiated by HPG axis, it is highly possible that 5 ppm geistein diet could stimulate HPG axis to regulate ovulation.

In my second project, lipodystrophic *Bscl2*$^{(-/-)}$ female mice showed delayed vaginal opening and accelerated mammary gland development at 5 weeks old. How did this happen? Because vaginal opening could be accelerated by 500 ppm genistein diet, it is possible that in *Bscl2*$^{(-/-)}$ females the delayed vaginal opening is caused by low levels of estrogen in the circulating systems. If this is true, the mammary gland development was accelerated when estrogen levels were low. It is possible that this is related to altered responsiveness to estrogen in the mammary gland epithelium, based on the reduced ERβ expression in the mammary gland epithelium.

In my third project, both mRNA and protein levels of *Olfm1* are highly expressed in the uterine luminal epithelium upon embryo implantation, but superovulation rescued

embryo implantation in *Olfm1*$^{(-/-)}$ females, indicating that uterine epithelial OLFM1 may not be essential for embryo implantation. One possibility is that other olfactomedin proteins or the presence of the truncated C terminus OLFM1 in the *Olfm1*$^{(-/-)}$ females may compensate for the loss of OLFM1 in the uterus. Three big questions remain from project 3 are how OLFM1 regulates olfaction, how the olfaction signal is relayed to affect female puberty and fertility, and whether similar mechanism exist for the male.

Besides, all the three projects have used mouse model, how to interpret the results for humans?

Humans are highly exposed to genistein through food. The doses of genistein diet in my study are all human relevant. Specifically, 500 ppm is found in some soy food, like soy bacon [122]; 100 ppm and 5 ppm could produce plasma levels of genistein in rodents that is similar to people who is on Asian or western diet respectively [142]. Mammary gland development during puberty and initiation of ovulation in human and mice shared similar molecular mechanism. My findings that all the three doses have some stimulation effects on mammary gland development or ovulation in female mice highlighted the risks of soy food on pubertal development of humans, especially girls.

BSCL2 mutation has been identified in human a few decades ago [425]. But it is still unknown whether *BSCL2* mutation and related lipodystrophy affect pubertal onset. *Bscl2*$^{(-/-)}$ mouse model recapitulates human congenital generalized lipodystrophy of *BSCL2* mutated patients . My findings suggested a novel role of *Bscl2* on mammary gland development during puberty and indicated *Bscl2* deletion did not impair the responses of mice to the environmental factor genistein, which would help us to understand the

mechanism of mammary gland development in humans, and also emphasized the interactive effects of genetic and environmental factors in the toxicology studies.

Olfaction is one of the key components for rodent reproduction. Although the importance of olfaction on human reproduction is still controversial, it is well known that olfaction system receive the olfactory signals from environment and project to multiple brain regions. The importance of olfaction on normal brain functions have been further indicated as olfactory dysfunction has been correlated with several brain diseases such as Alzheimer's disease, Parkinson's disease etc. [426-428]. And my finding suggested a pathway where *Olfm1* deletion impaired female reproduction through olfactory defects. It is possible that in humans, genetic mutation or physical disruption of the similar pathway might also impair the female reproduction. Furthermore, it has to be cautious to assess the toxicity of any volatile chemicals, as the direct damage on the olfaction system might also impair the fertility.

In summary, my PhD study used three animal models to investigate the influences of the environmental and genetic factors on female puberty and reproduction. Endocrine disruptors (e.g., genistein) and genetic factors (e.g., *Bscl2*, *Olfm1*) can affect female puberty and reproduction. The molecular mechanisms of each factor in influencing female puberty and reproduction remain to be further investigated.

REFERENCE

1. Dyrmundsson, O.R., *Natural Factors Affecting Puberty and Reproductive-Performance in Ewe Lambs - a Review.* Livestock Production Science, 1981. **8**(1): p. 55-65.
2. Daniel, Y., et al., *Analysis of 104 twin pregnancies conceived with assisted reproductive technologies and 193 spontaneously conceived twin pregnancies.* Fertil Steril, 2000. **74**(4): p. 683-9.
3. Christensen, A., et al., *Hormonal Regulation of Female Reproduction.* Hormone and Metabolic Research, 2012. **44**(8): p. 587-591.
4. Tena-Sempere, M., *Kisspeptin signaling in the brain: recent developments and future challenges.* Mol Cell Endocrinol, 2010. **314**(2): p. 164-9.
5. Wheeler, M.D., *Physical changes of puberty.* Endocrinol Metab Clin North Am, 1991. **20**(1): p. 1-14.
6. Judd, L.L., *The normal psychological development of the american adolescent; a review.* Calif Med, 1967. **107**(6): p. 465-70.
7. Sklar, C.A., S.L. Kaplan, and M.M. Grumbach, *Evidence for Dissociation between Adrenarche and Gonadarche - Studies in Patients with Idiopathic Precocious Puberty, Gonadal-Dysgenesis, Isolated Gonadotropin-Deficiency, and Constitutionally Delayed Growth and Adolescence.* Journal of Clinical Endocrinology & Metabolism, 1980. **51**(3): p. 548-556.
8. Klein, K.O., et al., *Estrogen levels in girls with premature thelarche compared with normal prepubertal girls as determined by an ultrasensitive recombinant cell bioassay.* Journal of Pediatrics, 1999. **134**(2): p. 190-192.
9. Apter, D., *Serum Steroids and Pituitary-Hormones in Female Puberty - Partly Longitudinal-Study.* Clinical Endocrinology, 1980. **12**(2): p. 107-120.

10. Rodriguez, I., et al., *Mouse vaginal opening is an apoptosis-dependent process which can be prevented by the overexpression of Bcl2.* Developmental Biology, 1997. **184**(1): p. 115-121.

11. Delclos, K.B., et al., *Overlapping but distinct effects of genistein and ethinyl estradiol (EE(2)) in female Sprague-Dawley rats in multigenerational reproductive and chronic toxicity studies.* Reprod Toxicol, 2009. **27**(2): p. 117-32.

12. Risma, K.A., A.N. Hirshfield, and J.H. Nilson, *Elevated luteinizing hormone in prepubertal transgenic mice causes hyperandrogenemia, precocious puberty, and substantial ovarian pathology.* Endocrinology, 1997. **138**(8): p. 3540-7.

13. Jefferson, W.N., E. Padilla-Banks, and R.R. Newbold, *Adverse effects on female development and reproduction in CD-1 mice following neonatal exposure to the phytoestrogen genistein at environmentally relevant doses.* Biol Reprod, 2005. **73**(4): p. 798-806.

14. Lomniczi, A., et al., *Epigenetic control of female puberty.* Nat Neurosci, 2013. **16**(3): p. 281-9.

15. Allen, E. and E.A. Doisy, *The induction of a sexually mature condition in immature females by injection of the ovarian follicular hormone.* Am J Physiol, 1924. **69**: p. 577–588.

16. Safranski, T.J., W.R. Lamberson, and D.H. Keisler, *Correlations among three measures of puberty in mice and relationships with estradiol concentration and ovulation.* Biol Reprod, 1993. **48**(3): p. 669-73.

17. Howlin, J., J. McBryan, and F. Martin, *Pubertal mammary gland development: insights from mouse models.* J Mammary Gland Biol Neoplasia, 2006. **11**(3-4): p. 283-97.

18. Brisken, C. and B. O'Malley, *Hormone action in the mammary gland.* Cold Spring Harb Perspect Biol, 2010. **2**(12): p. a003178.

19. Stocco, C., C. Telleria, and G. Gibori, *The molecular control of corpus luteum formation, function, and regression.* Endocr Rev, 2007. **28**(1): p. 117-49.

20. Terasawa, E. and D.L. Fernandez, *Neurobiological mechanisms of the onset of puberty in primates.* Endocr Rev, 2001. **22**(1): p. 111-51.

21. Schwanzel-Fukuda, M. and D.W. Pfaff, *Origin of luteinizing hormone-releasing hormone neurons.* Nature, 1989. **338**(6211): p. 161-4.

22. Schwanzel-Fukuda, M., *Origin and migration of luteinizing hormone-releasing hormone neurons in mammals.* Microsc Res Tech, 1999. **44**(1): p. 2-10.

23. Wierman, M.E., K. Kiseljak-Vassiliades, and S. Tobet, *Gonadotropin-releasing hormone (GnRH) neuron migration: initiation, maintenance and cessation as critical steps to ensure normal reproductive function.* Front Neuroendocrinol, 2011. **32**(1): p. 43-52.

24. Quanbeck, C., et al., *Two populations of luteinizing hormone-releasing hormone neurons in the forebrain of the rhesus macaque during embryonic development.* J Comp Neurol, 1997. **380**(3): p. 293-309.

25. Gore, A.C., J.L. Roberts, and M.J. Gibson, *Mechanisms for the regulation of gonadotropin-releasing hormone gene expression in the developing mouse.* Endocrinology, 1999. **140**(5): p. 2280-7.

26. Vician, L., et al., *Pubertal changes in pro-opiomelanocortin and gonadotropin-releasing hormone gene expression in the brain of the male monkey.* Mol Cell Neurosci, 1991. **2**(1): p. 31-8.

27. Terasawa, E., *Postnatal remodeling of gonadotropin-releasing hormone I neurons: toward understanding the mechanism of the onset of puberty.* Endocrinology, 2006. **147**(8): p. 3650-1.

28. Mitsushima, D., D.L. Hei, and E. Terasawa, *Gamma-Aminobutyric-Acid Is an Inhibitory Neurotransmitter Restricting the Release of Luteinizing-Hormone-Releasing Hormone*

before the Onset of Puberty. Proceedings of the National Academy of Sciences of the United States of America, 1994. **91**(1): p. 395-399.

29. Keen, K.L., et al., *Effects of pulsatile infusion of the GABA(A) receptor blocker bicuculline on the onset of puberty in female rhesus monkeys.* Endocrinology, 1999. **140**(11): p. 5257-5266.
30. Bourguignon, J.P., A. Gerard, and P. Franchimont, *Maturation of the Hypothalamic Control of Pulsatile Gonadotropin-Releasing-Hormone Secretion at Onset of Puberty .2. Reduced Potency of an Inhibitory Autofeedback.* Endocrinology, 1990. **127**(6): p. 2884-2890.
31. Lomniczi, A., H. Wright, and S.R. Ojeda, *Epigenetic regulation of female puberty.* Front Neuroendocrinol, 2015. **36**: p. 90-107.
32. Euling, S.Y., et al., *Role of environmental factors in the timing of puberty.* Pediatrics, 2008. **121**: p. S167-S171.
33. Louis, G.M.B., et al., *Environmental factors and puberty timing: Expert panel research needs.* Pediatrics, 2008. **121**: p. S192-S207.
34. Treloar, A.E., et al., *Variation of the Human Menstrual-Cycle through Reproductive Life.* Population Index, 1965. **31**(3): p. 269-&.
35. Westwood, F.R., *The female rat reproductive cycle: a practical histological guide to staging.* Toxicol Pathol, 2008. **36**(3): p. 375-84.
36. McGee, E.A. and A.J.W. Hsueh, *Initial and cyclic recruitment of ovarian follicles.* Endocrine Reviews, 2000. **21**(2): p. 200-214.
37. Murr, S.M., Geschwin.Ii, and G.E. Bradford, *Plasma Lh and Fsh during Different Estrous-Cycle Conditions in Mice.* Journal of Reproduction and Fertility, 1973. **32**(2): p. 221-230.

38. Butcher, R.L., W.E. Collins, and N.W. Fugo, *Plasma Concentration of Lh, Fsh, Prolactin, Progesterone and Estradiol-17beta Throughout 4-Day Estrous-Cycle of Rat.* Endocrinology, 1974. **94**(6): p. 1704-1708.

39. Oktem, O. and B. Urman, *Understanding follicle growth in vivo.* Hum Reprod, 2010. **25**(12): p. 2944-54.

40. Oktem, O. and K. Oktay, *The ovary: anatomy and function throughout human life.* Ann N Y Acad Sci, 2008. **1127**: p. 1-9.

41. Tomac, J., D. Cekinovic, and J. Arapovic, *Biology of the Corpus luteum.* Periodicum Biologorum, 2011. **113**(1): p. 43-49.

42. Hillier, S.G., P.F. Whitelaw, and C.D. Smyth, *Follicular Estrogen Synthesis - the 2-Cell, 2-Gonadotropin Model Revisited.* Molecular and Cellular Endocrinology, 1994. **100**(1-2): p. 51-54.

43. Beach, F.A., *Sexual attractivity, proceptivity, and receptivity in female mammals.* Horm Behav, 1976. **7**(1): p. 105-38.

44. Pfaff, D.W., Schwartz-Giblin, S., McCarthy, M., Kow, L.M., *Cellular and molecular mechanisms of female reproductive behaviors*. The Physiology of Reproduction, ed. E. Knobil, Neil,l J.D., . 1994, New York: Raven Press, Ltd.

45. Ittner, L.M. and J. Goetz, *Pronuclear injection for the production of transgenic mice.* Nature Protocols, 2007. **2**(5): p. 1206-1215.

46. Thrasher, J.D., F.I. Clark, and D.R. Clarke, *Changes in the vaginal epithelial cell cyle in relation to events of the estrous cycle.* Exp Cell Res, 1967. **45**(1): p. 232-6.

47. R., R.J., *The estrogen-progesterone induction of sexual receptivity in the spayed female mouse.* Endocrinology, 1944. **34**(4): p. 269.

48. Micevych, P. and K. Sinchak, *Temporal and Concentration-Dependent Effects of Oestradiol on Neural Pathways Mediating Sexual Receptivity.* Journal of Neuroendocrinology, 2013. **25**(11): p. 1012-1023.

49. Musatov, S., et al., *RNAi-mediated silencing of estrogen receptor {alpha} in the ventromedial nucleus of hypothalamus abolishes female sexual behaviors.* Proc Natl Acad Sci U S A, 2006. **103**(27): p. 10456-60.

50. Kudwa, A.E. and E.F. Rissman, *Double oestrogen receptor alpha and beta knockout mice reveal differences in neural oestrogen-mediated progestin receptor induction and female sexual behaviour.* J Neuroendocrinol, 2003. **15**(10): p. 978-83.

51. Mani, S.K., et al., *Differential response of progesterone receptor isoforms in hormone-dependent and -independent facilitation of female sexual receptivity.* Mol Endocrinol, 2006. **20**(6): p. 1322-32.

52. Lydon, J.P., et al., *Mice Lacking Progesterone-Receptor Exhibit Pleiotropic Reproductive Abnormalities.* Genes & Development, 1995. **9**(18): p. 2266-2278.

53. Mani, S.K., et al., *Dopamine requires the unoccupied progesterone receptor to induce sexual behavior in mice.* Mol Endocrinol, 1996. **10**(12): p. 1728-37.

54. Gomora-Arrati, P., et al., *GnRH mediates estrous behavior induced by ring A reduced progestins and vaginocervical stimulation.* Behav Brain Res, 2008. **187**(1): p. 1-8.

55. Garcia-Juarez, M., et al., *Leptin facilitates lordosis behavior through GnRH-1 and progestin receptors in estrogen-primed rats.* Neuropeptides, 2011. **45**(1): p. 63-7.

56. Sirinathsinghji, D.J., *GnRH in the spinal subarachnoid space potentiates lordosis behavior in the female rat.* Physiol Behav, 1983. **31**(5): p. 717-23.

57. Micevych, P.E. and P. Dewing, *Membrane-initiated estradiol signaling regulating sexual receptivity.* Front Endocrinol (Lausanne), 2011. **2**: p. 26.

58. Talbot, P., B.D. Shur, and D.G. Myles, *Cell adhesion and fertilization: steps in oocyte transport, sperm-zona pellucida interactions, and sperm-egg fusion.* Biol Reprod, 2003. **68**(1): p. 1-9.

59. Wu, A., et al., *Sperm surface arylsulfatase a can disperse the cumulus matrix of cumulus oocyte complexes.* Journal of Cellular Physiology, 2007. **213**(1): p. 201-211.

60. Roblero, L.S., M.D. Riffo, and H.B. Croxatto, *Cumulus Cell Dispersion Induced by Estradiol in Mouse Oviduct Invitro.* Gamete Research, 1989. **23**(4): p. 467-473.

61. Yasukawa, J.J. and R.K. Meyer, *Effect of progesterone and oestrone on the pre-implantation and implantation stages of embryo development in the rat.* J Reprod Fertil, 1966. **11**(2): p. 245-55.

62. Homa, S.T., J. Carroll, and K. Swann, *The role of calcium in mammalian oocyte maturation and egg activation.* Hum Reprod, 1993. **8**(8): p. 1274-81.

63. Kolle, S., et al., *Ciliary transport, gamete interaction, and effects of the early embryo in the oviduct: ex vivo analyses using a new digital videomicroscopic system in the cow.* Biol Reprod, 2009. **81**(2): p. 267-74.

64. Martinez-Frias, M.L., *Assessing pre-implantation embryo development in mice provides a rationale for understanding potential adverse effects of ART and PGD procedures.* Am J Med Genet A, 2012. **158A**(10): p. 2526-33.

65. Blakeley, P., et al., *Defining the three cell lineages of the human blastocyst by single-cell RNA-seq.* Development, 2015. **142**(20): p. 3613.

66. Gasperowicz, M. and D.R. Natale, *Establishing three blastocyst lineages--then what?* Biol Reprod, 2011. **84**(4): p. 621-30.

67. Marikawa, Y. and V.B. Alarcon, *Establishment of trophectoderm and inner cell mass lineages in the mouse embryo.* Mol Reprod Dev, 2009. **76**(11): p. 1019-32.

68. Paria, B.C., et al., *Deciphering the cross-talk of implantation: advances and challenges.* Science, 2002. **296**(5576): p. 2185-8.

69. Diao, H., et al., *Temporal expression pattern of progesterone receptor in the uterine luminal epithelium suggests its requirement during early events of implantation.* Fertil Steril, 2011. **95**(6): p. 2087-93.

70. Wetendorf, M. and F.J. DeMayo, *The progesterone receptor regulates implantation, decidualization, and glandular development via a complex paracrine signaling network.* Mol Cell Endocrinol, 2012. **357**(1-2): p. 108-18.

71. Finn, C.A. and A. McLaren, *A study of the early stages of implantation in mice.* J Reprod Fertil, 1967. **13**(2): p. 259-67.

72. Yoshinaga, K., *A sequence of events in the uterus prior to implantation in the mouse.* J Assist Reprod Genet, 2013. **30**(8): p. 1017-22.

73. Chen, Q., et al., *Navigating the site for embryo implantation: biomechanical and molecular regulation of intrauterine embryo distribution.* Mol Aspects Med, 2013. **34**(5): p. 1024-42.

74. Jasoni, C.L., R.W. Porteous, and A.E. Herbison, *Anatomical location of mature GnRH neurons corresponds with their birthdate in the developing mouse.* Dev Dyn, 2009. **238**(3): p. 524-31.

75. Wray, S., P. Grant, and H. Gainer, *Evidence That Cells Expressing Luteinizing-Hormone-Releasing Hormone Messenger-Rna in the Mouse Are Derived from Progenitor Cells in the Olfactory Placode.* Proceedings of the National Academy of Sciences of the United States of America, 1989. **86**(20): p. 8132-8136.

76. Kelly, M.J. and E.J. Wagner, *GnRH neurons and episodic bursting activity.* Trends Endocrinol Metab, 2002. **13**(10): p. 409-10.

77. Moenter, S.M., *Identified GnRH neuron electrophysiology: a decade of study.* Brain Res, 2010. **1364**: p. 10-24.

78. Constantin, S., K.J. Iremonger, and A.E. Herbison, *In vivo recordings of GnRH neuron firing reveal heterogeneity and dependence upon GABAA receptor signaling.* J Neurosci, 2013. **33**(22): p. 9394-401.

79. Moenter, S.M., R.C. Brand, and F.J. Karsch, *Dynamics of Gonadotropin-Releasing-Hormone (Gnrh) Secretion during the Gnrh Surge - Insights into the Mechanism of Gnrh Surge Induction.* Endocrinology, 1992. **130**(5): p. 2978-2984.

80. Caraty, A., A. Locatelli, and G.B. Martin, *Biphasic response in the secretion of gonadotrophin-releasing hormone in ovariectomized ewes injected with oestradiol.* J Endocrinol, 1989. **123**(3): p. 375-82.

81. Butler, J.A., M. Sjoberg, and C.W. Coen, *Evidence for oestrogen receptor alpha-immunoreactivity in gonadotrophin-releasing hormone-expressing neurones.* J Neuroendocrinol, 1999. **11**(5): p. 331-5.

82. Roy, D., N.L. Angelini, and D.D. Belsham, *Estrogen directly represses gonadotropin-releasing hormone (GnRH) gene expression in estrogen receptor-alpha (ER alpha)- and ER beta-expressing GT1-7 GnRH neurons.* Endocrinology, 1999. **140**(11): p. 5045-5053.

83. Martinez-Morales, J.R., et al., *Estrogen modulates norepinephrine-induced accumulation of adenosine cyclic monophosphate in a subpopulation of immortalized luteinizing hormone-releasing hormone secreting neurons from the mouse hypothalamus.* Neurosci Lett, 2001. **298**(1): p. 61-4.

84. Dufourny, L. and D.C. Skinner, *Colocalization of progesterone receptors and thyroid hormone receptors alpha in the ovine diencephalon: no effect of estradiol.* Neuroendocrinology, 2003. **77**(1): p. 51-8.

85. Campbell, R.E., *Defining the gonadotrophin-releasing hormone neuronal network: transgenic approaches to understanding neurocircuitry.* J Neuroendocrinol, 2007. **19**(7): p. 561-73.

86. Wintermantel, T.M., et al., *Definition of estrogen receptor pathway critical for estrogen positive feedback to gonadotropin-releasing hormone neurons and fertility.* Neuron, 2006. **52**(2): p. 271-80.

87. Herbison, A.E., *Estrogen positive feedback to gonadotropin-releasing hormone (GnRH) neurons in the rodent: the case for the rostral periventricular area of the third ventricle (RP3V).* Brain Res Rev, 2008. **57**(2): p. 277-87.

88. Decavel, C. and A.N. Van den Pol, *GABA: a dominant neurotransmitter in the hypothalamus.* J Comp Neurol, 1990. **302**(4): p. 1019-37.

89. van den Pol, A.N., J.P. Wuarin, and F.E. Dudek, *Glutamate, the dominant excitatory transmitter in neuroendocrine regulation.* Science, 1990. **250**(4985): p. 1276-8.

90. Roberts, C.B., P. Hemond, and K.J. Suter, *Synaptic integration in hypothalamic gonadotropin releasing hormone (GnRH) neurons.* Neuroscience, 2008. **154**(4): p. 1337-51.

91. Herbison, A.E. and S.M. Moenter, *Depolarising and Hyperpolarising Actions of GABA(A) Receptor Activation on Gonadotrophin-Releasing Hormone Neurones: Towards an Emerging Consensus.* Journal of Neuroendocrinology, 2011. **23**(7): p. 557-569.

92. Liu, X. and A.E. Herbison, *Estrous cycle- and sex-dependent changes in pre- and postsynaptic GABAB control of GnRH neuron excitability.* Endocrinology, 2011. **152**(12): p. 4856-64.

93. Zhang, C., et al., *gamma-Aminobutyric Acid B Receptor Mediated Inhibition of Gonadotropin-Releasing Hormone Neurons Is Suppressed by Kisspeptin-G Protein-Coupled Receptor 54 Signaling.* Endocrinology, 2009. **150**(5): p. 2388-2394.

94. Christian, C.A. and S.M. Moenter, *Critical roles for fast synaptic transmission in mediating estradiol negative and positive feedback in the neural control of ovulation.* Endocrinology, 2008. **149**(11): p. 5500-8.

95. Herbison, A.E. and S.M. Moenter, *Depolarising and hyperpolarising actions of GABA(A) receptor activation on gonadotrophin-releasing hormone neurones: towards an emerging consensus.* J Neuroendocrinol, 2011. **23**(7): p. 557-69.

96. Moenter, S.M., Z. Chu, and C.A. Christian, *Neurobiological mechanisms underlying oestradiol negative and positive feedback regulation of gonadotrophin-releasing hormone neurones.* J Neuroendocrinol, 2009. **21**(4): p. 327-33.

97. Hrabovszky, E., et al., *Glutamatergic and GABAergic innervation of human gonadotropin-releasing hormone-I neurons.* Endocrinology, 2012. **153**(6): p. 2766-76.

98. Christian, C.A., J. Pielecka-Fortuna, and S.M. Moenter, *Estradiol suppresses glutamatergic transmission to gonadotropin-releasing hormone neurons in a model of negative feedback in mice.* Biol Reprod, 2009. **80**(6): p. 1128-35.

99. Simerly, R.B., *Wired for reproduction: organization and development of sexually dimorphic circuits in the mammalian forebrain.* Annu Rev Neurosci, 2002. **25**: p. 507-36.

100. Iremonger, K.J., et al., *Glutamate regulation of GnRH neuron excitability.* Brain Res, 2010. **1364**: p. 35-43.

101. de Roux, N., et al., *Hypogonadotropic hypogonadism due to loss of function of the KiSS1-derived peptide receptor GPR54.* Proceedings of the National Academy of Sciences of the United States of America, 2003. **100**(19): p. 10972-10976.

102. Seminara, S.B., et al., *The GPR54 gene as a regulator of puberty.* New England Journal of Medicine, 2003. **349**(17): p. 1614-U8.

103. Kotani, M., et al., *The metastasis suppressor gene KiSS-1 encodes kisspeptins, the natural ligands of the orphan G protein-coupled receptor GPR54.* J Biol Chem, 2001. **276**(37): p. 34631-6.

104. Clarkson, J., et al., *Distribution of kisspeptin neurones in the adult female mouse brain.* J Neuroendocrinol, 2009. **21**(8): p. 673-82.

105. Rometo, A.M., et al., *Hypertrophy and increased kisspeptin gene expression in the hypothalamic infundibular nucleus of postmenopausal women and ovariectomized monkeys.* J Clin Endocrinol Metab, 2007. **92**(7): p. 2744-50.

106. Shahab, M., et al., *Increased hypothalamic GPR54 signaling: a potential mechanism for initiation of puberty in primates.* Proc Natl Acad Sci U S A, 2005. **102**(6): p. 2129-34.

107. Franceschini, I., et al., *Kisspeptin immunoreactive cells of the ovine preoptic area and arcuate nucleus co-express estrogen receptor alpha.* Neurosci Lett, 2006. **401**(3): p. 225-30.

108. Adachi, S., et al., *Involvement of anteroventral periventricular metastin/kisspeptin neurons in estrogen positive feedback action on luteinizing hormone release in female rats.* Journal of Reproduction and Development, 2007. **53**(2): p. 367-378.

109. Clarkson, J. and A.E. Herbison, *Postnatal development of kisspeptin neurons in mouse hypothalamus; Sexual dimorphism and projections to gonadotropin-releasing hormone neurons.* Endocrinology, 2006. **147**(12): p. 5817-5825.

110. Smith, J.T., et al., *Regulation of Kiss1 gene expression in the brain of the female mouse.* Endocrinology, 2005. **146**(9): p. 3686-92.

111. Kauffman, A.S., et al., *The kisspeptin receptor GPR54 is required for sexual differentiation of the brain and behavior.* J Neurosci, 2007. **27**(33): p. 8826-35.

112. Messager, S., et al., *Kisspeptin directly stimulates gonadotropin-releasing hormone release via G protein-coupled receptor 54.* Proc Natl Acad Sci U S A, 2005. **102**(5): p. 1761-6.

113. Han, S.K., et al., *Activation of gonadotropin-releasing hormone neurons by kisspeptin as a neuroendocrine switch for the onset of puberty.* Journal of Neuroscience, 2005. **25**(49): p. 11349-11356.

114. Roa, J. and M. Tena-Sempere, *Connecting metabolism and reproduction: roles of central energy sensors and key molecular mediators.* Mol Cell Endocrinol, 2014. **397**(1-2): p. 4-14.

115. Miller, B.H. and J.S. Takahashi, *Central circadian control of female reproductive function.* Front Endocrinol (Lausanne), 2013. **4**: p. 195.

116. Nagaraju, G.P., S.F. Zafar, and B.F. El-Rayes, *Pleiotropic effects of genistein in metabolic, inflammatory, and malignant diseases.* Nutr Rev, 2013. **71**(8): p. 562-72.

117. Kuiper, G.G.J.M., et al., *Interaction of estrogenic chemicals and phytoestrogens with estrogen receptor beta.* Endocrinology, 1998. **139**(10): p. 4252-4263.

118. Brzozowski, A.M., et al., *Molecular basis of agonism and antagonism in the oestrogen receptor.* Nature, 1997. **389**(6652): p. 753-8.

119. Barkhem, T., et al., *Differential response of estrogen receptor alpha and estrogen receptor beta to partial estrogen agonists/antagonists.* Molecular Pharmacology, 1998. **54**(1): p. 105-112.

120. Dai, S.Y., et al., *Unique Ligand Binding Patterns between Estrogen Receptor alpha and beta Revealed by Hydrogen-Deuterium Exchange.* Biochemistry, 2009. **48**(40): p. 9668-9676.

121. Mortensen, A., et al., *Analytical and compositional aspects of isoflavones in food and their biological effects.* Mol Nutr Food Res, 2009. **53 Suppl 2**: p. S266-309.

122. USDA, *USDA database for the isoflavone content of selected foods.* http://www.ars.usda.gov/nutrientdata/isoflav, 2008.

123. Chun, O.K., W.O. Song, and S.J. Chung, *Urinary Isoflavones and Their Metabolites Validate the Dietary Isoflavone Intakes in US Adults [electronic resource].* Journal of the American Dietetic Association, 2009. **109**(2): p. 245-254.

124. Wakai, K., et al., *Dietary intake and sources of isoflavones among Japanese.* Nutr Cancer, 1999. **33**(2): p. 139-45.

125. Surh, J., et al., *Estimated intakes of isoflavones and coumestrol in Korean population.* International Journal of Food Sciences and Nutrition, 2006. **57**(5-6): p. 325-344.

126. Seow, A., et al., *Isoflavonoid levels in spot urine are associated with frequency of dietary soy intake in a population-based sample of middle-aged and older Chinese in Singapore.* Cancer Epidemiology, Biomarkers & Prevention, 1998. **7**(2): p. 135-140.

127. FDA, *Food labeling: health claims; soy protein and coronary heart disease.* Fed Regist, 1999. **64**: p. 57700–33.

128. Patisaul, H.B. and W. Jefferson, *The pros and cons of phytoestrogens.* Front Neuroendocrinol, 2010. **31**(4): p. 400-19.

129. Yang, Z., et al., *Bioavailability and pharmacokinetics of genistein: mechanistic studies on its ADME.* Anticancer Agents Med Chem, 2012. **12**(10): p. 1264-80.

130. Mortensen, A., *Analytical and compositional aspects of isoflavones in food and their biological effects (vol 53, pg S266, 2009).* Mol Nutr Food Res, 2009. **53**(11): p. 1479-1479.

131. Piskula, M.K., J. Yamakoshi, and Y. Iwai, *Daidzein and genistein but not their glucosides are absorbed from the rat stomach.* Febs Letters, 1999. **447**(2-3): p. 287-291.

132. Setchell, K.D.R., et al., *Evidence for lack of absorption of soy isoflavone glycosides in humans, supporting the crucial role of intestinal metabolism for bioavailability.* American Journal of Clinical Nutrition, 2002. **76**(2): p. 447-453.

133. Steensma, A., M.E. Bienenmann-Ploum, and H.P.J.M. Noteborn, *Intestinal uptake of genistein and its glycoside in the rat using various isolated perfused gut segments.* Environmental Toxicology and Pharmacology, 2004. **17**(2): p. 103-110.

134. Coldham, N.G., et al., *Comparative metabolism of genistin by human and rat gut microflora: detection and identification of the end-products of metabolism.* Xenobiotica, 2002. **32**(1): p. 45-62.

135. Liu, Y. and M. Hu, *Absorption and metabolism of flavonoids in the caco-2 cell culture model and a perused rat intestinal model.* Drug Metab Dispos, 2002. **30**(4): p. 370-7.

136. Andlauer, W., J. Kolb, and P. Furst, *Absorption and metabolism of genistin in the isolated rat small intestine.* FEBS Lett, 2000. **475**(2): p. 127-30.

137. Zhang, L., Z. Zuo, and G. Lin, *Intestinal and hepatic glucuronidation of flavonoids.* Mol Pharm, 2007. **4**(6): p. 833-45.

138. Roberts-Kirchhoff, E.S., et al., *Metabolism of genistein by rat and human cytochrome P450s.* Chem Res Toxicol, 1999. **12**(7): p. 610-6.

139. Coldham, N.G. and M.J. Sauer, *Pharmacokinetics of [(14)C]Genistein in the rat: gender-related differences, potential mechanisms of biological action, and implications for human health.* Toxicol Appl Pharmacol, 2000. **164**(2): p. 206-15.

140. Zhou, S., et al., *Dose-dependent absorption, metabolism, and excretion of genistein in rats.* J Agric Food Chem, 2008. **56**(18): p. 8354-9.

141. Gilani, G.S., et al., *Distribution of isoflavones in samples of serum, liver and mammary glands of rats or pigs fed dietary isoflavones.* Ann Nutr Metab, 2011. **58**(3): p. 171-80.

142. Chang, H.C., et al., *Mass spectrometric determination of Genistein tissue distribution in diet-exposed Sprague-Dawley rats.* J Nutr, 2000. **130**(8): p. 1963-70.

143. Penza, M., et al., *Genistein accumulates in body depots and is mobilized during fasting, reaching estrogenic levels in serum that counter the hormonal actions of estradiol and organochlorines.* Toxicological Sciences, 2007. **97**(2): p. 299-307.

144. Watanabe, S., et al., *Pharmacokinetics of soybean isoflavones in plasma, urine and feces of men after ingestion of 60 g baked soybean powder (kinako).* J Nutr, 1998. **128**(10): p. 1710-5.

145. Morito, K., et al., *Interaction of phytoestrogens with estrogen receptors alpha and beta.* Biological & Pharmaceutical Bulletin, 2001. **24**(4): p. 351-6.

146. Gencel, V.B., et al., *Vascular effects of phytoestrogens and alternative menopausal hormone therapy in cardiovascular disease.* Mini Rev Med Chem, 2012. **12**(2): p. 149-74.

147. Jacobs, A., et al., *Efficacy of isoflavones in relieving vasomotor menopausal symptoms - A systematic review.* Mol Nutr Food Res, 2009. **53**(9): p. 1084-97.

148. Lanou, A.J., *Soy foods: are they useful for optimal bone health?* Ther Adv Musculoskelet Dis, 2011. **3**(6): p. 293-300.

149. Hilakivi-Clarke, L., J.E. Andrade, and W. Helferich, *Is Soy Consumption Good or Bad for the Breast?* Journal of Nutrition, 2010. **140**(12): p. 2326s-2334s.

150. Rozman, K.K., et al., *NTP-CERHR expert panel report on the reproductive and developmental toxicity of genistein.* Birth Defects Res B Dev Reprod Toxicol, 2006. **77**(6): p. 485-638.

151. Ryokkynen, A., J.V. Kukkonen, and P. Nieminen, *Effects of dietary genistein on mouse reproduction, postnatal development and weight-regulation.* Anim Reprod Sci, 2006. **93**(3-4): p. 337-48.

152. Piotrowska, K., et al., *Changes in male reproductive system and mineral metabolism induced by soy isoflavones administered to rats from prenatal life until sexual maturity.* Nutrition, 2011. **27**(3): p. 372-9.

153. Roberts, D., et al., *Effects of chronic dietary exposure to genistein, a phytoestrogen, during various stages of development on reproductive hormones and spermatogenesis in rats.* Endocrine, 2000. **13**(3): p. 281-6.

154. Wisniewski, A.B., et al., *Exposure to genistein during gestation and lactation demasculinizes the reproductive system in rats.* J Urol, 2003. **169**(4): p. 1582-6.

155. Klein, S.L., et al., *Early exposure to genistein exerts long-lasting effects on the endocrine and immune systems in rats.* Molecular Medicine, 2002. **8**(11): p. 742-749.

156. Svechnikov, K., et al., *Influence of long-term dietary administration of procymidone, a fungicide with anti-androgenic effects, or the phytoestrogen genistein to rats on the pituitary-gonadal axis and Leydig cell steroidogenesis.* Journal of Endocrinology, 2005. **187**(1): p. 117-24.

157. Lee, B.J., et al., *Effects of exposure to genistein during pubertal development on the reproductive system of male mice.* J Reprod Dev, 2004. **50**(4): p. 399-409.

158. Michael McClain, R., et al., *Acute, subchronic and chronic safety studies with genistein in rats.* Food Chem Toxicol, 2006. **44**(1): p. 56-80.

159. Slikker, W., Jr., et al., *Gender-based differences in rats after chronic dietary exposure to genistein.* Int J Toxicol, 2001. **20**(3): p. 175-9.

160. Delclos, K.B., et al., *Effects of dietary genistein exposure during development on male and female CD (Sprague-Dawley) rats.* Reprod Toxicol, 2001. **15**(6): p. 647-63.

161. Kyselova, V., et al., *Body and organ weight, sperm acrosomal status and reproduction after genistein and diethylstilbestrol treatment of CD1 mice in a multigenerational study.* Theriogenology, 2004. **61**(7-8): p. 1307-25.

162. Fritz, W.A., et al., *Dietary diethylstilbestrol but not genistein adversely affects rat testicular development.* J Nutr, 2003. **133**(7): p. 2287-93.

163. Sherrill, J.D., et al., *Developmental exposures of male rats to soy isoflavones impact Leydig cell differentiation.* Biol Reprod, 2010. **83**(3): p. 488-501.

164. Lehraiki, A., et al., *Genistein impairs early testosterone production in fetal mouse testis via estrogen receptor alpha.* Toxicology in Vitro, 2011. **25**(8): p. 1542-1547.

165. Assinder, S., et al., *Adult-only exposure of male rats to a diet of high phytoestrogen content increases apoptosis of meiotic and post-meiotic germ cells.* Reproduction, 2007. **133**(1): p. 11-9.

166. Cederroth, C.R., et al., *Potential detrimental effects of a phytoestrogen-rich diet on male fertility in mice.* Mol Cell Endocrinol, 2010. **321**(2): p. 152-60.

167. Al-Nakkash, L., et al., *Genistein induces estrogen-like effects in ovariectomized rats but fails to increase cardiac GLUT4 and oxidative stress.* J Med Food, 2010. **13**(6): p. 1369-75.

168. Rimoldi, G., et al., *Effects of chronic genistein treatment in mammary gland, uterus, and vagina.* Environ Health Perspect, 2007. **115 Suppl 1**: p. 62-8.

169. Diel, P., et al., *The differential ability of the phytoestrogen genistein and of estradiol to induce uterine weight and proliferation in the rat is associated with a substance specific modulation of uterine gene expression.* Mol Cell Endocrinol, 2004. **221**(1-2): p. 21-32.

170. Moller, F.J., et al., *Long-term dietary isoflavone exposure enhances estrogen sensitivity of rat uterine responsiveness mediated through estrogen receptor alpha.* Toxicol Lett, 2010. **196**(3): p. 142-53.

171. Akbas, G.E., X. Fei, and H.S. Taylor, *Regulation of HOXA10 expression by phytoestrogens.* Am J Physiol Endocrinol Metab, 2007. **292**(2): p. E435-42.

172. Li, W. and Y.H. Liu, *Effects of phytoestrogen genistein on genioglossus function and oestrogen receptors expression in ovariectomized rats.* Arch Oral Biol, 2009. **54**(11): p. 1029-34.

173. Carbonel, A.A., et al., *Effects of high-dose isoflavones on rat uterus.* Rev Assoc Med Bras, 2011. **57**(5): p. 534-9.

174. Diel, P., et al., *Comparative responses of three rat strains (DA/Han, Sprague-Dawley and Wistar) to treatment with environmental estrogens.* Arch Toxicol, 2004. **78**(4): p. 183-93.

175. Hertrampf, T., et al., *Effects of genistein on the mammary gland proliferation of adult ovariectomised Wistar rats.* Planta Med, 2006. **72**(4): p. 304-10.

176. Molzberger, A.F., et al., *In utero and postnatal exposure to isoflavones results in a reduced responsivity of the mammary gland towards estradiol.* Mol Nutr Food Res, 2012. **56**(3): p. 399-409.

177. Nagao, T., et al., *Reproductive effects in male and female rats of neonatal exposure to genistein.* Reprod Toxicol, 2001. **15**(4): p. 399-411.

178. Jefferson, W.N., et al., *Oral exposure to genistin, the glycosylated form of genistein, during neonatal life adversely affects the female reproductive system.* Environ Health Perspect, 2009. **117**(12): p. 1883-9.

179. Jefferson, W.N., et al., *Neonatal exposure to genistein disrupts ability of female mouse reproductive tract to support preimplantation embryo development and implantation.* Biol Reprod, 2009. **80**(3): p. 425-31.

180. Jefferson, W.N., et al., *Neonatal Phytoestrogen Exposure Alters Oviduct Mucosal Immune Response to Pregnancy and Affects Preimplantation Embryo Development in the Mouse.* Biol Reprod, 2012.

181. Jefferson, W.N., et al., *Neonatal exposure to genistein induces estrogen receptor (ER)alpha expression and multioocyte follicles in the maturing mouse ovary: evidence for ERbeta-mediated and nonestrogenic actions.* Biol Reprod, 2002. **67**(4): p. 1285-96.

182. Newbold, R.R., et al., *Uterine adenocarcinoma in mice treated neonatally with genistein.* Cancer Res, 2001. **61**(11): p. 4325-8.

183. Padilla-Banks, E., W.N. Jefferson, and R.R. Newbold, *Neonatal exposure to the phytoestrogen genistein alters mammary gland growth and developmental programming of hormone receptor levels.* Endocrinology, 2006. **147**(10): p. 4871-82.

184. Patisaul, H.B., et al., *Dietary soy supplements produce opposite effects on anxiety in intact male and female rats in the elevated plus-maze.* Behavioral Neuroscience, 2005. **119**(2): p. 587-594.

185. Li, W. and Y.H. Liu, *Effects of phytoestrogen genistein on genioglossus function and oestrogen receptors expression in ovariectomized rats.* Archives of Oral Biology, 2009. **54**(11): p. 1029-1034.

186. Hooper, L., et al., *Effects of soy protein and isoflavones on circulating hormone concentrations in pre- and post-menopausal women: a systematic review and meta-analysis.* Hum Reprod Update, 2009. **15**(4): p. 423-440.

187. Bhattarai, J.P., I.M. Abraham, and S.K. Han, *Genistein excitation of gonadotrophin-releasing hormone neurones in juvenile female mice.* Journal of Neuroendocrinology, 2013. **25**(5): p. 497-505.

188. Medigovic, I., et al., *Effects of genistein on gonadotropic cells in immature female rats.* Acta Histochem, 2012. **114**(3): p. 270-5.

189. Myllymaki, S., et al., *In vitro effects of diethylstilbestrol, genistein, 4-tert-butylphenol, and 4-tert-octylphenol on steroidogenic activity of isolated immature rat ovarian follicles.* Toxicol Appl Pharmacol, 2005. **204**(1): p. 69-80.

190. Rice, S., H.D. Mason, and S.A. Whitehead, *Phytoestrogens and their low dose combinations inhibit mRNA expression and activity of aromatase in human granulosa-luteal cells.* Journal of Steroid Biochemistry and Molecular Biology, 2006. **101**(4-5): p. 216-225.

191. Lewis, R.W., et al., *The effects of the phytoestrogen genistein on the postnatal development of the rat.* Toxicological Sciences, 2003. **71**(1): p. 74-83.

192. Losa, S.M., et al., *Neonatal exposure to genistein adversely impacts the ontogeny of hypothalamic kisspeptin signaling pathways and ovarian development in the peripubertal female rat.* Reprod Toxicol, 2011. **31**(3): p. 280-9.

193. Lephart, E.D., et al., *Neurobehavioral effects of dietary soy phytoestrogens.* Neurotoxicol Teratol, 2002. **24**(1): p. 5-16.

194. Bateman, H.L. and H.B. Patisaul, *Disrupted female reproductive physiology following neonatal exposure to phytoestrogens or estrogen specific ligands is associated with decreased GnRH activation and kisspeptin fiber density in the hypothalamus.* Neurotoxicology, 2008. **29**(6): p. 988-97.

195. Mueller, J.K. and S. Heger, *Endocrine disrupting chemicals affect the gonadotropin releasing hormone neuronal network.* Reprod Toxicol, 2014. **44**: p. 73-84.

196. Patisaul, H.B., et al., *Genistein affects ER beta- but not ER alpha-dependent gene expression in the hypothalamus.* Endocrinology, 2002. **143**(6): p. 2189-97.

197. Adgent, M.A., et al., *Early-life soy exposure and age at menarche.* Paediatric and Perinatal Epidemiology, 2012. **26**(2): p. 163-175.

198. Parent, A.S., et al., *The timing of normal puberty and the age limits of sexual precocity: variations around the world, secular trends, and changes after migration.* Endocrine Reviews, 2003. **24**(5): p. 668-93.

199. Setchell, K.D., et al., *Exposure of infants to phyto-oestrogens from soy-based infant formula.* Lancet, 1997. **350**(9070): p. 23-7.

200. Yum, T., S. Lee, and Y. Kim, *Association between precocious puberty and some endocrine disruptors in human plasma.* Journal of Environmental Science and Health, Part A, 2013. **48**: p. 912-917.

201. Thigpen, J.E., et al., *Dietary phytoestrogens accelerate the time of vaginal opening in immature CD-1 mice.* Comp Med, 2003. **53**(6): p. 607-15.

202. Nikaido, Y., et al., *Effects of prepubertal exposure to xenoestrogen on development of estrogen target organs in female CD-1 mice.* In Vivo, 2005. **19**(3): p. 487-94.

203. Kaludjerovic, J. and W.E. Ward, *Neonatal exposure to daidzein, genistein, or the combination modulates bone development in female CD-1 mice.* J Nutr, 2009. **139**(3): p. 467-73.

204. Goran, M.I., et al., *Developmental changes in energy expenditure and physical activity in children: evidence for a decline in physical activity in girls before puberty.* Pediatrics, 1998. **101**(5): p. 887-91.

205. Kennedy, G.C. and J. Mitra, *Body Weight and Food Intake as Initiating Factors for Puberty in Rat.* Journal of Physiology-London, 1963. **166**(2): p. 408-&.

206. Caron, E., et al., *Alteration in Neonatal Nutrition Causes Perturbations in Hypothalamic Neural Circuits Controlling Reproductive Function.* Journal of Neuroscience, 2012. **32**(33): p. 11486-11494.

207. Wagner, I.V., et al., *Effects of obesity on human sexual development.* Nature Reviews Endocrinology, 2012. **8**(4): p. 246-254.

208. Frisch, R.E. and J.W. Mcarthur, *Menstrual Cycles - Fatness as a Determinant of Minimum Weight for Height Necessary for Their Maintenance or Onset.* Science, 1974. **185**(4155): p. 949-951.

209. He, D.Q., et al., *Effects of glucose and related substrates on the recovery of the electrical activity of gonadotropin-releasing hormone pulse generator which is decreased by insulin-induced hypoglycemia in the estrogen-primed ovariectomized rat.* Brain Research, 1999. **820**(1-2): p. 71-76.

210. Hiney, J.K., et al., *Insulin-like growth factor I of peripheral origin acts centrally to accelerate the initiation of female puberty.* Endocrinology, 1996. **137**(9): p. 3717-28.

211. Pralong, F.P., *Insulin and NPY pathways and the control of GnRH function and puberty onset.* Mol Cell Endocrinol, 2010. **324**(1-2): p. 82-6.

212. Zhang, Y.Y., et al., *Positional Cloning of the Mouse Obese Gene and Its Human Homolog (Vol 372, Pg 425, 1994).* Nature, 1995. **374**(6521): p. 479-479.

213. Woods, S.C. and D.A. D'Alessio, *Central Control of Body Weight and Appetite.* Journal of Clinical Endocrinology & Metabolism, 2008. **93**(11): p. S37-S50.

214. Friedman, J.M., *Leptin at 14 y of age: an ongoing story.* American Journal of Clinical Nutrition, 2009. **89**(3): p. 973s-979s.

215. Ahima, R.S., D. Prabakaran, and J.S. Flier, *Postnatal leptin surge and regulation of circadian rhythm of leptin by feeding. Implications for energy homeostasis and neuroendocrine function.* J Clin Invest, 1998. **101**(5): p. 1020-7.

216. Garcia-Mayor, R.V., et al., *Serum leptin levels in normal children: relationship to age, gender, body mass index, pituitary-gonadal hormones, and pubertal stage.* J Clin Endocrinol Metab, 1997. **82**(9): p. 2849-55.

217. Ahima, R.S., et al., *Leptin accelerates the onset of puberty in normal female mice.* J Clin Invest, 1997. **99**(3): p. 391-5.

218. El-Eshmawy, M.M., I.A. Abdel Aal, and A.K. El Hawary, *Association of ghrelin and leptin with reproductive hormones in constitutional delay of growth and puberty.* Reprod Biol Endocrinol, 2010. **8**: p. 153.

219. Bouchard, C., *Genetics of obesity in humans: current issues.* Ciba Found Symp, 1996. **201**: p. 108-15; discussion 115-7, 188-93.

220. Coleman, D.L., *Obese and diabetes: two mutant genes causing diabetes-obesity syndromes in mice.* Diabetologia, 1978. **14**(3): p. 141-8.

221. Chehab, F.F., M.E. Lim, and R. Lu, *Correction of the sterility defect in homozygous obese female mice by treatment with the human recombinant leptin.* Nat Genet, 1996. **12**(3): p. 318-20.

222. Zhao, J., et al., *Leptin receptor expression increases in placenta, but not hypothalamus, during gestation in Mus musculus and Myotis lucifugus.* Placenta, 2004. **25**(8-9): p. 712-722.

223. Chien, E.K., et al., *Increase in serum leptin and uterine leptin receptor messenger RNA levels during pregnancy in rats.* Biochemical and Biophysical Research Communications, 1997. **237**(2): p. 476-480.

224. van der Lely, A.J., et al., *Biological, physiological, pathophysiological, and pharmacological aspects of ghrelin.* Endocr Rev, 2004. **25**(3): p. 426-57.

225. Tschop, M., et al., *Circulating Ghrelin levels are decreased in human obesity.* Diabetes, 2001. **50**(4): p. 707-709.

226. Broglio, F., et al., *Ghrelin: endocrine, metabolic and cardiovascular actions.* J Endocrinol Invest, 2005. **28**(5 Suppl): p. 23-5.

227. Soriano-Guillen, L., et al., *Ghrelin levels from fetal life through early adulthood: Relationship with endocrine and metabolic and anthropometric measures.* Journal of Pediatrics, 2004. **144**(1): p. 30-35.

228. Fernandez-Fernandez, R., et al., *Effects of ghrelin upon gonadotropin-releasing hormone and gonadotropin secretion in adult female rats: In vivo and in vitro studies.* Neuroendocrinology, 2005. **82**(5-6): p. 245-255.

229. Fernandez-Fernandez, R., et al., *Effects of chronic hyperghrelinemia on puberty onset and pregnancy outcome in the rat.* Endocrinology, 2005. **146**(7): p. 3018-3025.

230. Claudel, T., et al., *Crosstalk between xenobiotics metabolism and circadian clock.* Febs Letters, 2007. **581**(19): p. 3626-3633.

231. Gachon, F., et al., *The mammalian circadian timing system: from gene expression to physiology.* Chromosoma, 2004. **113**(3): p. 103-112.

232. Tsang, A.H., J.L. Barclay, and H. Oster, *Interactions between endocrine and circadian systems.* J Mol Endocrinol, 2014. **52**(1): p. R1-16.

233. Schibler, U., J. Ripperger, and S.A. Brown, *Peripheral circadian oscillators in mammals: time and food.* J Biol Rhythms, 2003. **18**(3): p. 250-60.

234. Mendoza, J., P. Pevet, and E. Challet, *High-fat feeding alters the clock synchronization to light.* J Physiol, 2008. **586**(Pt 24): p. 5901-10.

235. Grosbellet, E., et al., *Leptin normalizes photic synchronization in male ob/ob mice, via indirect effects on the suprachiasmatic nucleus.* Endocrinology, 2014: p. en20141570.

236. Zigman, J.M., et al., *Expression of ghrelin receptor mRNA in the rat and the mouse brain.* J Comp Neurol, 2006. **494**(3): p. 528-48.

237. Lamont, E.W., et al., *Ghrelin receptor-knockout mice display alterations in circadian rhythms of activity and feeding under constant lighting conditions.* Eur J Neurosci, 2014. **39**(2): p. 207-17.

238. Munger, S.D., T. Leinders-Zufall, and F. Zufall, *Subsystem Organization of the Mammalian Sense of Smell.* Annual Review of Physiology, 2009. **71**: p. 115-140.

239. Petrulis, A., *Chemosignals, hormones and mammalian reproduction.* Hormones and Behavior, 2013. **63**(5): p. 723-741.

240. Martinez-Marcos, A., *On the organization of olfactory and vomeronasal cortices.* Progress in Neurobiology, 2009. **87**(1): p. 21-30.

241. Kang, N., M.J. Baum, and J.A. Cherry, *A direct main olfactory bulb projection to the 'vomeronasal' amygdala in female mice selectively responds to volatile pheromones from males.* European Journal of Neuroscience, 2009. **29**(3): p. 624-634.

242. Mohedano-Moriano, A., et al., *Centrifugal telencephalic afferent connections to the main and accessory olfactory bulbs.* Frontiers in Neuroanatomy, 2012. **6**.

243. Petrulis, A., *Chemosignals, hormones and mammalian reproduction.* Horm Behav, 2013. **63**(5): p. 723-41.

244. Yoon, H., L.W. Enquist, and C. Dulac, *Olfactory inputs to hypothalamic neurons controlling reproduction and fertility.* Cell, 2005. **123**(4): p. 669-82.

245. Dicke, M. and M.W. Sabelis, *Infochemical terminology: based on cost-benefit analysis rather than origin of compounds?* Functional Ecology, 1988. **2**(2): p. 131-139.

246. Tirindelli, R., et al., *From Pheromones to Behavior.* Physiological Reviews, 2009. **89**(3): p. 921-956.

247. Keller, M., et al., *Destruction of the main olfactory epithelium reduces female sexual behavior and olfactory investigation in female mice.* Chemical Senses, 2006. **31**(4): p. 315-323.

248. Keller, M., et al., *The vomeronasal organ is required for the expression of lordosis behaviour, but not sex discrimination in female mice.* European Journal of Neuroscience, 2006. **23**(2): p. 521-530.

249. Whitten, W.K., *Occurrence of Anoestrus in Mice Caged in Groups.* Journal of Endocrinology, 1959. **18**(1): p. 102-107.

250. Whitten, W.K., *Modification of the Oestrous Cycle of the Mouse by External Stimuli Associated with the Male - Changes in the Oestrous Cycle Determined by Vaginal Smears.* Journal of Endocrinology, 1958. **17**(3): p. 307-313.

251. Ma, W.D., Z.S. Miao, and M.V. Novotny, *Induction of estrus in grouped female mice (Mus domesticus) by synthetic analogues of preputial gland constituents.* Chemical Senses, 1999. **24**(3): p. 289-293.

252. Jemiolo, B., S. Harvey, and M. Novotny, *Promotion of the Whitten Effect in Female Mice by Synthetic Analogs of Male Urinary Constituents.* Proceedings of the National Academy of Sciences of the United States of America, 1986. **83**(12): p. 4576-4579.

253. Fabre-Nys, C., K.M. Kendrick, and R.J. Scaramuzzi, *The "ram effect": new insights into neural modulation of the gonadotropic axis by male odors and socio-sexual interactions.* Front Neurosci, 2015. **9**: p. 111.

254. Curry, J.J., *Alterations in Incidence of Mating and Copulation-Induced Ovulation after Olfactory Bulb Ablation in Female Rats.* Journal of Endocrinology, 1974. **62**(2): p. 245-250.

255. Sanchez, M.A. and R. Dominguez, *Differential effects of unilateral lesions in the medial amygdala on spontaneous and induced ovulation.* Brain Res Bull, 1995. **38**(4): p. 313-7.

256. Bagga, N., et al., *Cholinergic activation of medial preoptic area by amygdala for ovulation in rat.* Physiol Behav, 1984. **32**(1): p. 45-8.

257. Arai, Y., *Effect of electrochemical stimulation of the amygdala on induction of ovulation in different types of persistent estrous rats and castrated male rats with an ovarian transplant.* Endocrinol Jpn, 1971. **18**(2): p. 211-4.

258. Ellendorff, F., et al., *Effects of electrical stimulation of the amygdala on gonadotropin release and ovulation in the rat.* Proc Soc Exp Biol Med, 1973. **142**(2): p. 417-20.

259. Beltramino, C. and S. Taleisnik, *Effect of electrochemical stimulation in the olfactory bulbs on the release of gonadotropin hormones in rats.* Neuroendocrinology, 1979. **28**(5): p. 320-8.

260. Vandenbe.Jg, *Male Odor Accelerates Female Sexual Maturation in Mice.* Endocrinology, 1969. **84**(3): p. 658-&.

261. Snyder, D.A., et al., *Olfactomedin: purification, characterization, and localization of a novel olfactory glycoprotein.* Biochemistry, 1991. **30**(38): p. 9143-53.

262. Karavanich, C.A. and R.R. Anholt, *Molecular evolution of olfactomedin.* Mol Biol Evol, 1998. **15**(6): p. 718-26.

263. Tomarev, S.I. and N. Nakaya, *Olfactomedin Domain-Containing Proteins: Possible Mechanisms of Action and Functions in Normal Development and Pathology.* Molecular Neurobiology, 2009. **40**(2): p. 122-138.

264. Lencinas, A., et al., *Olfactomedin-1 activity identifies a cell invasion checkpoint during epithelial-mesenchymal transition in the chick embryonic heart.* Dis Model Mech, 2013. **6**(3): p. 632-42.

265. Kodithuwakku, S.P., et al., *Hormonal regulation of endometrial olfactomedin expression and its suppressive effect on spheroid attachment onto endometrial epithelial cells.* Hum Reprod, 2011. **26**(1): p. 167-75.

266. Moreno, T.A. and M. Bronner-Fraser, *Noelins modulate the timing of neuronal differentiation during development.* Dev Biol, 2005. **288**(2): p. 434-47.

267. Moreno, T.A. and M. Bronner-Fraser, *The secreted glycoprotein noelin-1 promotes neurogenesis in Xenopus.* Developmental Biology, 2001. **240**(2): p. 340-360.

268. Nakaya, N., et al., *Olfactomedin 1 Interacts with the Nogo A Receptor Complex to Regulate Axon Growth.* Journal of Biological Chemistry, 2012. **287**(44): p. 37171-37184.

269. Nakaya, N., et al., *Zebrafish olfactomedin 1 regulates retinal axon elongation in vivo and is a modulator of Wnt signaling pathway.* Journal of Neuroscience, 2008. **28**(31): p. 7900-10.

270. Cheng, A.W., et al., *Pancortin-2 interacts with WAVE1 and Bcl-xL in a mitochondria-associated protein complex that mediates ischemic neuronal death.* Journal of Neuroscience, 2007. **27**(7): p. 1519-1528.

271. Rice, H.C., et al., *Pancortins interact with amyloid precursor protein and modulate cortical cell migration.* Development, 2012. **139**(21): p. 3986-96.

272. Janowski, D., et al., *Incidence of apoptosis and transcript abundance in bovine follicular cells is associated with the quality of the enclosed oocyte.* Theriogenology, 2012. **78**(3): p. 656-69 e1-5.

273. Bohr, D.C., et al., *Increased expression of olfactomedin-1 and myocilin in podocytes during puromycin aminonucleoside nephrosis.* Nephrol Dial Transplant, 2011. **26**(1): p. 83-92.

274. Danielson, P.E., et al., *Four structurally distinct neuron-specific olfactomedin-related glycoproteins produced by differential promoter utilization and alternative mRNA splicing from a single gene.* J Neurosci Res, 1994. **38**(4): p. 468-78.

275. Nagano, T., et al., *Differentially expressed olfactomedin-related glycoproteins (Pancortins) in the brain.* Molecular Brain Research, 1998. **53**(1-2): p. 13-23.

276. Yokoe, H. and R.R.H. Anholt, *Molecular-Cloning of Olfactomedin, an Extracellular-Matrix Protein-Specific to Olfactory Neuroepithelium.* Proc Natl Acad Sci U S A, 1993. **90**(10): p. 4655-4659.

277. Veroni, C., et al., *beta-dystrobrevin, a kinesin-binding receptor, interacts with the extracellular matrix components pancortins.* J Neurosci Res, 2007. **85**(12): p. 2631-9.

278. Kondo, D., et al., *Localization of olfactomedin-related glycoprotein isoform (BMZ) in the Golgi apparatus of glomerular podocytes in rat kidneys.* Journal of the American Society of Nephrology, 2000. **11**(5): p. 803-813.

279. Munro, S. and H.R. Pelham, *A C-terminal signal prevents secretion of luminal ER proteins.* Cell, 1987. **48**(5): p. 899-907.

280. Ando, K., et al., *Expression and characterization of disulfide bond use of oligomerized A2-Pancortins: extracellular matrix constituents in the developing brain.* Neuroscience, 2005. **133**(4): p. 947-57.

281. Nagano, T., et al., *A2-Pancortins (Pancortin-3 and -4) are the dominant pancortins during neocortical development.* J Neurochem, 2000. **75**(1): p. 1-8.

282. Nakaya, N., et al., *Deletion in the N-terminal half of olfactomedin 1 modifies its interaction with synaptic proteins and causes brain dystrophy and abnormal behavior in mice.* Exp Neurol, 2013. **250**: p. 205-18.

283. Hilakivi-Clarke, L., J.E. Andrade, and W. Helferich, *Is soy consumption good or bad for the breast?* J Nutr, 2010. **140**(12): p. 2326S-2334S.

284. Parent, A.S., et al., *The timing of normal puberty and the age limits of sexual precocity: Variations around the world, secular trends, and changes after migration.* Endocrine Reviews, 2003. **24**(5): p. 668-693.

285. Euling, S.Y., et al., *Role of environmental factors in the timing of puberty.* Pediatrics, 2008. **121 Suppl 3**: p. S167-71.

286. Mouritsen, A., et al., *Hypothesis: exposure to endocrine-disrupting chemicals may interfere with timing of puberty.* International Journal of Andrology, 2010. **33**(2): p. 346-359.

287. Euling, S.Y., et al., *Examination of US puberty-timing data from 1940 to 1994 for secular trends: panel findings.* Pediatrics, 2008. **121 Suppl 3**: p. S172-91.

288. Aksglaede, L., et al., *Recent Decline in Age at Breast Development: The Copenhagen Puberty Study.* Pediatrics, 2009. **123**(5): p. E932-E939.

289. Ebling, F.J., *The neuroendocrine timing of puberty.* Reproduction, 2005. **129**(6): p. 675-83.

290. Spearow, J.L., et al., *Genetic variation in susceptibility to endocrine disruption by estrogen in mice.* Science, 1999. **285**(5431): p. 1259-61.

291. Xiao, S., et al., *Preimplantation exposure to bisphenol A (BPA) affects embryo transport, preimplantation embryo development, and uterine receptivity in mice.* Reprod Toxicol, 2011. **32**(4): p. 434-41.

292. Zhao, F., et al., *Postweaning exposure to dietary zearalenone, a mycotoxin, promotes premature onset of puberty and disrupts early pregnancy events in female mice.* Toxicol Sci, 2013. **132**(2): p. 431-42.

293. Byers, S.L., et al., *Mouse estrous cycle identification tool and images.* PLoS One, 2012. **7**(4): p. e35538.

294. Fenton, S.E., et al., *Persistent abnormalities in the rat mammary gland following gestational and lactational exposure to 2,3,7,8-tetrachlorodibenzo-p-dioxin (TCDD).* Toxicological Sciences, 2002. **67**(1): p. 63-74.

295. Ye, X., et al., *Unique uterine localization and regulation may differentiate LPA3 from other lysophospholipid receptors for its role in embryo implantation.* Fertil Steril, 2011. **95**(6): p. 2107-13, 2113 e1-4.

296. Diao, H., et al., *Altered spatiotemporal expression of collagen types I, III, IV, and VI in Lpar3-deficient peri-implantation mouse uterus.* Biol Reprod, 2011. **84**(2): p. 255-65.

297. Ye, X., et al., *LPA3-mediated lysophosphatidic acid signalling in embryo implantation and spacing.* Nature, 2005. **435**(7038): p. 104-8.

298. Stocco, C., C. Telleria, and G. Gibori, *The molecular control of corpus luteum formation, function, and regression.* Endocrine Reviews, 2007. **28**(1): p. 117-149.

299. Richert, M.M., et al., *An atlas of mouse mammary gland development.* J Mammary Gland Biol Neoplasia, 2000. **5**(2): p. 227-41.

300. Mucignat-Caretta, C., A. Caretta, and A. Cavaggioni, *Acceleration of puberty onset in female mice by male urinary proteins.* J Physiol, 1995. **486 (Pt 2)**: p. 517-22.

301. Adams, G.P. and M.H. Ratto, *Ovulation-inducing factor in seminal plasma: a review.* Anim Reprod Sci, 2013. **136**(3): p. 148-56.

302. Rasier, G., et al., *Female sexual maturation and reproduction after prepubertal exposure to estrogens and endocrine disrupting chemicals: a review of rodent and human data.* Mol Cell Endocrinol, 2006. **254-255**: p. 187-201.

303. Diel, P., et al., *Phytoestrogens and carcinogenesis-differential effects of genistein in experimental models of normal and malignant rat endometrium.* Human Reproduction, 2001. **16**(5): p. 997-1006.

304. Heldring, N., et al., *Estrogen receptors: How do they signal and what are their targets.* Physiological Reviews, 2007. **87**(3): p. 905-931.

305. Cheng, G., et al., *Estrogen receptors ER alpha and ER beta in proliferation in the rodent mammary gland.* Proc Natl Acad Sci U S A, 2004. **101**(11): p. 3739-46.

306. Luetteke, N.C., et al., *Targeted inactivation of the EGF and amphiregulin genes reveals distinct roles for EGF receptor ligands in mouse mammary gland development.* Development, 1999. **126**(12): p. 2739-50.

307. Ciarloni, L., S. Mallepell, and C. Brisken, *Amphiregulin is an essential mediator of estrogen receptor alpha function in mammary gland development.* Proc Natl Acad Sci U S A, 2007. **104**(13): p. 5455-5460.

308. Sternlicht, M.D. and S.W. Sunnarborg, *The ADAM17-amphiregulin-EGFR axis in mammary development and cancer.* J Mammary Gland Biol Neoplasia, 2008. **13**(2): p. 181-94.

309. Li, R., et al., *Postweaning dietary genistein exposure advances puberty without significantly affecting early pregnancy in C57BL/6J female mice.* Reprod Toxicol, 2014. **44**: p. 85-92.

310. McNally, S. and F. Martin, *Molecular regulators of pubertal mammary gland development.* Ann Med, 2011. **43**(3): p. 212-34.

311. Walters, L.M., A.W. Rourke, and V.P. Eroschenko, *Purified methoxychlor stimulates the reproductive tract in immature female mice.* Reprod Toxicol, 1993. **7**(6): p. 599-606.

312. Macias, H. and L. Hinck, *Mammary gland development.* Wiley Interdiscip Rev Dev Biol, 2012. **1**(4): p. 533-57.

313. Sinkevicius, K.W., et al., *An estrogen receptor-alpha knock-in mutation provides evidence of ligand-independent signaling and allows modulation of ligand-induced pathways in vivo.* Endocrinology, 2008. **149**(6): p. 2970-9.

314. Korach, K.S., et al., *Estrogen receptor gene disruption: molecular characterization and experimental and clinical phenotypes.* Recent Prog Horm Res, 1996. **51**: p. 159-86; discussion 186-8.

315. Palmieri, C., et al., *Estrogen receptor beta in breast cancer.* Endocr Relat Cancer, 2002. **9**(1): p. 1-13.

316. Krege, J.H., et al., *Generation and reproductive phenotypes of mice lacking estrogen receptor beta.* Proc Natl Acad Sci U S A, 1998. **95**(26): p. 15677-82.

317. Forster, C., et al., *Involvement of estrogen receptor beta in terminal differentiation of mammary gland epithelium.* Proc Natl Acad Sci U S A, 2002. **99**(24): p. 15578-83.

318. Thigpen, J.E., et al., *Variations in phytoestrogen content between different mill dates of the same diet produces significant differences in the time of vaginal opening in CD-1 mice and F344 rats but not in CD Sprague-Dawley rats.* Environ Health Perspect, 2007. **115**(12): p. 1717-26.

319. Caligioni, C.S., *Assessing reproductive status/stages in mice.* Curr Protoc Neurosci, 2009. **Appendix 4**: p. Appendix 4I.

320. Kaplowitz, P.B., *Link between body fat and the timing of puberty.* Pediatrics, 2008. **121 Suppl 3**: p. S208-17.

321. Aksglaede, L., et al., *Age at puberty and the emerging obesity epidemic.* PLoS One, 2009. **4**(12): p. e8450.

322. Zhao, F., et al., *Multigenerational exposure to dietary zearalenone (ZEA), an estrogenic mycotoxin, affects puberty and reproduction in female mice.* Reprod Toxicol, 2014.

323. Zhao, F., et al., *Timing and recovery of postweaning exposure to diethylstilbestrol on early pregnancy in CD-1 mice.* Reprod Toxicol, 2014. **49C**: p. 48-54.

324. Chen, W., et al., *Berardinelli-seip congenital lipodystrophy 2/seipin is a cell-autonomous regulator of lipolysis essential for adipocyte differentiation.* Mol Cell Biol, 2012. **32**(6): p. 1099-111.

325. Magre, J., et al., *Identification of the gene altered in Berardinelli-Seip congenital lipodystrophy on chromosome 11q13.* Nat Genet, 2001. **28**(4): p. 365-70.

326. Lundin, C., et al., *Membrane topology of the human seipin protein.* FEBS Lett, 2006. **580**(9): p. 2281-4.

327. Sim, M.F., et al., *Analyzing the functions and structure of the human lipodystrophy protein seipin.* Methods Enzymol, 2014. **537**: p. 161-75.

328. Cui, X., et al., *Seipin ablation in mice results in severe generalized lipodystrophy.* Hum Mol Genet, 2011. **20**(15): p. 3022-30.

329. Prieur, X., et al., *Thiazolidinediones partially reverse the metabolic disturbances observed in Bscl2/seipin-deficient mice.* Diabetologia, 2013. **56**(8): p. 1813-25.

330. Chen, W., et al., *The human lipodystrophy gene product Berardinelli-Seip congenital lipodystrophy 2/seipin plays a key role in adipocyte differentiation.* Endocrinology, 2009. **150**(10): p. 4552-61.

331. Agarwal, A.K. and A. Garg, *Congenital generalized lipodystrophy: significance of triglyceride biosynthetic pathways.* Trends Endocrinol Metab, 2003. **14**(5): p. 214-21.

332. Jiang, M., et al., *Lack of testicular seipin causes teratozoospermia syndrome in men.* Proc Natl Acad Sci U S A, 2014. **111**(19): p. 7054-9.

333. Cartwright, B.R. and J.M. Goodman, *Seipin: from human disease to molecular mechanism.* J Lipid Res, 2012. **53**(6): p. 1042-55.

334. Van Maldergem, L., et al., *Genotype-phenotype relationships in Berardinelli-Seip congenital lipodystrophy.* J Med Genet, 2002. **39**(10): p. 722-33.

335. Zhao, F., et al., *Postweaning exposure to dietary zearalenone, a mycotoxin, promotes premature onset of puberty and disrupts early pregnancy events in female mice.* Toxicological Sciences, 2013. **132**(2): p. 431-42.

336. Murr, S.M., Geschwind, II, and G.E. Bradford, *Plasma LH and FSH during different oestrous cycle conditions in mice.* J Reprod Fertil, 1973. **32**(2): p. 221-30.

337. Wang, H. and S.K. Dey, *Roadmap to embryo implantation: clues from mouse models.* Nat Rev Genet, 2006. **7**(3): p. 185-99.

338. Walmer, D.K., et al., *Lactoferrin expression in the mouse reproductive tract during the natural estrous cycle: correlation with circulating estradiol and progesterone.* Endocrinology, 1992. **131**(3): p. 1458-66.

339. Wagner, I.V., et al., *Effects of obesity on human sexual development.* Nat Rev Endocrinol, 2012. **8**(4): p. 246-54.

340. Thigpen, J.E., et al., *Phytoestrogen content of purified, open- and closed-formula laboratory animal diets.* Laboratory Animal Science, 1999. **49**(5): p. 530-536.

341. Thigpen, J.E., et al., *The estrogenic content of rodent diets, bedding, cages, and water bottles and its effect on bisphenol A studies.* J Am Assoc Lab Anim Sci, 2013. **52**(2): p. 130-41.

342. Degen, G.H., et al., *Estrogenic isoflavones in rodent diets.* Toxicol Lett, 2002. **128**(1-3): p. 145-57.

343. Takashima-Sasaki, K., et al., *Effect of exposure to high isoflavone-containing diets on prenatal and postnatal offspring mice.* Biosci Biotechnol Biochem, 2006. **70**(12): p. 2874-82.

344. Casanova, M., et al., *Developmental effects of dietary phytoestrogens in Sprague-Dawley rats and interactions of genistein and daidzein with rat estrogen receptors alpha and beta in vitro (vol 51, pg 236, 1999).* Toxicological Sciences, 1999. **52**(2): p. Cp2-Cp2.

345. Thigpen, J.E., et al., *Selecting the appropriate rodent diet for endocrine disruptor research and testing studies.* ILAR J, 2004. **45**(4): p. 401-16.

346. Ito, D., et al., *Characterization of seipin/BSCL2, a protein associated with spastic paraplegia 17.* Neurobiol Dis, 2008. **31**(2): p. 266-77.

347. Brisken, C., et al., *A paracrine role for the epithelial progesterone receptor in mammary gland development.* Proc Natl Acad Sci U S A, 1998. **95**(9): p. 5076-81.

348. Shyamala, G., et al., *Transgenic mice carrying an imbalance in the native ratio of A to B forms of progesterone receptor exhibit developmental abnormalities in mammary glands.* Proc Natl Acad Sci U S A, 1998. **95**(2): p. 696-701.

349. Kingsley-Kallesen, M., et al., *The mineralocorticoid receptor may compensate for the loss of the glucocorticoid receptor at specific stages of mammary gland development.* Molecular Endocrinology, 2002. **16**(9): p. 2008-2018.

350. Weihua, Z., et al., *Estrogen receptor (ER) beta, a modulator of ERalpha in the uterus.* Proc Natl Acad Sci U S A, 2000. **97**(11): p. 5936-41.

351. Elias, C.F., *Leptin action in pubertal development: recent advances and unanswered questions.* Trends Endocrinol Metab, 2012. **23**(1): p. 9-15.

352. Savage, D.B., *Mouse models of inherited lipodystrophy.* Disease Models & Mechanisms, 2009. **2**(11-12): p. 554-562.

353. Cunningham, M.J., D.K. Clifton, and R.A. Steiner, *Leptin's actions on the reproductive axis: perspectives and mechanisms.* Biol Reprod, 1999. **60**(2): p. 216-22.

354. Relic, B., et al., *Genistein induces adipogenesis but inhibits leptin induction in human synovial fibroblasts.* Lab Invest, 2009. **89**(7): p. 811-22.

355. Szkudelski, T., et al., *Genistein restricts leptin secretion from rat adipocytes.* J Steroid Biochem Mol Biol, 2005. **96**(3-4): p. 301-7.

356. Kim, H.K., et al., *Genistein decreases food intake, body weight, and fat pad weight and causes adipose tissue apoptosis in ovariectomized female mice.* J Nutr, 2006. **136**(2): p. 409-14.

357. Clegg, D.J., et al., *Gonadal hormones determine sensitivity to central leptin and insulin.* Diabetes, 2006. **55**(4): p. 978-87.

358. McBryan, J., et al., *Amphiregulin: role in mammary gland development and breast cancer.* J Mammary Gland Biol Neoplasia, 2008. **13**(2): p. 159-69.

359. Hovey, R.C. and L. Aimo, *Diverse and active roles for adipocytes during mammary gland growth and function.* J Mammary Gland Biol Neoplasia, 2010. **15**(3): p. 279-90.

360. Landskroner-Eiger, S., et al., *Morphogenesis of the developing mammary gland: stage-dependent impact of adipocytes.* Dev Biol, 2010. **344**(2): p. 968-78.

361. Couldrey, C., et al., *Adipose tissue: a vital in vivo role in mammary gland development but not differentiation.* Dev Dyn, 2002. **223**(4): p. 459-68.

362. Yokoe, H. and R.R. Anholt, *Molecular cloning of olfactomedin, an extracellular matrix protein specific to olfactory neuroepithelium.* Proc Natl Acad Sci U S A, 1993. **90**(10): p. 4655-9.

363. Zeng, L.C., Z.G. Han, and W.J. Ma, *Elucidation of subfamily segregation and intramolecular coevolution of the olfactomedin-like proteins by comprehensive phylogenetic analysis and gene expression pattern assessment.* FEBS Lett, 2005. **579**(25): p. 5443-53.

364. Anholt, R.R., *Olfactomedin proteins: central players in development and disease.* Front Cell Dev Biol, 2014. **2**: p. 6.

365. Karavanich, C.A. and R.R.H. Anholt, *Molecular evolution of olfactomedin.* Molecular Biology and Evolution, 1998. **15**(6): p. 718-726.

366. Nakaya, N., et al., *Olfactomedin 1 interacts with the Nogo A receptor complex to regulate axon growth.* J Biol Chem, 2012. **287**(44): p. 37171-84.

367. Nagano, T., et al., *Differentially expressed olfactomedin-related glycoproteins (Pancortins) in the brain.* Brain Res Mol Brain Res, 1998. **53**(1-2): p. 13-23.

368. Barembaum, M., et al., *Noelin-1 is a secreted glycoprotein involved in generation of the neural crest.* Nature Cell Biology, 2000. **2**(4): p. 219-225.

369. Cheng, A., et al., *Pancortin-2 interacts with WAVE1 and Bcl-xL in a mitochondria-associated protein complex that mediates ischemic neuronal death.* J Neurosci, 2007. **27**(7): p. 1519-28.

370. Xiao, S., et al., *Differential gene expression profiling of mouse uterine luminal epithelium during periimplantation.* Reprod Sci, 2014. **21**(3): p. 351-62.

371. Denker, H.W., *Implantation: a cell biological paradox.* J Exp Zool, 1993. **266**(6): p. 541-58.

372. Cowell, T.P., *Implantation and development of mouse eggs transferred to the uteri of non-progestational mice.* J Reprod Fertil, 1969. **19**(2): p. 239-45.

373. Parr, E.L., H.N. Tung, and M.B. Parr, *Apoptosis as the Mode of Uterine Epithelial-Cell Death during Embryo Implantation in Mice and Rats.* Biology of Reproduction, 1987. **36**(1): p. 211-225.

374. Allen C. Enders, S.S., *A morphological analysis of the early implantation stages in the rat.* American Journal of Anatomy, 1967. **120**(2): p. 185-225.

375. Paria, B.C., H. Song, and S.K. Dey, *Implantation: molecular basis of embryo-uterine dialogue.* Int J Dev Biol, 2001. **45**(3): p. 597-605.

376. Diao, H., et al., *Distinct spatiotemporal expression of serine proteases prss23 and prss35 in periimplantation mouse uterus and dispensable function of prss35 in fertility.* PLoS One, 2013. **8**(2): p. e56757.

377. Ushinohama, K., et al., *Impaired ovulation by 2,3,7,8 tetrachlorodibenzo-p-dioxin (TCDD) in immature rats treated with equine chorionic gonadotropin.* Reprod Toxicol, 2001. **15**(3): p. 275-80.

378. Larder, R., et al., *Hypothalamic dysregulation and infertility in mice lacking the homeodomain protein Six6.* J Neurosci, 2011. **31**(2): p. 426-38.

379. Diaczok, D., et al., *Deletion of Otx2 in GnRH neurons results in a mouse model of hypogonadotropic hypogonadism.* Mol Endocrinol, 2011. **25**(5): p. 833-46.

380. Diao, H., et al., *Broad gap junction blocker carbenoxolone disrupts uterine preparation for embryo implantation in mice.* Biol Reprod, 2013. **89**(2): p. 31.

381. Diao, H., et al., *Progesterone receptor-mediated up-regulation of transthyretin in preimplantation mouse uterus.* Fertil Steril, 2010. **93**(8): p. 2750-3.

382. Brisken, C. and B. O'Malley, *Hormone Action in the Mammary Gland.* Cold Spring Harbor Perspectives in Biology, 2010. **2**(12).

383. Dudas, B., A. Mihaly, and I. Merchenthaler, *Topography and associations of luteinizing hormone-releasing hormone and neuropeptide Y-immunoreactive neuronal systems in the human diencephalon.* J Comp Neurol, 2000. **427**(4): p. 593-603.

384. Pepin, D., et al., *The imitation switch ATPase Snf2l is required for superovulation and regulates Fgl2 in differentiating mouse granulosa cells.* Biol Reprod, 2013. **88**(6): p. 142.

385. Sarkar, D.K., et al., *Gonadotropin-releasing hormone surge in pro-oestrous rats.* Nature, 1976. **264**(5585): p. 461-3.

386. Whitten, W.K., *Modification of the oestrous cycle of the mouse by external stimuli associated with the male; changes in the oestrous cycle determined by vaginal smears.* Journal of Endocrinology, 1958. **17**(3): p. 307-13.

387. Knapska, E., et al., *Functional internal complexity of amygdala: focus on gene activity mapping after behavioral training and drugs of abuse.* Physiol Rev, 2007. **87**(4): p. 1113-73.

388. Barkan, D., et al., *Leptin induces ovulation in GnRH-deficient mice.* FASEB J, 2005. **19**(1): p. 133-5.

389. Koos, R.D., et al., *Perfusion of the rat ovary in vitro: methodology, induction of ovulation, and pattern of steroidogenesis.* Biol Reprod, 1984. **30**(5): p. 1135-41.

390. Smarr, B.L., E. Morris, and H.O. de la Iglesia, *The dorsomedial suprachiasmatic nucleus times circadian expression of Kiss1 and the luteinizing hormone surge.* Endocrinology, 2012. **153**(6): p. 2839-50.

391. Herbison, A.E., et al., *Gonadotropin-releasing hormone neuron requirements for puberty, ovulation, and fertility.* Endocrinology, 2008. **149**(2): p. 597-604.

392. Owen, B.M., et al., *FGF21 contributes to neuroendocrine control of female reproduction.* Nat Med, 2013. **19**(9): p. 1153-6.

393. Pinilla, L., et al., *Kisspeptins and reproduction: physiological roles and regulatory mechanisms.* Physiol Rev, 2012. **92**(3): p. 1235-316.

394. Nagai, K., et al., *Olfactory stimulatory with grapefruit and lavender oils change autonomic nerve activity and physiological function.* Auton Neurosci, 2014. **185**: p. 29-35.

395. Trejo-Munoz, L., et al., *Temporal modulation of the canonical clockwork in the suprachiasmatic nucleus and olfactory bulb by the mammary pheromone 2MB2 in pre-visual rabbits.* Neuroscience, 2014. **275**: p. 170-83.

396. Amir, S., et al., *Olfactory stimulation enhances light-induced phase shifts in free-running activity rhythms and Fos expression in the suprachiasmatic nucleus.* Neuroscience, 1999. **92**(4): p. 1165-70.

397. Smarr, B.L., J.J. Gile, and H.O. de la Iglesia, *Oestrogen-independent circadian clock gene expression in the anteroventral periventricular nucleus in female rats: possible role as an integrator for circadian and ovarian signals timing the luteinising hormone surge.* J Neuroendocrinol, 2013. **25**(12): p. 1273-9.

398. Lewkowitz-Shpuntoff, H.M., et al., *Olfactory phenotypic spectrum in idiopathic hypogonadotropic hypogonadism: pathophysiological and genetic implications.* J Clin Endocrinol Metab, 2012. **97**(1): p. E136-44.

399. Chamero, P., et al., *G protein G alpha o is essential for vomeronasal function and aggressive behavior in mice.* Proceedings of the National Academy of Sciences of the United States of America, 2011. **108**(31): p. 12898-12903.

400. Hasen, N.S. and S.C. Gammie, *Trpc2-deficient lactating mice exhibit altered brain and behavioral responses to bedding stimuli.* Behav Brain Res, 2011. **217**(2): p. 347-53.

401. Tirindelli, R., et al., *From pheromones to behavior.* Physiol Rev, 2009. **89**(3): p. 921-56.

402. Petrulis, A., *Chemosignals and hormones in the neural control of mammalian sexual behavior.* Front Neuroendocrinol, 2013. **34**(4): p. 255-67.

403. Gandelman, R., M.X. Zarrow, and V.H. Denenberg, *Reproductive and maternal performance in the mouse following removal of the olfactory bulbs.* J Reprod Fertil, 1972. **28**(3): p. 453-6.

404. Kimoto, H. and K. Touhara, *Induction of c-Fos expression in mouse vomeronasal neurons by sex-specific non-volatile pheromone(s).* Chem Senses, 2005. **30 Suppl 1**: p. i146-7.

405. Kang, N., et al., *Sex difference in Fos induced by male urine in medial amygdala-projecting accessory olfactory bulb mitral cells of mice.* Neurosci Lett, 2006. **398**(1-2): p. 59-62.

406. Logan, D.W., et al., *Learned recognition of maternal signature odors mediates the first suckling episode in mice.* Curr Biol, 2012. **22**(21): p. 1998-2007.

407. Lee, A.C., J.W. He, and M.H. Ma, *Olfactory Marker Protein Is Critical for Functional Maturation of Olfactory Sensory Neurons and Development of Mother Preference.* Journal of Neuroscience, 2011. **31**(8): p. 2974-2982.

408. Colledge, W.H., H. Mei, and X. d'Anglemont de Tassigny, *Mouse models to study the central regulation of puberty.* Mol Cell Endocrinol, 2010. **324**(1-2): p. 12-20.

409. Sultana, A., et al., *Deletion of olfactomedin 2 induces changes in the AMPA receptor complex and impairs visual, olfactory, and motor functions in mice.* Exp Neurol, 2014. **261**: p. 802-11.

410. Ertzeid, G. and R. Storeng, *Adverse effects of gonadotrophin treatment on pre- and postimplantation development in mice.* J Reprod Fertil, 1992. **96**(2): p. 649-55.

411. Beaumont, H.M. and A.F. Smith, *Embryonic mortality during the pre- and post-implantation periods of pregnancy in mature mice after superovulation.* J Reprod Fertil, 1975. **45**(3): p. 437-48.

412. Tapia, A., et al., *Bioinformatic detection of E47, E2F1 and SREBP1 transcription factors as potential regulators of genes associated to acquisition of endometrial receptivity.* Reprod Biol Endocrinol, 2011. **9**: p. 14.

413. Lee, J., et al., *Differentially expressed genes implicated in unexplained recurrent spontaneous abortion.* Int J Biochem Cell Biol, 2007. **39**(12): p. 2265-77.

414. Dharmaraj, N., S.J. Gendler, and D.D. Carson, *Expression of human MUC1 during early pregnancy in the human MUC1 transgenic mouse model.* Biol Reprod, 2009. **81**(6): p. 1182-8.

415. Hillier, B.J. and V.D. Vacquier, *Amassin, an olfactomedin protein, mediates the massive intercellular adhesion of sea urchin coelomocytes.* J Cell Biol, 2003. **160**(4): p. 597-604.

416. Dorn, L.D., *Psychological and Social Problems in Children with Premature Adrenarche and Precocious Puberty.* When Puberty Is Precocious, 2007: p. 309-327.

417. Cheng, G., et al., *Beyond overweight: nutrition as an important lifestyle factor influencing timing of puberty.* Nutrition Reviews, 2012. **70**(3): p. 133-152.

418. Day, F.R., et al., *Puberty timing associated with diabetes, cardiovascular disease and also diverse health outcomes in men and women: the UK Biobank study.* Scientific Reports, 2015. **5**.

419. Stoll, B.A., *Western diet, early puberty, and breast cancer risk.* Breast Cancer Research and Treatment, 1998. **49**(3): p. 187-193.

420. Ehrlich, S., *Effect of fertility and infertility on longevity.* Fertility and Sterility, 2015. **103**(5): p. 1129-1135.

421. Klein, J. and M.V. Sauer, *Assessing fertility in women of advanced reproductive age.* Am J Obstet Gynecol, 2001. **185**(3): p. 758-70.

422. Yum, T., S. Lee, and Y. Kim, *Association between precocious puberty and some endocrine disruptors in human plasma.* J Environ Sci Health A Tox Hazard Subst Environ Eng, 2013. **48**(8): p. 912-7.

423. Lavie, C.J., A. De Schutter, and R.V. Milani, *Healthy obese versus unhealthy lean: the obesity paradox.* Nature Reviews Endocrinology, 2015. **11**(1): p. 55-62.

424. Chen, W.Q., et al., *Berardinelli-Seip Congenital Lipodystrophy 2/Seipin Is a Cell-Autonomous Regulator of Lipolysis Essential for Adipocyte Differentiation.* Molecular and Cellular Biology, 2012. **32**(6): p. 1099-1111.

425. Han, M., et al., *Embryonic exposures of lithium and homocysteine and folate protection affect lipid metabolism during mouse cardiogenesis and placentation.* Reprod Toxicol, 2016. **61**: p. 82-96.

426. Wesson, D.W., et al., *Olfactory dysfunction correlates with amyloid-beta burden in an Alzheimer's disease mouse model.* J Neurosci, 2010. **30**(2): p. 505-14.

427. Berendse, H.W., et al., *Motor and non-motor correlates of olfactory dysfunction in Parkinson's disease.* J Neurol Sci, 2011. **310**(1-2): p. 21-4.

428. Braga-Neto, P., et al., *Clinical correlates of olfactory dysfunction in spinocerebellar ataxia type 3.* Parkinsonism Relat Disord, 2011. **17**(5): p. 353-6.